

VOLUME XXXVII

GEMS & GEMOLOGY

SUMMER 2001



Featuring:

*Chinese Freshwater
Cultured Pearls*

*"Golden" South Sea
Cultured Pearls*

Imitation Asterism



pg. 108



pg. 115

EDITORIAL _____

- 95 **The G&G Twenty Year Index: Two Decades of Evolution**
Alice S. Keller

FEATURE ARTICLES _____

- 96 **The Current Status of Chinese Freshwater Cultured Pearls**
Shigeru Akamatsu, Li Tajima Zansheng, Thomas M. Moses, and Kenneth Scarratt
Based on recent visits to the pearl farms of Hanzhou Province, the authors report on the latest techniques being used to produce Chinese freshwater cultured pearls.

- 114 **Spectral Reflectance and Fluorescence Characteristics of Natural-Color and Heat-Treated "Golden" South Sea Cultured Pearls**
Shane Elen

UV-Vis reflectance spectra and fluorescence characteristics are useful in distinguishing undrilled natural- and treated-color yellow cultured pearls produced from the *Pinctada maxima* mollusk.

NOTES AND NEW TECHNIQUES _____

- 124 **A New Method for Imitating Asterism**
Shane F. McClure and John I. Koivula

A new polishing process is being used to create the appearance of asterism in gems that have seldom if ever shown this phenomenon previously.

REGULAR FEATURES _____

130 **Gem Trade Lab Notes**

- "Banded" twinned diamond crystal
- Diamonds with unusual inclusions
- Feldspar with chrome diopside inclusions
- Gibbsite dyed to imitate nephrite
- Devitrified glass resembling jade
- Early Japanese assembled cultured blister pearls
- Dyed black faceted cultured pearls
- New imitation: "Shell pearls" with a calcite bead

137 **Thank You, Donors**138 **Gem News International**

- Royal Asscher cut
- Canadian diamonds
- PDAC conference
- A diamond table with trigons
- "Burmite"
- Cat's-eye amethyst
- Brownish red to orange gems from Afghanistan/Pakistan
- Clinohumite from Tanzania
- An engraved emerald
- Unusual rutilated quartz
- Rubies and ruby deposits of eastern Madagascar
- Ruby crystal with a mobile bubble
- Green sapphire with pyrochlore inclusions
- Vortex (Yogo Gulch) sapphire mine update
- "Canary" tourmaline from Malawi
- Bismuth-bearing liddicoatite from Nigeria
- "Jurassic Bugs" amber imitation
- Assembled diamond imitations from Brazil
- Enamel-backed quartz as a star sapphire imitation
- Goldschmidt conference
- Moscow gemological conference
- Harvard tourmaline exhibit

160 **Book Reviews**163 **Gemological Abstracts**171 **Guidelines for Authors**

pg. 133



pg. 149

GEMS & GEMOLOGY

EDITORIAL STAFF

Editor-in-Chief
Richard T. Liddicoat

Publisher
William E. Boyajian

Associate Editor
John Sinkankas

Technical Editor
Carol M. Stockton

Assistant Editor
Stuart Overlin
soverlin@gia.edu

Contributing Editor
John I. Koivula

Editor
Alice S. Keller
5345 Armada Drive
Carlsbad, CA 92008
(760) 603-4504
akeller@gia.edu

Senior Editor
Brendan M. Laurs
blaurs@gia.edu

Subscriptions
Debbie Ortiz
(800) 421-7250, ext. 7142
Fax: (760) 603-4595
dortiz@gia.edu

Editors, Gem Trade Lab Notes
Thomas M. Moses, Ilene Reinitz,
Shane F. McClure, and
Mary L. Johnson

Editor, Gem News International
Brendan M. Laurs

Editors, Book Reviews
Susan B. Johnson
Jana E. Miyahira-Smith

Editor, Gemological Abstracts
A. A. Levinson

Web Site: www.gia.edu/gandg

PRODUCTION STAFF

Art Director
Karen Myers

Technical Writer
Barak Green

Research Assistant
Alethea Inns

EDITORIAL REVIEW BOARD

Alan T. Collins
London, United Kingdom

G. Robert Crowningshield
New York, New York

John Emmett
Brush Prairie, Washington

Emmanuel Fritsch
Nantes, France

C. W. Fryer
Santa Monica, California

Henry A. Hänni
Basel, Switzerland

C. S. Hurlbut, Jr.
Cambridge, Massachusetts

Alan Jobbins
Caterham, United Kingdom

Mary L. Johnson
Carlsbad, California

Anthony R. Kampf
Los Angeles, California

Robert E. Kane
Helena, Montana

John I. Koivula
Carlsbad, California

A. A. Levinson
Calgary, Alberta, Canada

Thomas M. Moses
New York, New York

Kurt Nassau
P.O. Lebanon, New Jersey

George Rossman
Pasadena, California

Kenneth Scarratt
New York, New York

Karl Schmetzer
Petershausen, Germany

James E. Shigley
Carlsbad, California

Christopher P. Smith
Lucerne, Switzerland

SUBSCRIPTIONS

Subscriptions to addresses in the U.S. are priced as follows: **\$69.95** for one year (4 issues), **\$179.95** for three years (12 issues). Subscriptions sent elsewhere are **\$80.00** for one year, **\$210.00** for three years.

Special annual subscription rates are available for GIA Alumni Association members and students actively involved in a GIA program: **\$59.95** to addresses in the U.S., **\$70.00** elsewhere. Your student number must be listed at the time your subscription is entered. Current issues may be purchased for **\$17.50** in the U.S.A., **\$22.00** elsewhere. Discounts are given for bulk orders of 10 or more of any one issue. A limited number of back issues of *G&G* are also available for purchase. Please address all inquiries regarding subscriptions and the purchase of single copies or back issues to the Subscriptions Department (see above), or visit www.gia.edu/gandg.

To obtain a Japanese translation of *Gems & Gemology*, contact GIA Japan, Okachimachi Cy Bldg., 5-15-14 Ueno, Taitoku, Tokyo 110, Japan. Our Canadian goods and service registration number is 126142892RT.

MANUSCRIPT SUBMISSIONS

Gems & Gemology welcomes the submission of articles on all aspects of the field. Please see the Guidelines for Authors in this issue of the journal, or contact the Senior Editor for a copy. Letters on articles published in *Gems & Gemology* are also welcome.

COPYRIGHT AND REPRINT PERMISSIONS

Abstracting is permitted with credit to the source. Libraries are permitted to photocopy beyond the limits of U.S. copyright law for private use of patrons. Instructors are permitted to photocopy isolated articles for noncommercial classroom use without fee. Copying of the photographs by any means other than traditional photocopying techniques (Xerox, etc.) is prohibited without the express permission of the photographer (where listed) or author of the article in which the photo appears (where no photographer is listed). For other copying, reprint, or republication permission, please contact the Editor.

Gems & Gemology is published quarterly by the Gemological Institute of America, a nonprofit educational organization for the jewelry industry, 5345 Armada Drive, Carlsbad, CA 92008.

Postmaster: Return undeliverable copies of *Gems & Gemology* to 5345 Armada Drive, Carlsbad, CA 92008.

Any opinions expressed in signed articles are understood to be the opinions of the authors and not of the publisher.

ABOUT THE COVER

"Golden" South Sea cultured pearls have become increasingly popular. Although distinguishing natural- from treated-color yellow pearls is fairly straightforward when they have been treated with inorganic chemicals or dyes after drilling, this separation is more difficult when the pearls have been heat treated prior to drilling. Shane Elen addresses this difficulty in his article on South Sea "golden" pearls, and suggests that UV-Vis reflectance spectroscopy can be used in conjunction with other detection methods to identify pearls that have been heat treated to attain their yellow color.

This necklace is composed of 29 natural-color cultured pearls that range from 13.0 to 17.3 mm. Each of the natural-color cultured pearls in the earrings measures 13 × 14 mm. Courtesy of Tara & Sons, New York.

Photo by Harold & Erica Van Pelt—Photographers, Los Angeles, California.

Color separations for *Gems & Gemology* are by the LTC Group/Pacific Color, Carlsbad, California. Printing is by Fry Communications, Inc., Mechanicsburg, Pennsylvania.

© 2001 Gemological Institute of America All rights reserved. ISSN 0016-626X

The *G&G Twenty Year Index:* Two Decades of Evolution

It has been just over 20 years since *Gems & Gemology* was redesigned and the “new” format introduced. Looking at the dozens of covers of these issues, which dominate the walls of my office, I think of the incredible effort that went into each one—the thousands of hours that our authors and staff invested in every issue to do the research, write and refine the articles, and acquire the best illustrations. I also think of Harold and Erica Van Pelt, who photographed the vast majority of the cover images, as well as the many individuals who loaned valuable gemstones and jewelry for them to capture on film.

What am I proudest of? The quality of the information and the depth of knowledge each issue represents. Today, 20 years after the first issue of the redesigned *G&G* appeared, the articles in that issue—on peridot from Zabargad, cubic zirconia, and the detection of diamond simulants—are just as solid and useful as they were in April 1981. Certainly, since then there have been new peridot localities, changes in CZ, and more diamond simulants, but these articles continue to serve as a solid base for ongoing research on those topics.

In the past two decades, we have published over 5,500 pages of timely—and timeless—articles, Lab Notes, Gem News entries, Book Reviews, and Gemological Abstracts. This is truly a treasure chest of information. But how do you access it? How do you find what you need?

We are pleased to provide a solution: our *Twenty Year Index* (1981–2000). We have revised and updated the subject and author listings from our first 15 years, and added the annual indexes for the last five.

In the course of preparing this *Index*, we were all struck by the changes that were necessary since our first index was published in Winter 1981—changes not only in gemology, but also in geography and technology, many of them interrelated.

For example, the most significant change to the geopolitical landscape since the Spring 1981 issue has been the breakup of the Soviet Union. For our industry, however, this change has been more profound than the simple replacement of names on a map. With the new socioeconomic climate in this region has come an influx of natural gem materials onto the world market—most notably from the release of diamonds that were in the government stockpile, but also from renewed mining activity for such classic gems as demantoid garnets. There also has been an unprecedented impact on the availability of synthetic gem materials—new synthetic rubies, sapphires, emeralds, and quartz varieties, to name but a few. Russian high

pressure/high temperature (HPHT) presses are now synthesizing diamonds in virtually every color.

In other regions, names that were unknown to most of us only five years ago are now part of the gemological parlance—Tunduru in Tanzania, Ilakaka in Madagascar, Ekati in Canada. The availability of these significant new deposits of sapphires, rubies, and diamonds has shifted the balance of supply and demand. At the same time, it has presented greater challenges to gemologists in identifying sources and treatments.

Scientific advances in the U.S. and elsewhere also have brought us synthetic moissanite, the first diamond simulant to match the thermal properties of diamond. Whereas there was almost nothing written on diamond treatments in the 1980s, articles on diamonds that have been fracture filled or HPHT processed are prominent in the current index. Our first index simply referred to “spectroscopy.” Today, there are entries for more than 10 different types of spectroscopy. Laser Raman microspectrometry—which we first reported on only three years ago—is now used routinely in major gem labs around the world to identify inclusions and gem materials, as well as to recognize HPHT annealing in diamonds.

For this veteran of two decades of *G&G*, the Author Index offered a distinct pleasure as I was reminded of those who have contributed so much to the journal. “Godfathers” of gemological research such as Robert Crowningshield, Edward Gübelin, Richard T. Liddicoat, and Kurt Nassau were joined by an impressive group of new researchers such as Emmanuel Fritsch, Henry Hänni, Bob Kammerling, Bob Kane, John Koivula, Shane McClure, Tom Moses, Ken Scarratt, Karl Schmetzer, and James Shigley, among many others.

We hope that you too will enjoy using the index and find it a valuable reference tool. Explore the thousands of entries to learn what you *need* to know to stay abreast of the rapidly evolving world of gemology.



Alice S. Keller
Editor
akeller@gia.edu

Note: See the ad on page 159 of this issue to purchase a printed copy of the Gems & Gemology Twenty Year Index, or access it free of charge by visiting us online at www.gia.edu/gandg.



THE CURRENT STATUS OF CHINESE FRESHWATER CULTURED PEARLS

By Shigeru Akamatsu, Li Tajima Zansheng,
Thomas M. Moses, and Kenneth Scarratt

Chinese freshwater cultured pearls (FWCPs) are assuming a growing role at major gem and jewelry fairs, and in the market at large. Yet, it is difficult to obtain hard information on such topics as quantities produced, in what qualities, and the culturing techniques used because pearl culturing in China covers such a broad area, with thousands of individual farms, and a variety of culturing techniques are used. This article reports on recent visits by two of the authors (SA and LTZ) to Chinese pearl farms in Hanzhou Province to investigate the latest pearl-culturing techniques being used there, both in tissue nucleation and, much less commonly, bead (typically shell but also wax) nucleation. With improved techniques, using younger *Hyriopsis Cumingi* mussels, pearl culturers are producing freshwater cultured pearls in a variety of attractive colors that are larger, rounder, and with better luster. Tissue-nucleated FWCPs can be separated from natural and bead-nucleated cultured pearls with X-radiography.

The popularity of Chinese freshwater cultured pearls (FWCPs) has risen dramatically in the world's markets. The unique characteristics of the Chinese FWCP—in terms of size, shape, and color—have been key to this popularity (figure 1). Chinese FWCPs are available in sizes ranging from 2 mm to over 10 mm; in an interesting variety of shapes such as round, oval, drop, button, and baroque; and in rich colors such as orange and purple, often with a metallic luster. The vast majority of these Chinese FWCPs are nucleated by mantle tissue only, although some nucleation with spherical beads has taken place (Bosshart et al., 1993; "China producing nucleated rounds," 1995; Matlins, 1999; "China starts...," 2000; Scarratt et al., 2000). This makes them distinct from the overwhelming majority of cultured pearls from other localities, which are bead nucleated. Despite the growing popularity of Chinese FWCPs, details concerning their history, culturing areas, production figures, culturing techniques, and the characteristics of the pearls themselves are not widely known. In response to the growing

demand for information, two of the authors (SA and LTZ) visited six FWCP farms and one nucleus manufacturer in China's Zhejiang district; they also examined hundreds of Chinese FWCPs. The trip was made from July 25 to 29, 2000; information in this article has been confirmed and updated since then based on the second author's monthly trips to the pearl-farming areas to visit his pearl factory in Zhuji City, as well as to purchase freshwater cultured pearls for export. In addition, the first author has visited Chinese freshwater pearl-culturing areas several times during the past two years. This article reports on the current status of the Chinese freshwater cultured pearl, both the various culturing techniques used and the cultured pearls themselves, updating (and superseding) the pearl-culturing information in Scarratt et al. (2000).

See end of article for About the Authors information and Acknowledgments.
GEMS & GEMOLOGY, Vol. 37, No. 2, pp. 96–113
© 2001 Gemological Institute of America



Figure 1. Chinese freshwater cultured pearls occur in a variety of attractive shapes and colors, as well as in sizes over 10 mm. The potato-shaped Chinese FWCPs in the strand on the left range from 9.3×11.3 mm to 10.6×12.7 mm. The near-round Chinese FWCPs on the right are approximately 9–10 mm. Photo © Harold & Erica Van Pelt.

HISTORY

The culturing of freshwater pearls was widespread in China by the 13th century. Tiny figures of Buddha formed of lead were cemented onto the nacreous interior of the shell produced by the freshwater mussel *Cristaria plicata* (zhou wen guan bang in Chinese). Over time, the mollusk coated the lead figures with nacre, and the blister pearls thus cultured were used as temple decorations or amulets (Ward, 1985; Webster, 1994). Even now, this culturing technique survives, although the images are larger and nucleated with wax rather than lead (figure 2). Today, images of Buddha, flowers, birds, animals, and other forms are molded with wax and inserted into the mussels. A similar technique is used to create the mabé-type hemispheric composite cultured blister pearls in white- and black-lipped pearl oysters, as well as in abalone (Wentzell, 1998).

Freshwater pearl culturing was attempted in Japan around 1910, but success was not achieved until 1924, when growers changed from the “Karasu” mussel (*C. plicata*) to the “Ikecho” mussel (*Hyriopsis schlegeli*). Following this success, commercial freshwater pearl culturing began in Japan in 1928. A bead-nucleating technique was first adopted, but growers eventually recognized that tissue nucleation produced better results. In 1946, freshwater-pearl farmers switched to tissue

nucleation, creating unique freshwater cultured pearls. Since then, Japanese FWCPs have been highly prized as “Biwas” (named after Lake Biwa,

Figure 2. The culturing of freshwater blister pearls was widespread in China by the 13th century. Tiny figures of Buddha were cemented onto the inner shell of freshwater mussels (*Cristaria plicata*), where they were coated with nacre. The same culturing technique survives today. Instead of tiny lead figures, larger wax images are commonly used to produce a variety of forms, although Buddha (as seen in this 8.3×10.8 cm shell) is still popular. Photo by Shigeru Akamatsu.





Figure 3. Most of the Chinese FWCPs cultivated with *Cristaria plicata* were of low quality: irregular shaped with many wrinkles on their surface (hence called “Rice Krispies”; here, 5 × 8 mm to 9 × 14 mm, produced in 1976). These pearls first appeared on the market in the late 1960s and early 1970s, with 600 grams imported into Japan in 1971. The quantity increased dramatically over the next several years (with Japanese imports of 49 tons in 1984), but the boom had faded by the late 1980s. Photo by Maha Tannous.

Figure 4. Chinese pearl farmers greatly improved the quality of their product in the 1990s by changing the mussel species from *Cristaria plicata* to *H. Cumingi*, the Chinese “triangle” mussel. With the use of *H. Cumingi* both as donor of the mantle tissue and for culturing, they produced larger cultured pearls with a smoother surface, rounder shape, and better color and luster. In particular, the color and luster of the mother-of-pearl in the tissue-donor mussel has a strong influence on the color and luster of the final cultured pearl; notice the differences among these four mussels, all of which were used to provide mantle tissue nuclei. Although earlier culturing with *H. Cumingi* was done using 2–2.5 year old mussels, these one-year old mussels are typical of the age at which *H. Cumingi* are nucleated today. Photo by Shigeru Akamatsu.



where most were grown). Over time, improvements in the culturing technique produced more pearls of better quality, and the Japanese freshwater pearl culturing industry flourished. Pearl culturing at Lake Kasumigaura began in 1962, and in 1980 production reached a peak of 6.3 tons. Production began to decline because of water contamination and the high mortality of the mussels (Toyama, 1991). By 1998, production of Japanese freshwater cultured pearls had dropped to 214 kg, only 3.4% of the peak in 1980 (“Statistics of fishery and cultivation,” 2000).

It was in the late 1960s and early 1970s that China started full-scale FWCP production, and low-quality irregular-shaped cultured pearls with wrinkles on their surface (commonly known as “Rice Krispie” pearls) appeared in the market (Hiratsuka, 1985; figure 3). According to trade statistics published by the Japanese Ministry of Finance, in 1971 Japan imported only 600 grams of this material. Over the next 13 years, however, these imports increased dramatically: They reached 7.5 tons in 1978, 34 tons in 1983, and over 49 tons in 1984. Most were not consumed by the Japanese market, but instead were exported to Germany, Switzerland, Hong Kong, the Middle East, and the U.S. by Japanese distributors (Chinese FWCPs accounted for more than half the pearls exported from Japan in 1984). In the late 1980s, however, the demand for such low-quality pearls quickly died down, and the Chinese FWCP almost disappeared from the world market.

In the 1990s, however, Chinese FWCPs reappeared, with their quality remarkably improved (“China starts pearling revolution,” 2000). Culturers had changed the species of mussel from *C. plicata* to *Hyriopsis cumingi*, which is generally called the “triangle mussel” (*san jiao* or *san jiao bang* in Chinese) because of its shape (figure 4; Fukushima, 1991). The triangle mussel inhabits wide areas along the Chang Jiang (Yangtze) River. Using the new mussel, growers started to cultivate 3–4 mm pearls with a smooth surface. Although some of these Chinese FWCPs were near-round, more often the commercial product had a bulbous oval “potato” shape (again, see figure 1). Over the last decade, quality continued to improve. Chinese cultivators now produce FWCPs in sizes from 2 mm to over 10 mm, in shapes from extreme baroque to perfect round, and in colors from white to pastel orange and purple, often with a metallic luster.

CULTURING AREAS AND PRODUCTION AMOUNT

The culturing region for Chinese FWCPs extends over wide areas along the Chang Jiang (also known as the Yangtze) River (figure 5). The provinces of Jiangsu, Zhejiang, Anhui, Fujian, Hunan, and Jiangxi are the main culturing areas, with Jiangsu and Zhejiang accounting for nearly 70% of the total FWCP production (He Xiao Fa, pers. comm., August 2000).

It is generally thought that pearls cultured in southern farms grow faster, coinciding with the rapid growth of the mussel. By contrast, pearls cultured in northern farms grow more slowly, but their compact nacre gives them a better luster. For this reason, some farmers who own both northern and southern farms initially cultivate pearls in the southern farms to accelerate nacre growth, then move the mussels to northern farms one year before harvest to improve the luster. In addition, northern farmers often buy nucleated mussels from southern cultivators. According to several pearl culturers in the cities of Zhuji and Shaoxing, transferring mussels from one farm to another during the pearl growth period (which may take up to six years) is not uncommon in China.

No accurate production figures exist for Chinese FWCPs. Two major culturers, He Xiao Fa of Shanxiahua Pearl Co. Ltd. and Ruan Tiejun of Fuyuan Pearl Jewelry Co. Ltd., estimate that annual production is currently about 1,000 tons. Because there are several thousand pearl farms, many of which are very small, it is impossible to give an accurate count. The farms range from major operations with over one million mussels, to tiny roadside swamps diverted from rice paddy fields that contain tens of thousands of mussels (see, e.g., figure 6). The mussels are suspended in nets (each typically containing two to three mussels; figure 7) from buoys that are often made of Styrofoam or recycled plastic bottles.

RECENT DEVELOPMENTS IN TISSUE NUCLEATION

From observations made during our frequent visits, and from conversations with several leading pearl farmers, we confirmed that the vast majority of freshwater cultured pearls produced in China today are, as stated in Scarratt et al. (2000), mantle-tissue nucleated. As the recent improvement in quality demonstrates, the growth techniques used to create the Chinese product have changed. Some of the changes can be counted as major technical improvements.



Figure 5. Freshwater pearl culturing areas extend widely along the Chang Jiang (Yangtze) River, including the provinces of Jiangsu, Zhejiang, Anhui, Fujian, Hunan, and Jiangxi. Mussels that have been tissue nucleated are not always cultivated in a single farm for the entire culturing process. Often they are transferred to other farms in different provinces, where cultivation continues.

New Mussel Species Used for Culturing. As noted above and in Scarratt et al. (2000), Chinese pearl cultivators have changed from the *C. plicata* mussel to the *H. cumingi* ("triangle") mussel. *H. cumingi* is a large bivalve of the same genus as the *H. schlegeli* used for pearl cultivation in Japan's Lake Biwa. Triangle mussels can produce attractive FWCPs with a smooth surface. With the introduction of hatchery techniques to propagate the *H. Cumingi*, mass production of mussels has become possible and enormous amounts are now used for pearl culturing.



Figure 6. In China, the number of farms culturing freshwater pearls is too large to be counted accurately. They vary in size from large lakes (left) to small farms converted from rice paddy fields (right). Note the soil piled around the paddy field to keep the water deep enough (1.5 m) for pearl culturing. Photos by Shigeru Akamatsu (left) and Li Tajima Zansheng (right).

A Longer Culturing Period. In the past, it was common for growers to perform tissue nucleation on two-and-a-half-year-old mussels, cultivate them for two to three years thereafter, and harvest 4–7 mm pearls (see, e.g., Jobbins and Scarratt, 1990). In recent years, however, some growers have been operating on significantly younger mussels, approximately one to one-and-a-half years old (figure 8, right), and cultivating them for four to six years. By extending the period between insertion of the tissue nuclei and the harvest, they have succeeded in producing commercial quantities of FWCPs larger than 8 mm. A one-year-old mussel has a small shell, one valve of which weighs only 10 grams (average dimensions: 7.2 × 4.3 cm) at the time of nucleation. That same valve will attain a shell weight at harvest after

five years of 260 grams (up to 16.4 × 10.5 cm), more than 25 times its starting weight (figure 8, left). The pearls grow as the mussels grow, but the rate of growth is not always proportional.

Even though the cultivation period from nucleation to harvest is the same for any given mussel, the growth rate of the many pearls nucleated in that mussel is not the same. Consequently, FWCPs of various sizes are harvested from a single mussel (figure 9). Table 1 lists the different sizes of FWCPs removed from a sample harvest of four mussels that were cultivated for 4.5 years in a farm in Shaoxing.

Figure 7. During pearl cultivation, two to three mussels typically are put in a net and suspended in the water from Styrofoam buoys or recycled plastic bottles. Photo by Shigeru Akamatsu.



Figure 8. A one-year-old “triangle” mussel at the time of tissue nucleation is very small (right)—an average of 7.2 × 4.3 cm, with an approximate shell weight (one valve) of 10 grams. A six-year-old *H. cumingi* mussel at the time of harvest (left) after five years of cultivation is very large—up to 16.4 × 10.5 cm, with a single valve now 260 grams in weight. Photo by Li Tajima Zansheng.



These results also indicate that cultivation periods of 4.5 years can produce FWCP sizes of over 9 mm. Note that these mussels were older and larger when the nuclei were inserted than is currently practiced

Improvement in the Mantle Tissue Nucleus. In earlier freshwater pearl culturing, a common technique was to cut a 2 × 2 mm piece of tissue from the mantle of a 2.5-year-old mussel, fold it, and then insert it into a pocket made in the mantle lobe of a host mussel (Jobbins and Scarratt, 1990). Because this piece of tissue was too thick to be worked into a round shape, most of the FWCPs produced had shapes such as rice, oval, and baroque. Recently, pearl farmers have changed the nature of the mantle-tissue nuclei. Instead of taking the tissue from a 2.5-year-old mussel, growers now use a one-year-old (*H. cumingi*) mussel for this part of the procedure. When a piece of tissue is removed from such a young mussel, it is thin enough to be rolled into a round ball. So the culturer now cuts a larger (but thinner) 4 × 4 mm piece of mantle tissue (figure 10), and makes it as round as possible by rolling it before nucleation (figure 11).

Improvements in the Nucleation Technique. From their experience, pearl culturers identified that the posterior mantle lobe of the mussel, where the mother-of-pearl has the desired color and luster, is the key location to produce a better-quality pearl with fine color and luster (again, see figure 4). So they started to cut pieces of tissue from the posterior part of the sacrificed “donor” mussel and then placed them into pockets in the same posterior mantle lobes of the host mussel (figure 12). With this new technique,



Figure 9. All the Chinese FWCPs in this photo were tissue nucleated and harvested from both valves of one mussel after 4.5 years. Even though the culturing conditions were the same, the resulting FWCPs range from 5 to 9 mm. Photo by Shigeru Akamatsu.

pearl culturers are improving the color and luster of their FWCPs. Figure 13, taken in April 2001, shows a group of technicians performing different stages of the pearl nucleation technique at this pearl-processing operation in a suburb of Zhuji City.

Another improvement is the reduction in the number of tissue pieces used to nucleate a single mussel. In the past, when cultivators used relatively large, 2.5-year-old mussels to begin the process, about 20 pieces usually were inserted in each mantle lobe of the bivalve—for a total of about 40 pieces in a single mussel (Farn, 1986; Scarratt et al., 2000). Now, some growers typically insert 14 or fewer pieces of tissue in each mantle lobe of a one-year-old mussel—for a total of 28 or fewer in each mussel (figure 14).

TABLE 1. Freshwater cultured pearls produced from four mussels harvested in Shaoxing after cultivation for 4.5 years.^a

Size (mm)	Mussel 1		Mussel 2		Mussel 3		Mussel 4	
	No. of FWCPs	% of total	No. of FWCPs	% of total	No. of FWCPs	% of total	No. of FWCPs	% of total
4	0	0	1	2.9	2	3.8	0	0
5	4	9.5	5	14.3	20	37.7	1	3.0
6	12	28.6	13	37.1	21	39.6	8	24.2
7	13	31.0	12	34.3	6	11.3	16	48.5
8	10	23.8	3	8.6	3	5.7	8	24.2
9	3	7.1	1	2.9	1	1.9	0	0
Total	42		35		53		33	

^aNote that these mussels were older when they were nucleated, and had more nuclei inserted, than pearl farmers now prefer.

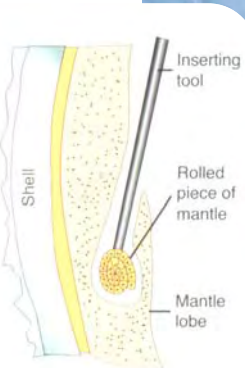
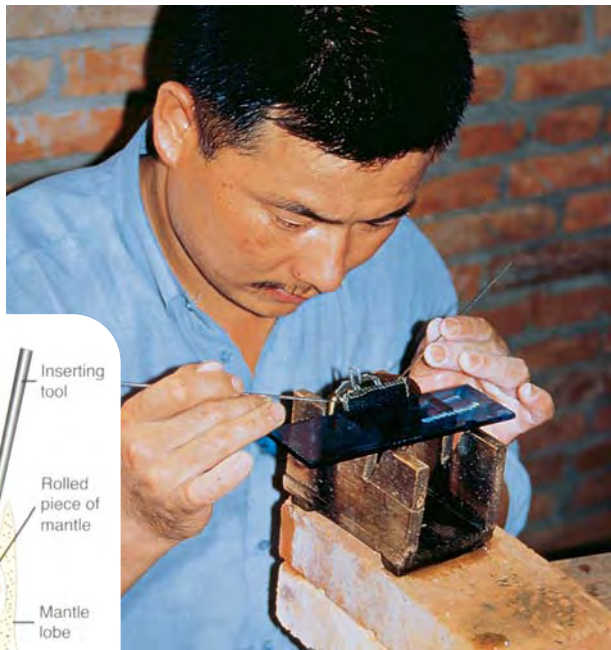


Figure 10. Using a knife, the technician cuts a piece approximately 4×4 mm from a strip of tissue that was removed from the mantle lobe of an H. Cumingi mussel of about the same age as the one-year-old H. Cumingi into which it will be inserted. Photo by Shigeru Akamatsu.



Figure 11. Just before nucleation, the thin pieces of mantle tissue are rolled as round as possible. Because the piece of mantle tissue is so thin, it can be rolled into a round ball more efficiently than the thicker (2×2 mm) pieces of tissue that were typically used in the past. Photo by Shigeru Akamatsu.

Figure 12. The operator places a one-year-old mussel on a fixing stand and opens the shell with care, making pockets in the posterior mantle lobes and inserting rolled pieces of mantle into them, as illustrated in the diagram (inset). A skilled technician can operate on 120 mussels a day. Photo by Shigeru Akamatsu.



Movement of Mussels Among Different Farms. We observed not only that culturers sold the live, operated mussels for further growth in the farm of another producer, but also that as they recognized deficiencies or changes in the environments of their farms, they often moved their own mussels to more suitable farms. Culturers also have found that the change in farms places the mussels under a type of “stress” that activates their respiration so that they produce more carbon dioxide (Koji Wada, pers. comm., 2001). The carbon dioxide converts to carbonate ions that combine with the calcium ions to form more calcium carbonate crystals. This improves the nacre growth, thus promoting good luster and color, as well as larger pearls.

FWCP CULTIVATION WITH SOLID NUCLEI

Although, as noted above, the vast majority of Chinese FWCPs currently are tissue nucleated, various methods to culture the FWCP by inserting a solid bead nucleus are being practiced (“China producing nucleated rounds,” 1995). Use of a bead nucleus is still being done on a limited scale only, because of the higher cost of production and the inferior quality of the pearls produced. According to

Chinese pearl-culturing textbooks (Li and Zhang, 1997; Li, 1997), the main methods used to bead nucleate Chinese FWCPs are as described below.

Insertion of Bead Nuclei into Mantle Pockets. The Chinese textbooks cited above report that pockets are cut into the mantle lobes of large and healthy five- to eight-year-old *H. cumingi* mussels, and the same round shell beads typically used for saltwater pearl culturing are inserted together with pieces of tissue cut from the mantle of another *H. Cumingi* mussel (figure 15). The implantations typically take place from March through May and from September through November, but the latter period yields better results.

The spherical bead nucleus varies from less than 2 mm to over 8 mm, while the piece of mantle tissue usually is smaller than 2×2 mm. For the best product, the size of the piece of tissue must be consistent with the size of the bead nucleus. When the piece of tissue is too large relative to the bead, pearls with a poor shape, wrinkles, or blemishes commonly result. Conversely, according to the textbooks, if the piece of tissue is too small, it can easily separate from the nucleus, resulting in a tissue-nucleated FWCP and the possible expulsion of the bead. The solid nucleus normally is cut from the interior of a Chinese or American freshwater

Figure 14. Shown here is a one-year-old mussel just after a tissue-nucleating operation in July 2000. In accordance with the current practice of this cultivator, 14 pieces of mantle tissue were inserted into the posterior part of each of the two mantle lobes (to produce a total of 28 pearls). In recent years, fewer pieces of mantle tissue have been used to facilitate the production of larger FWCPs. Photo by Shigeru Akamatsu.



*Figure 13. Several technicians are simultaneously preparing the mantle tissue and inserting the pieces into the young *H. Cumingi* mussels at this pearl-processing operation in a suburb of Zhuji City. Photo by Li Tajima Zansheng.*

mussel (see “The Bead Nucleus” section below), but paraffin wax also is used by some pearl farmers.

When paraffin is used, typically spherical wax beads about 2 mm in diameter are inserted into a mussel (*H. cumingi*) to produce 5–7 mm FWCPs (figure 16). If these cultured pearls are heated when drilled, the liquefied paraffin will ooze out of the drill hole, leaving a small hollow core. Solvents such as bleaching reagents can easily enter such hollow FWCPs, facilitating this processing. Thus, the use of paraffin nuclei has a possible three-fold purpose: (1) produce round pearls, (2) lower the cost of the nucleus, and (3) facilitate processing after harvest.

Modified Direct (or “D”) Operation. This method is similar to that used in South Sea and Tahitian pearl cultivation, with the exception that (as noted above)

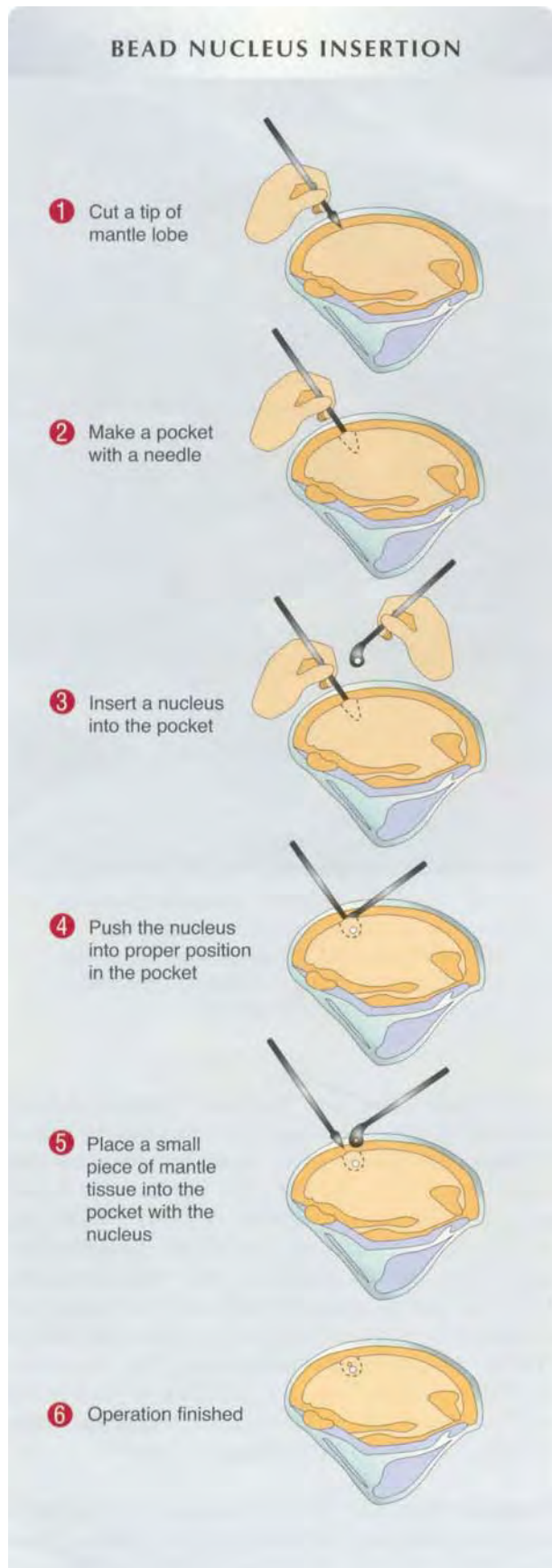


Figure 16. Recently, small paraffin balls also have been used as bead nuclei. When the cultured pearl is heated during drilling, the wax can melt out, leaving a small void that makes treatment easier. The cultured pearls shown here are 5–7 mm in diameter. Photo by Maha Tannous.

the bead nuclei are inserted into the mantle of the host mussel for (freshwater) Chinese cultured pearls, whereas for (saltwater) South Sea and Tahitian cultured pearls the bead is inserted into the gonad. After a mussel nucleated by the usual tissue-insertion operation is harvested, the technicians carefully cut out the FWCPs and then, rather than discarding the animal, they insert a shell bead nucleus into each pearl sac where a tissue-nucleated FWCP had grown (figure 17). With this procedure, there is no need to insert a piece of tissue with the bead nucleus because the pearl sac is already formed. Usually bead nuclei 5–6 mm in diameter are inserted into pearl sacs formed in the mantle lobes, and culturing continues for one to two years. Because at the time of the first harvest the mussel is already a little old, the color and luster of the bead-nucleated pearl produced by this second procedure typically will not be as good as that of the original tissue-nucleated FWCP (Li and Zhang, 1997; Li, 1997). Nevertheless, some attractive pearls have been cultured by this process (figure 18).

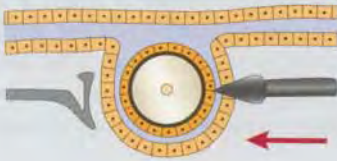
Figure 15. Bead nucleation of Chinese FWCPs usually involves insertion of the bead nucleus together with a piece of mantle tissue into a pocket made in the mantle lobe. Most commonly the beads are fashioned from the shell of a Chinese or American freshwater mussel. Adapted from Li (1997).

BEAD NUCLEATION by DIRECT OPERATION

- 1 Place a curved holder on the inner surface of the mantle next to the pearl sac



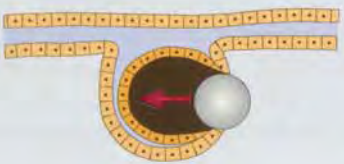
- 2 Cut open the tip of the pearl sac with a bladed needle



- 3 Remove the cultured pearl from the pearl sac by pushing with the curved holder



- 4 Insert a bead nucleus into the new vacant pearl sac and continue cultivation; there is no need for a piece of mantle to accompany the bead because the pearl sac is already formed



- 5 A bead-nucleated pearl is produced

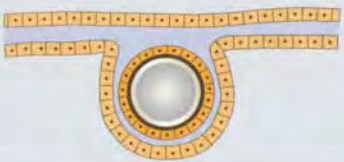


Figure 18. These Chinese FWCPs were bead nucleated by a modified “D” operation. The cross-section is 8 mm in diameter; the whole samples range from 7.5 mm in diameter to 9 × 10 mm. Photo by Maha Tannous.

Insertion of the Bead into the Mussel’s Body. To make FWCPs over 10 mm, relatively large nuclei (8 to 12 mm in diameter) are inserted together with pieces of tissue into the body of the *H. cumingi* mussel—as distinct from the mantle lobes in the bead-nucleation procedure described earlier—usually under the liver and/or the heart (figure 19). This is the same technique currently used to produce Kasumiga freshwater cultured pearls in Japan (Hänni, 2000).

The Bead Nucleus. Japan was once the only country that manufactured shell bead nuclei for pearl culturing, but now China also produces and supplies shell beads to Chinese pearl culturers. By visiting one of the nucleus manufacturers—Theng Xuan An of Penfei Youhezenzhu Co., Zhuji—two of the authors (SA and LTZ) learned about some of the Chinese nuclei. In China today, bead nuclei for saltwater as well as freshwater pearl culturing are fashioned

Figure 17. Some Chinese pearl farmers use a direct (or “D”) operation modified from a similar process used to produce saltwater cultured pearls in the South Seas and Tahiti. After removing the tissue-nucleated FWCP, the technician inserts a shell bead nucleus into the existing pearl sac to grow another pearl. Mantle tissue is not needed in this case because the pearl sac is already formed. Adapted from Li (1997).

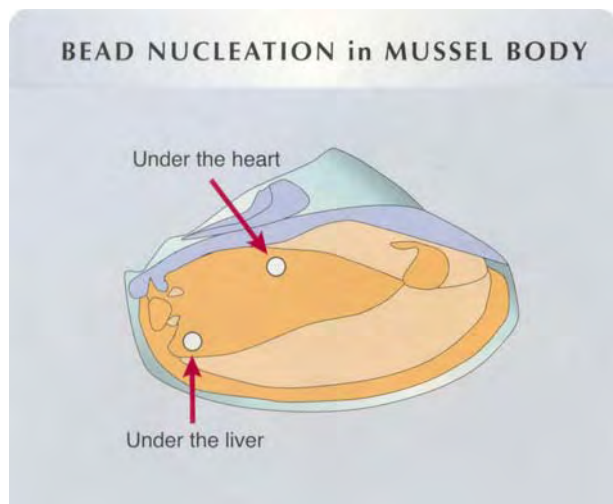


Figure 19. To produce FWCPs over 10 mm, some cultivators insert larger (8–12 mm diameter) but fewer (usually one or two) bead nuclei together with pieces of mantle tissue into the body of the mussel under the liver and/or the heart. Adapted from Li (1997).

from both Chinese and American freshwater mussel shells; Mr. Theng's factory uses the same triangle mussel in which the freshwater pearls are cultured as the shell for beads, too. We are aware that shells cut from other mussels, such as *Lamprotula leai*, are also used for bead cultivation in China (D. Fiske, pers. comm., 2001). To fashion the nuclei (typically 5–7 mm in diameter), Penfei Youhezenzhu Co. uses machines imported from

Figure 20. Commercial round Chinese FWCPs range from 2 mm to over 13 mm. The sizes of tissue-nucleated FWCPs are closely related to the culturing period: 2 mm FWCPs such as the one on the far left can be produced by a culturing period of less than two years, but the 13 mm FWCP on the far right typically requires more than six years. Note also the range of colors and the metallic luster in some of these samples. Photo by Li Tajima Zansheng.



Japan and the same procedure as is used in Japan. These beads are also exported to other pearl-producing countries such as Japan and Tahiti.

Reports in the trade literature have suggested that some bead nuclei are made by grinding tissue-nucleated FWCPs into a round shape (Matlins, 1999; Roskin, 2000). In our visits with a Chinese nucleus manufacturer and numerous pearl culturers, we found no evidence of such nuclei. Recently, one of the authors (SA) asked a Japanese nucleus manufacturer to fashion such nuclei from tissue-nucleated 10 mm "potato" FWCPs to examine the appearance and potential effectiveness of such a bead. By the usual shell-bead manufacturing procedure, the FWCPs were ground to round. The result was not satisfactory, because the nacre peeled unevenly during grinding to produce a poor sphere.

CHARACTERISTICS OF CHINESE FWCPs

Materials and Methods. As described in the introduction, Chinese FWCPs are distinctive in terms of size, shape, color, and luster. Their internal structure also is unique. To study these characteristics, two of the authors (SA and LTZ) examined approximately 500 sample Chinese FWCPs—ranging from 2 mm to 13 mm (figure 20)—that were selected from the stock (about 100 kg) of Stream Co. These are representative in color and luster of the better-quality cultured pearls being sold in China at this time. The stock was harvested from a few Zhuji and Shaoxing pearl farms in July 2000. The buyers at Stream Co. purchased all of these samples as tissue-nucleated FWCPs; only a few farms in these areas culture bead-nucleated FWCPs.

All of the pearls were examined visually by two of the authors (SA and LTZ). Approximately 50 tissue-nucleated FWCPs were cut in half so that we could examine the internal structure with a loupe.

Structure. Because the vast majority of Chinese FWCPs are tissue nucleated, solid nuclei are not normally seen. Most of the sawn tissue-nucleated FWCP sections showed traces of the tissue nucleus at the center, although in some samples they were difficult to discern (figure 21). For this reason, as discussed in depth in Scarratt et al. (2000), the separation of natural from tissue-nucleated cultured pearls is best done with X-radiography (see Appendix A). The cross-sections of the more strongly colored samples also showed distinct concentric color bands



Figure 21. The evidence of tissue nucleation in Chinese FWCPs can be very subtle. In most of these four tissue-nucleated samples, the nucleus can be seen as a fine line toward the center of the sphere. Because such sawn sections are a highly destructive means of identifying the type of nucleus, and even they may not reveal the necessary evidence (if, for example, the tissue nucleus is slightly off-center), X-radiography is the best method to separate tissue-nucleated cultured pearls from their natural or bead-nucleated counterparts. During cultivation, growth rings of different colors form in some FWCPs. Photo by Shigeru Akamatsu.

between nacreous layers. These bands seem to be related to the same mechanism that produces the various colors observed in the shell nacre of the host *H. cumingi* mussel (figure 22).

Shape. In the past, Chinese FWCPs were typically elongated and wrinkled or pitted (again, see figure 3). Although most Chinese FWCPs continue to be oval or other shapes, the improvements in culturing techniques described above (e.g., the use of younger, thinner pieces of mantle tissue that can be rolled into a ball) have brought a greater number of round and near-round FWCPs to the marketplace (figure 23).

Today, the most popular shapes are round, near-round, oval, button, drop, semi-baroque, and others such as sticks and crosses. This wide variety of shapes is characteristic of FWCPs from sources around the world. The group we examined were specifically selected to be round to near round.

Color. Chinese FWCPs occur in three main hues—white, orange, and purple—all of which were represented in our sample. Combinations of tone and saturation yield a broad range of color appearances (figure 24) from which very attractive and distinc-



Figure 22. When the periostracum (the outer layer of the shell) of the triangle mussel *H. Cumingi* is removed, the beautiful color and luster of the nacre are revealed. Insertion of mantle tissue taken from the posterior of the mussel into the posterior of the live mussel is the key to producing better color and luster. Photo by Shigeru Akamatsu.

tive jewelry has been fashioned (figure 25). Pearl dealers have described some Chinese FWCPs as “wine,” “cognac,” “lavender” (figure 26), “blueberry,” and “apricot.” This color range is believed to be associated with: (1) the color of the mother-of-pearl in the donor mussel from which the piece of mantle tissue was taken, (2) the environmental conditions of the culturing farm, and/or (3) the age

Figure 23. The new tissue-nucleation techniques being used in China have led to a greater number of round freshwater cultured pearls in the marketplace. Photo by Shigeru Akamatsu.





Figure 24. Chinese FWCPs occur in different tones, saturations, and combinations of white, orange, and purple. Photo by Li Tajima Zansheng.

Figure 25. This contemporary jewelry takes advantage of the combination of unusual colors offered by Chinese FWCPs. Jewelry courtesy of Stream Co.; photo © A.Takagi/Bexem Co. Ltd.



of the host mussel. The first of these probably has the greatest effect on the color of an individual FWCP (Li and Zhang, 1997).

Luster. Our sample Chinese FWCPs demonstrated a wide range of luster, from dull and chalky to metallic. On the basis of on-site investigations and interviews with several cultivators in Shaoxing, two of the authors (SA and LTZ) concluded that the following four factors can influence the luster of Chinese FWCPs:

- The nature of the piece of mantle tissue used
- The location in the mussel where the tissue piece is inserted
- The age of the mussel that has been nucleated
- The environmental conditions of the culturing farm

As an example of this last item, experienced cultivators know that the water quality at Shaoxing pearl farms is different from that of pearl farms along the Chang Jiang River.

Pearl farmers carefully choose mussels with shell nacre that shows good luster as the source of the mantle tissue to be used in the nucleation process. As noted above, to achieve the best luster (and color), the technicians insert the pieces of tissue into the posterior of the mantle lobe. This region of the mantle also experiences the most growth. A young mussel bears lustrous pearls, but as it becomes older (more than five or six years), the luster of the pearl gradually decreases as its size increases. Pearl culturers claim that the water quality (probably the difference in mineral content) of their farms is the key to producing pearls with a shiny metallic luster, but that regardless of the farm the metallic luster will disappear if the cultured pearl is left in a mussel that is more than five or six years old.

In addition to these four factors, the mussel species itself will affect pearl luster. Pearls with very fine luster are produced when the pieces of mantle tissue are cut from the mantle of a *C. plicata* and inserted into the mantle of an *H. cumingi*. However, almost all of the pearls produced with this combination have heavy surface wrinkles.

CONCLUSION

Annual production of freshwater cultured pearls in China is estimated at about 1,000 tons, with approximately 650 tons usable in the jewelry trade. However, the present expansion of cultivation indicates a sub-

stantial increase within the next two or three years. Although more high-quality FWCPs are being produced as cultivation methods improve, most of the Chinese FWCPs are still of moderate to low quality.

The improvements in size, shape, surface condition, luster, and color seen in recent years are the result of many advances in the culturing materials and techniques used. These include changing mussel species from *C. plicata* to *H. cumingi*, nucleation of younger (one-year-old) mussels, improvement in the tissue nucleation (rolling a thinner piece of mantle into a round shape and inserting fewer pieces into the host mussel), a relatively longer culturing period, and a frequent change of culturing farms.

Bead-nucleation techniques also are being developed, but our experience indicates that bead-nucleated FWCPs continue to represent a very small percentage of the total production in China. This appears to be due to the technical difficulties and culturing costs involved. For example, bead nucleation doubles the labor required because both a bead and a piece of tissue must be inserted into the pocket, whereas tissue nucleation requires only a single action to insert the piece of tissue. In any event, as discussed in Appendix A, the separation of bead-nucleated from tissue-nucleated cultured pearls, and of the tissue-nucleated product from its natural counterparts, is readily accomplished with contemporary X-radiography techniques.

While this information represents the study of several pearl operations and hundreds of FWCPs, the fact that China has many thousands of pearl farms and produces tons of cultured pearls annually makes it impossible to provide a complete story. We believe, however, that the information we have provided is representative of the Chinese product seen in the market today and that the new nucleation and culturing techniques promise an even better product in the future.



Figure 26. Lavender is one of the distinctive colors in which Chinese FWCPs occur. The rounds in the strand are approximately 9.5 mm in diameter; the cultured pearl in the ring is 12.3 mm. Photo © Harold & Erica Van Pelt.

ABOUT THE AUTHORS

Mr. Akamatsu is former manager of the Pearl Research Laboratory and currently general manager of the Sales Promotion Department, K. Mikimoto & Co. Ltd., Tokyo, Japan. Mr. Li, who started his Chinese freshwater cultured pearl business in 1985, is president of Stream Co., Tokyo and Hong Kong; in 1998, he established a pearl-processing operation in Zhuji City, China. Mr. Scaratt is laboratory director at the AGTA Gemological Testing Center, New York; and Mr. Moses is vice president of Identification Services at the GIA Gem Trade Laboratory, New York.

ACKNOWLEDGMENTS

The authors express heart-felt appreciation to He Xiao Fa, director of Shanxiahu Pearl Co. Ltd. in Zhuji City, and Lou Yong Qi, director of Echolou Pearl Co. in Zhuji City, for giving them the opportunity to visit several pearl farms, and for providing numerous FWCP samples. The authors also gratefully acknowledge Mikio Ibuki, executive manager of the Japan Pearl Exporters Association (JPEA), for supplying Kasumiga cultured pearls. Last, the authors thank Katsumi Isono, president of Miyake Nucleus Manufacturing Co. in Matsubara City, Osaka, for fashioning bead nuclei from tissue-nucleated "potato" FWCPs for the purposes of this research.

APPENDIX A: IDENTIFYING CHINESE FRESHWATER CULTURED PEARLS BY X-RADIOGRAPHY

Cultured pearls form a significant portion of all gem materials traded. Yet the one nondestructive method that can be used to identify the growth technique or separate cultured from natural pearls—X-radiography—is available only to a limited number of gemologists who have access to the necessary equipment. Nevertheless, it is important that all gemologists understand the principles behind X-radiography and its capabilities in pearl identification. While the general method and operating procedures have been published by, for example, Webster (1994) and Kennedy (1998), this box provides specific information regarding the use of X-radiography in the identification of freshwater cultured pearls (FWCPs) grown by a variety of techniques in China. The information is based on the experience of two of the authors (TMM and KS) with taking and interpreting tens of thousands of pearl X-radiographs over the last two decades, many of which were of Chinese FWCPs.

Pearl Structure. Both natural and cultured freshwater pearls are formed of concentric layers, of variable thickness, that are comprised of aragonite and/or calcite along with some organic matter. As the pearl grows, more organic matter may be accumulated during one period than another, as seen in figure A-1. Some pearls—natural or cultured by tissue nucleation—have a growth structure similar to that between points A and B in figure A-1, whereas others have one similar to that between points B and C throughout. Most Chinese freshwater cultured pearls (FWCPs) that are nucleated only with tissue also contain a characteristically shaped cavity near their center. If such samples are sawn adjacent to this cavity, it may reveal itself only as a fine line (figure A-2). For a more complete explanation of the growth structure of pearls, see chapter 22 of Webster (1994).

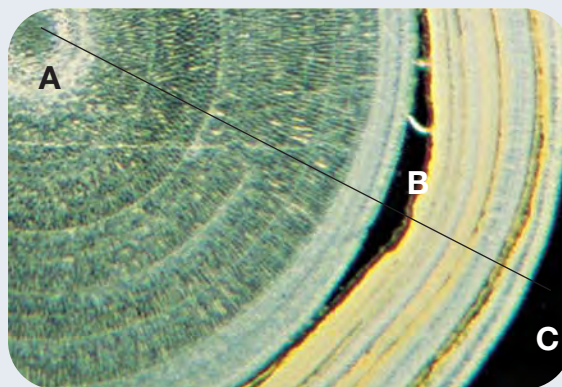
To better understand the identification criteria discussed below, it is important to note the less obvious organic layers between points B and C in figure A-1, as well as the obvious ones. Note also the concentric growth between A and B in figure A-1, and the structures in figure A-2.

X-radiography Equipment. For more than 70 years, X-radiography has formed the backbone of pearl identification. Fortunately for the industry, there are a number (albeit limited) of gemologists with extensive experience in producing and interpreting X-radiographs. Although pearl X-ray units have gone through many incarnations, today there are several industrial units that are well suited to perform the tasks required for Chinese FWCP identification.

While we recognize that the latest digital or similar X-radiography units give the user a degree of convenience, it is the experience of these authors (TMM and KS) that the identification of Chinese FWCPs requires a resolution that at this time is available only through the use of very fine-grain X-ray film—wet radiography. The instruments used by the authors are Faxitron models 43855B and 43856A. These air-cooled units are powered by normal electrical outlets, have variable kV and mA control, and offer an extended timed exposure capability. The distance between the X-ray tube target and the sample is adjusted by moving the shelving under the pearls.

Procedures. The samples should be placed in direct contact with a sheet of high-resolution fine-grain industrial X-ray film; the film and the as-yet-unidentified pearls are then placed in a position—and at a distance—that will allow all the samples to be contained within the X-ray beam (figure A-3). Next, depending first on the size of the pearls, X-rays are generated for a specifically timed exposure at predetermined kV and mA settings. Then, based on the internal structures observed in the resulting X-radiograph, the technician may increase or decrease the

Figure A-1. In this thin section of a natural freshwater pearl, the center of the pearl is located at the top left (A). Note the various stages of growth along the line A-B-C. Between A and B is an evenly deposited arrangement of concentric layers, inside of which are radially arranged crystals. At B the structure abruptly changes, with a large organically lined void that is followed by several yellow and dark, mostly organic, layers interspersed with the more crystalline (gray) layers toward the edge of the pearl (C).



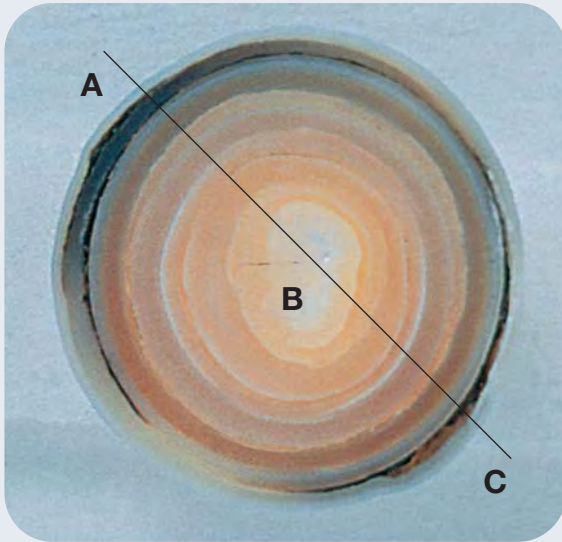


Figure A-2. In this sawn half of a known tissue-nucleated cultured pearl, the slight dark line in the center (at B) is the only visual evidence of the tissue implant. Note, however, as in figure A-1 the varying amounts of organic material (dark) associated with the concentric growth structures.

exposure times, target-to-pearl distances, and kV and mA settings.

All X-radiographs are normally examined at magnifications between 2× and 10× (hence the need for fine-grained film) using a variety of back-illumination techniques. The X-radiograph may show one or more of the following features, depending on the nature of the sample:

1. *If the sample was a coherent solid composed of aragonite or calcite, without any organic matter:* The image would be simply an opaque white disc against a black background. That is, the aragonite or calcite would have absorbed the X-rays and left the film immediately below it unexposed (white), whereas the remainder of the film would have been fully exposed and thus black when processed. This is how the shell bead portion of a bead-nucleated cultured pearl would look, and is not uncommon for a non-nacreous (e.g., conch) “pearl.”
2. *If the sample was aragonite or calcite with internal organic material or voids:* The image would reflect the difference in the ability of the X-rays to pass through the aragonite or calcite, the organic material, and any voids present. Organic layers and voids pass X-rays more readily than calcium carbonate does, so they reveal themselves on the processed X-ray film as dark gray to black lines or shapes set against the white background of the cal-

cium carbonate. If voids are present, the contrast between these and the calcium carbonate generally will be greater than that for organic material.

If one takes the more familiar example of a human bone contained within the flesh of the human body, a similar principle applies. The human bone absorbs the X-rays more than the flesh that surrounds it and thus stands out clearly as “white” against the gray to black areas that comprise the flesh (organic). In addition, any fractures or fissures in the bone (voids) will appear black on the processed film.

Once the initial observations have been completed, the technician takes additional X-radiographs, now optimized for the suspected type of pearl—natural, cultured (bead or tissue nucleated), etc.—being examined, in several different directions, to provide images that can be interpreted as characteristic of the sample in three dimensions.

The scattering of X-rays as they pass through and around a pearl may at times reduce the quality of the image. Two techniques that the authors have found to be successful in absorbing the scattered X-rays (and thus enhancing the image) are: (1) for necklaces, immersing the pearls in a scatter-reducing fluid; and (2) for single pearls, surrounding the sides of the sample with a thin layer of lead foil.

Characteristics of Tissue-Nucleated and Bead-Nucleated Chinese FWCPs. X-radiographs of tissue-nucleated FWCPs will show features that depend to some extent on when they were grown. “Rice Krispie” tissue-nucleated Chinese FWCPs grown in the 1970s typically have somewhat twisted internal organic structures and voids (figure A-4, left). X-radiographs of more recently grown tissue-nucleated Chinese FWCPs—with

Figure A-3. The samples (here, a baroque strand ranging from 12.0 × 9.15 to 15.20 × 11.15 mm) are placed on the film immediately below the X-ray beam in the Faxitron unit. Photo by E. Schrader.



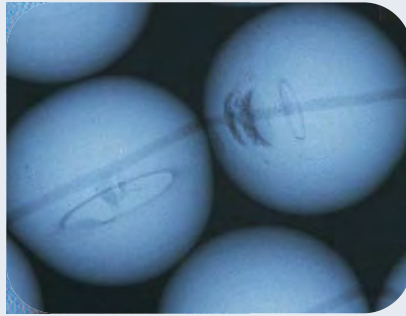
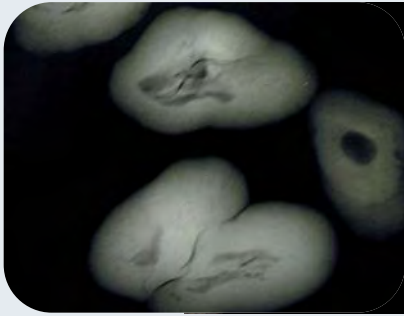


Figure A-4. The dark gray “twisted” structures shown on the left are typical of the tissue-nucleated Chinese FWCPs produced in the 1970s. In the X-radiograph on the right of more recent FWCPs, ovoids mark the original tissue implant.

their characteristic implant lines—were published by Scarratt et al. (2000; figure A-4, right). In both cases, the X-radiographs are totally unlike those of either natural pearls (figure A-5) or of cultured pearls produced from a shell bead nucleus.

The X-radiographs of shell bead-nucleated Chinese FWCPs resemble those of shell bead-nucleated saltwater cultured pearls (figure A-6). Centrally located beads with no internal growth structures are separated from the nacre overgrowth by a layer that is mostly organic. Any possible confusion with tissue-nucleated FWCPs caused by dark areas on the X-radiograph inside the area of the central bead would be dispelled by X-radiographs taken in other directions.

The X-radiographs of wax bead-nucleated Chinese FWCPs also show characteristic features (figure A-7). Each contains a nearly circular central area that is black or dark gray. Additional layers are defined by fine black concentric growth structures within the white crystalline areas of the Chinese FWCP (which are not visible in figure A-7). There are similarities between the X-radiographic struc-

tures seen in this type of Chinese FWCP and those sometimes observed in natural pearls. However, natural pearls differ from Chinese FWCPs in that they show additional structures within the central area.

The short descriptions given here about the equipment needed, procedures, and expected results must be supplemented by operator experience—the most important element.

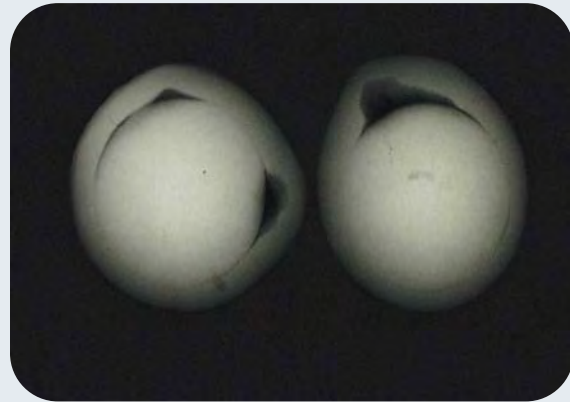


Figure A-6. This radiographic image of shell bead-nucleated Chinese freshwater cultured pearls is typical of the images seen for this product.

Figure A-5. Natural pearls typically do not show evidence of a nucleus, only the structures that indicate organic matter or voids. Note also the concentric rings throughout this pearl.

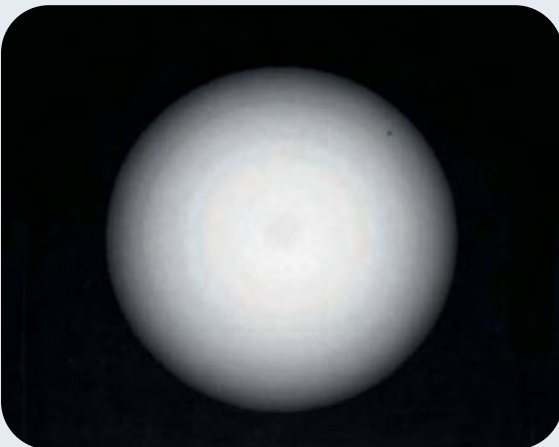
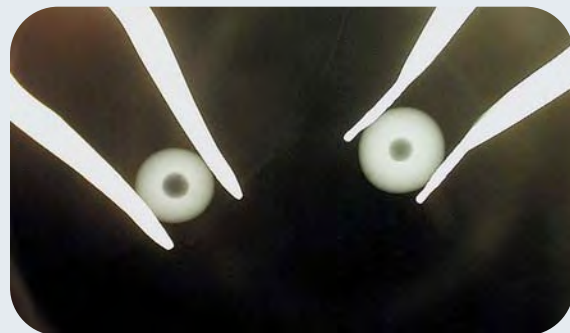



Figure A-7. Recently produced wax bead-nucleated Chinese FWCPs have the characteristic radiographic structures shown here.



REFERENCES

- Bosshart G., Ho H., Jobbins E.A., Scarratt K. (1993) Freshwater pearl cultivation in Vietnam. *Journal of Gemmology*, Vol. 23, No. 6, pp. 326–332.
- China producing nucleated rounds (1995) *Jewellery News Asia*, No. 129, pp. 56–58.
- China starts pearling revolution (2000) *Jewellery News Asia*, No. 186, p. 62.
- Farn A. (1986) *Pearls: Natural, Cultured and Imitation*. Butterworths, London, p. 76.
- Fukushima Y. (1991) The freshwater pearl in China. *Pearls of the World II*, Les Joyaux special edition, Shinsoshoku Co., Tokyo, pp. 127–134.
- Hänni H. (2000) Gem news: Freshwater cultured “Kasumiga pearls,” with Akoya cultured pearl nuclei. *Gems & Gemology*, Vol. 36, No. 2, pp. 167–168.
- Hiratsuka T. (1985) The Chinese freshwater pearl. *Pearls of the World*, Les Joyaux special edition, Shinsoshoku Co., Tokyo, pp. 95–100.
- Jobbins E.A., Scarratt K. (1990) Some aspects of pearl production with particular reference to cultivation at Yangxin, China. *Journal of Gemmology*, Vol. 22, No. 1, pp. 3–15.
- Kennedy S.J. (1998) Pearl identification. *Australian Gemmologist*, Vol. 20, No. 1, pp. 2–19.
- Li H.P., Zhang X.P. (1997) Chapter 4: Nucleating operation. In *Danshui Zenzhubang Yangyu* [Freshwater Pearl Mussel Cultivation], Science Technology Literature Press, Beijing, pp. 36–67 (in Chinese).
- Li S.R. (1997) Chapter 2: Nucleus Inserting Operation, 2—Bead nucleus inserting operation. In *Danshui Zenzhu Peiyu Jishu* [Freshwater pearl cultivation technique]. Jin Dun Press, Beijing, pp. 71–78 (in Chinese).
- Matlins A. (1999) Large Chinese freshwater cultured pearls. *Journal of the Accredited Gemologists Association*, Winter 99–00, pp. 1, 3, 5.
- Roskin G. (2000) Are freshwater Chinese pearls being misrepresented? *Jewelers' Circular Keystone*, Vol. 171, No. 3, pp. 36, 38.
- Scarratt K., Moses T., Akamatsu S. (2000) Characteristics of nuclei in Chinese freshwater cultured pearls. *Gems & Gemology*, Vol. 36, No. 2, pp. 100–102.
- Statistics of fishery and cultivation (2000) *Almanac of Fishery Agency*. Ministry of Agriculture, Forestry and Fisheries, Tokyo.
- Toyama T. (1991) Freshwater pearl—Status of, and future. *Pearls of the World II*, Les Joyaux special edition, Shinsoshoku Co., Tokyo, pp. 119–126.
- Ward F. (1985) Pearl. *National Geographic*, Vol. 168, No. 2, August, pp. 192–223.
- Webster R. (1994) *Gems—Their Sources, Descriptions and Identification*, 5th ed. Rev. by P.G. Read, Butterworth-Heinemann Ltd., Oxford, England, 1026 pp.
- Wentzell C.Y. (1998) Cultured abalone blister pearls from New Zealand. *Gems & Gemology*, Vol. 34, No. 3, pp. 184–200.



GEMS & GEMOLOGY

A wealth of information at your fingertips.

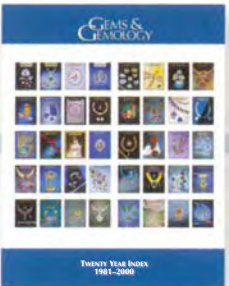
There's nothing like having what you need, when you need it. That's why no gemological reference library is complete without GEMS & GEMOLOGY. In addition to in-depth research and locality articles, every beautifully illustrated issue features unique sections like Lab Notes and Gem News. Taken together, they provide a depth and breadth of gemological information you simply cannot find anywhere else. Take advantage of this special offer and complete your back issues today!

1981-2000
FREE Twenty Year Index!

With any three years of back issues

ORDER TODAY!

Call Toll Free 800-421-7250 ext. 7142
or 760-603-4000, ext. 7142



(Please see the ad on page 129 of this issue for a list of topics covered in specific back issues, and please mention this offer when ordering.)

SPECTRAL REFLECTANCE AND FLUORESCENCE CHARACTERISTICS OF NATURAL-COLOR AND HEAT-TREATED “GOLDEN” SOUTH SEA CULTURED PEARLS

By Shane Elen

A comparison study was made between the yellow and white nacre of the gold-lipped *Pinctada maxima* oyster shell and 65 yellow cultured pearls, both natural and treated color, produced from this mollusk. The yellow nacre of this shell has a characteristic absorption feature in the UV region between 330 and 385 nm; the strength of this feature increases as the color becomes more saturated. White shell nacre fluoresces very light blue or very light yellow to long-wave UV radiation, whereas yellow shell nacre fluoresces greenish to brownish yellow or brown. Natural-color yellow cultured pearls from *P. maxima* exhibited absorption and fluorescence characteristics similar to those of the yellow shell nacre. In contrast, the absorption feature in the UV was either weak or absent in yellow cultured pearls reportedly produced by a method involving heat treatment, and their fluorescence was generally very light blue or light yellow.

The popularity of “golden” cultured pearls from the South Seas (figure 1) has increased steadily over the last 10 years (Vock, 1997; “Prices of golden...,” 2000). As demand for these cultured pearls has grown, treated-color “golden” cultured pearls have also entered the marketplace. A portion of the South Sea yellow cultured pearls harvested are well shaped with few blemishes but with less desirable color—either very light (Federman, 1995) or uneven. The most common methods used to produce or enhance yellow coloration in South Sea “golden” cultured pearls involve treatment with a chemical or an organic dye. The fact that so many different chemicals and dyes could be used for this purpose complicates a comprehensive study of these treatment methods. However, inorganic chemicals are routinely identified using EDXRF; and dyes, since they usually are applied after the pearls are drilled, generally are easy to identify with magnification.

The Ballerina Pearl Co. (New York City) developed a method in the early 1990s to treat these poorly colored South Sea cultured pearls to produce a more uniform and desirable yellow. These were

first marketed in 1993 with full disclosure that they were treated (Vock, 1997). Details of the proprietary process are not known, but it has been reported that the treatment, which is believed to be stable, is applied to undrilled cultured pearls and involves the use of heat without the application of dyes or bleaching (Vock, 1997). Inasmuch as the report did not exclude chemicals other than bleach, it is possible that chemicals also may be involved in the treatment. It is probable that other companies are treating “golden” pearls using a similar process.

The challenge for the gem and jewelry industry is to separate natural-color cultured pearls, of any color, from treated ones (Sheung, 1998). Although, as noted above, drilled treated cultured pearls generally can be distinguished from natural-color cultured pearls by microscopy (Hargett, 1989), undrilled cultured pearls—especially in the absence of obvious visual features—are much

See end of article for About the Authors information and Acknowledgments.
GEMS & GEMOLOGY, Vol. 37, No. 2, pp. 114–123
© 2001 Gemological Institute of America



Figure 1. These natural-color and heat-treated cultured pearls range from 12.5 to 13.6 mm; the natural-color cultured pearls are on the top right and bottom left. Note the area of “golden” nacre along the periphery of the white nacreous region in the gold-lipped *Pinctada maxima* shell (18.0 cm in diameter). Photo by Maha Tannous.

more difficult to identify. The present report compares heat-treated yellow cultured pearls to natural shell nacre and natural-color yellow cultured pearls from the *Pinctada maxima* to identify criteria that can be used to separate treated from natural-color material, especially when the samples are undrilled.

BACKGROUND

The gold-lipped *P. maxima* oyster has a characteristic yellow to “golden” nacre inside the shell along the periphery of the white nacreous region (Gervis and Sims, 1992, p. 4; again, see figure 1). Pearls produced from this oyster, either natural or cultured, are typically white, “silver,” or yellow (South Sea Pearl Consortium, 1996) and include so-called “golden” pearls.

The post-harvest color treatment of cultured pearls, of any color, falls into two categories: prior to drilling and after drilling. Heat treatment (Vock, 1997) and gamma irradiation (Ken-Tang Chow, 1963) may be performed pre- or post-drilling. As noted above, however, dyes and chemicals typically are used only after drilling (Komatsu, 1999), to facilitate their entry parallel to the nacre layers. Generally, such treatments affect the organic material (i.e., conchiolin) between the nacre layers; they have less influence on the crystalline nacre (Gauthier and Lasnier, 1990).

The most obvious indication of these treatments (with the exception of irradiation) is an unusual color concentration in the form of a colored layer (visible in the drill hole) or a colored spot or streak visible on the surface (Komatsu, 1999). Color from dyes or chemicals typically becomes concentrated in surface defects such as cracks, pits, or blemishes (Newman, 1999, p. 94). Dimples or protrusions in the nacre are particularly likely to exhibit concentrations of color. These areas are often more porous (as indicated by a cloudy or milky appearance prior to treatment), which allows the dye or chemical to become concentrated (T. Moses, pers. comm., 2000). These features sometimes are eye-visible, but usually they can be detected only with microscopy.

Typically, detection of a treated yellow color in undrilled cultured pearls relies on the presence of surface color concentrations. When such features are absent, however, identification is more of a challenge. Inasmuch as the Ballerina process is applied prior to drilling, this is the situation for yellow cultured pearls treated by this technique.

Due to the nature of the chemicals and dyes typically used in most post-drilling treatments, many color-treated natural and cultured pearls can be identified using X-ray fluorescence (XRF) or Raman spectrometry (see box A). However, the author did not find these techniques useful for the heat-treated “golden” pearls tested for this study. Thus, the pur-

BOX A: ADVANCED IDENTIFICATION OF COLOR TREATMENTS IN NATURAL AND CULTURED PEARLS

Advanced testing often can be used to identify color-treated cultured pearls. These techniques include X-ray fluorescence (XRF), Raman and luminescence spectrometry, and UV-Vis spectrophotometry. XRF is useful for detecting the presence of inorganic treatments such as silver salts (black) or iodine (yellow; figure A-1). In most cases, organic treatments and biological pigments cannot be detected by this method, but their presence can sometimes be determined using Raman spectrometry (figure A-2). UV-

Vis spectrophotometry frequently is used to identify the presence of chromophores responsible for natural coloring in Tahitian black cultured pearls, as indicated by an absorption at 700 nm (Komatsu and Akamatsu, 1978; figure A-3). Luminescence can verify the presence of porphyrins (Miyoshi et al., 1987) responsible for the reddish brown fluorescence observed in natural-color black cultured pearls originating from the *Pinctada margaritifera*, *Pteria sterna*, and *Pteria penguin* oysters (figure A-4).

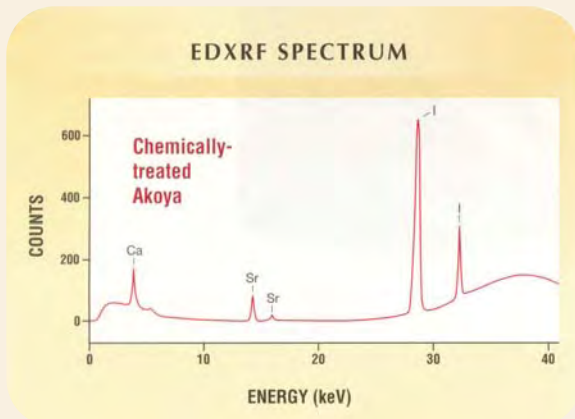


Figure A-1. The iodine (I) peaks in this energy-dispersive X-ray fluorescence (EDXRF) spectrum of a yellow Akoya cultured pearl indicate chemical treatment.

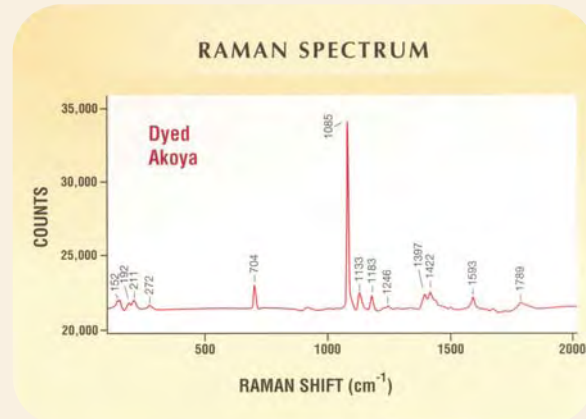


Figure A-2. In this Raman spectrum of an orangy yellow Akoya cultured pearl, the series of peaks above 1085 cm⁻¹ indicate treatment with an organic dye.

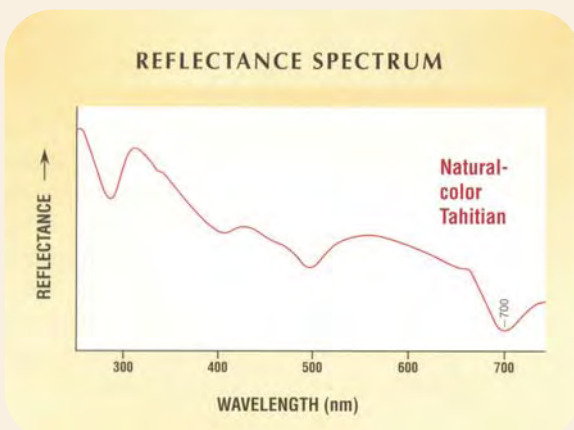


Figure A-3. In a UV-Vis (ultraviolet-visible) reflectance spectrum, an absorption maximum at 700 nm is characteristic of natural-color black cultured pearls from the *Pinctada margaritifera* oyster.

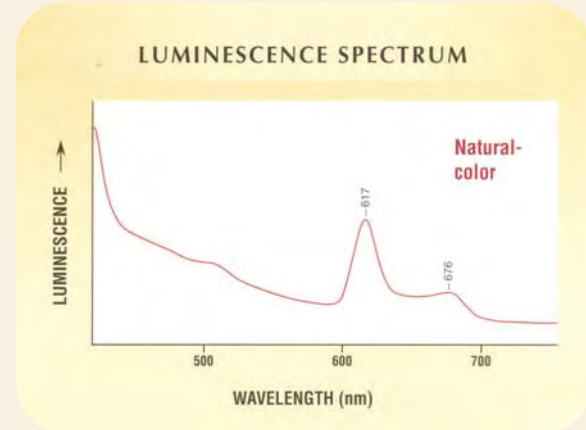


Figure A-4. This luminescence spectrum of a cultured black pearl from *Pinctada margaritifera* shows fluorescence peaks at 617 and 676 nm due to porphyrins, which are responsible for the reddish brown fluorescence to 365 nm UV or 405 nm blue light.



Figure 2. These five samples, each about 9 mm in diameter, show the range of color seen in the *Pinctada maxima* shell nacre samples. Photo by Maha Tannous.

pose of the present research was to determine other nondestructive spectral or fluorescence characteristics that could be used to aid in the identification of heat-treated yellow cultured pearls from the *P. maxima* that either are undrilled or have drill holes that are inaccessible for examination.

For convenience and brevity, natural-color yellow cultured pearls will henceforth be abbreviated as NYCPCs, and reportedly heat-treated yellow cultured pearls as HTYCPCs. Note, too, that the hue, tone, and saturation terms used to describe the colors of the shell and cultured pearl samples are based on the new (2000) GIA pearl grading system.

MATERIALS AND METHODS

To establish the characteristics of known *untreated* material, we obtained a total of 42 samples of nacre from seven gold-lipped *P. maxima* shells that originated from Australia (2 shells), the Amami Islands in Japan (2), and the Philippines (3). The samples, each approximately 9 mm in diameter, were removed with a diamond saw while the shells were completely immersed in water, since overheating could affect their color (Webster, 1994) and thus their fluorescence or spectral characteristics. Two samples of white nacre and four samples of yellow nacre were obtained from each shell, for a total of 14 white nacre and 28 yellow nacre samples.

In addition, 53 NYCPCs, ranging from 9.1 to 15.7 mm, were obtained from several reputable sources. They were reportedly from Indonesia (5), the Philippines (23), Japan (3), Australia (6), and the "South Seas" in general (16). Forty-five were undrilled and eight were drilled. Twelve undrilled treated-color yellow cultured pearls, which were reportedly heat treated, were also obtained for the study; they ranged from 11.8 to 13.1 mm. We believe that these samples originated from the gold-lipped variety of the *P. maxima*; we could not confirm whether the process has been applied to cultured pearls from the silver-lipped *P. maxima*. No strongly



Figure 3. The natural-color yellow cultured pearls ranged from very light yellow to orange (as shown here) or greenish yellow. These pearls are 11.6–13.6 mm in diameter. Photo by Maha Tannous.

saturated yellow cultured pearls of known pedigree, natural or treated, were available for characterization.

All of the cultured pearls were examined with a GIA Gem Instruments Mark VII microscope using fluorescent and fiber-optic lighting. Initially six NYCPCs and six HTYCPCs were analyzed with a Renishaw 2000 Ramascope laser Raman microspectrometer and a Thermo Noran Spectrace 5000 EDXRF spectrometer. Inasmuch as neither technique revealed any distinct differences between the natural- and the treated-color samples, further testing by Raman and EDXRF was discontinued.

UV-Vis reflectance spectra and fluorescence observations were obtained for each sample using a Hitachi 4001 spectrophotometer and a UVP model B100 AP long-wave ultraviolet lamp. Reflectance spectra were collected from 250 to 2500 nm, although only the pertinent data range (i.e., 250–700 nm) is illustrated in this article. At least two spectra were obtained in different regions for each cultured pearl that showed uneven color or fluorescence distribution. A total of 162 reflectance spectra were collected: 42 on the shell nacre samples, 94 on the natural-color cultured pearls, and 26 on the treated cultured pearls. Acquisition of luminescence spectra with a Spectronic AB2 luminescence spectrometer was unsuccessful, due to instrument configuration, sample shape, and the generally desaturated fluorescence colors. Therefore, fluorescence color and distribution were observed visually in a darkened room with the aid of UV contrast goggles.

RESULTS

Visual Appearance. Fourteen of the shell nacre samples were white, and 28 ranged from light to dark yellow (see, e.g., figure 2). The natural-color cultured pearls ranged from very light yellow to orange or greenish yellow (see, e.g., figure 3); a few exhibited slightly uneven color distribution. The HTYCPCs ranged from light yellow to orange yellow (see, e.g., figure 4), with the majority being light yellow.



Figure 4. The heat-treated yellow cultured pearls ranged from light yellow to moderate orangy yellow. The samples shown here are 11.3–12.6 mm in diameter. Photo by Maha Tannous.

Small, localized spots of concentrated color were visible in 10 of the 12 HTYCPs, with either the unaided eye or magnification (figure 5). The remaining two did not exhibit any visible or microscopic evidence of treatment.

UV-Vis Reflectance Spectra and Fluorescence. Shell Nacre Samples. The UV-Vis spectra revealed a decrease in reflectance due to absorption between 330 and 460 nm for all 28 yellow shell nacre samples as compared to the samples of white shell nacre. This broad region of absorption is actually composed of two features: one in the UV region from 330 to 385 nm, with a maximum between 350 and 365 nm; and the other in the visible region from 385 to 460 nm, with a maximum between 420 and 435 nm. The spectra of the white shell nacre samples showed no absorption features in this broad region. Examination of the reflectance spectra for a series of five samples that ranged from white to dark yellow revealed an increase in the general absorption between 330 and 460 nm as the strength of the yellow coloration increased (figure 6).

Typically, dark yellow shell nacre exhibited moderate brown, greenish brown, or greenish yellow fluorescence, and light yellow shell nacre fluoresced light brown or light yellow (see, e.g., figure 7). Most of the white shell nacre samples showed moderate-to-strong very light blue fluorescence, although some appeared to exhibit a slight trace of yellow.

Natural-Color Cultured Pearls. The spectra for these samples (figure 8) exhibited absorption characteristics similar to those of the yellow shell nacre, except that the maximum in the UV varied from 350 to 385 nm. All but four of the 94 spectra obtained on these samples exhibited the two absorption features between 330 and 460 nm. In the four spectra that did not show these features, the regions

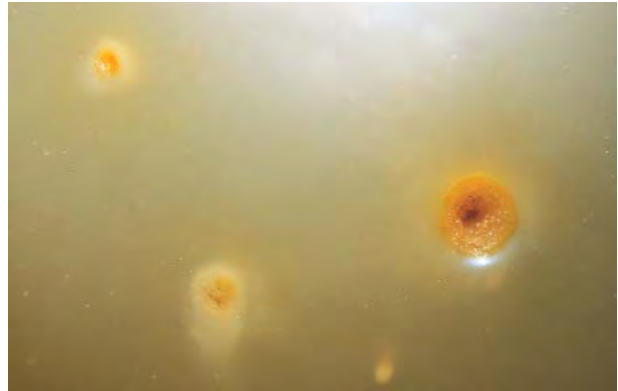
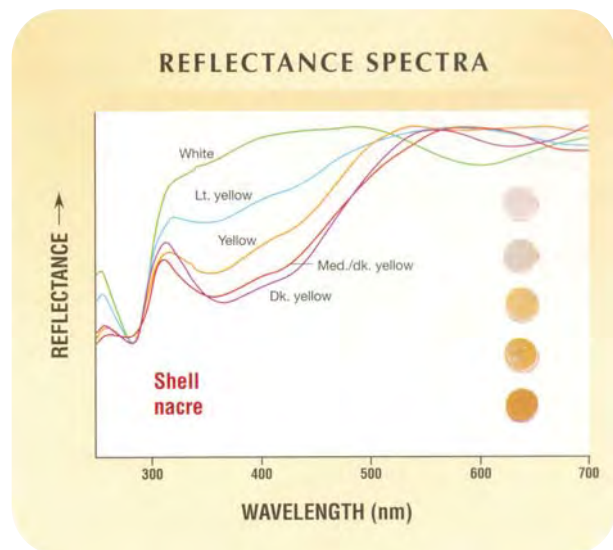


Figure 5. Small spots of concentrated color are evident within blemishes on this yellow cultured pearl that reportedly has been heat treated. Photomicrograph by Shane Elen; magnified 5x.

analyzed were white areas on unevenly colored samples; and these results were similar to the reflectance spectra obtained for white shell nacre. As the yellow color of the cultured pearls increased in saturation, the long-wave UV fluorescence progressed from light yellow or light brown, to greenish yellow, greenish brown, or brown.

Heat-Treated Cultured Pearls. Five of the 26 reflectance spectra obtained from the HTYCPs

Figure 6. These reflectance spectra of five shell nacre samples—ranging from white through dark yellow—show increasing absorption from 330 to 460 nm as the color intensifies. Note in particular the increasing absorption in the UV region from 330 to 385 nm.



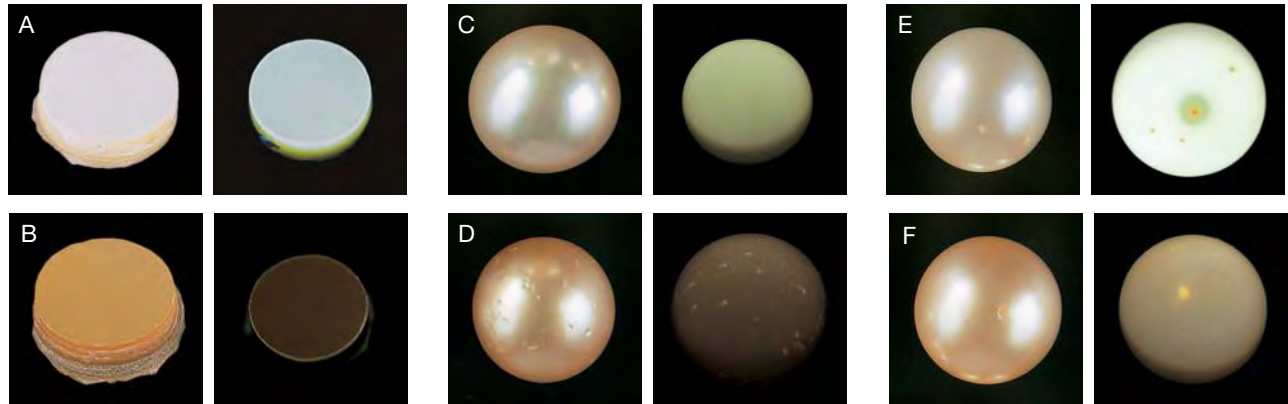


Figure 7. The typical fluorescence reactions of natural- and treated-color cultured pearls when exposed to 365 nm (long-wave) UV radiation are illustrated here. Shown in normal lighting (left in each pair) and with long-wave UV (right) are: (A) white shell nacre, (B) yellow shell nacre, (C) 13.6 mm natural-color light yellow cultured pearl, (D) 12.5 mm natural-color orangy yellow cultured pearl, (E) 12.6 mm heat-treated light yellow cultured pearl, and (F) 12.6 mm heat-treated orangy yellow cultured pearl. Normal lighting photos by Maha Tannous; fluorescence photos by Shane Elen.

exhibited a weak absorption feature in the UV region around 345 nm (see, e.g., figure 9). These spectra represented five of the 12 treated cultured pearls studied. Spectra taken from other areas on these same five HTYCPs, and from the remaining seven HTYCPs, exhibited very weak or no absorption in the UV region. All 26 spectra showed an absorption feature in the blue region between 415 and 430 nm.

Generally, the fluorescence of the HTYCPs was slightly uneven, and appeared unrelated to the dis-

tribution of bodycolor. In one HTYCP, however, fluorescence did appear to be related to the uneven distribution of the yellow color: Light yellow and light brown fluorescence corresponded directly to areas of light yellow and light orangy yellow. Eight of the HTYCPs, which were light in tone and saturation, fluoresced moderate to strong light yellow; two—also light in tone and saturation—exhibited a very light blue fluorescence. The sample with the

Figure 8. As was the case with the shell nacre samples, the reflectance spectra of the natural-color yellow cultured pearls showed increasing absorption in the 330–460 nm region with greater saturation of color.

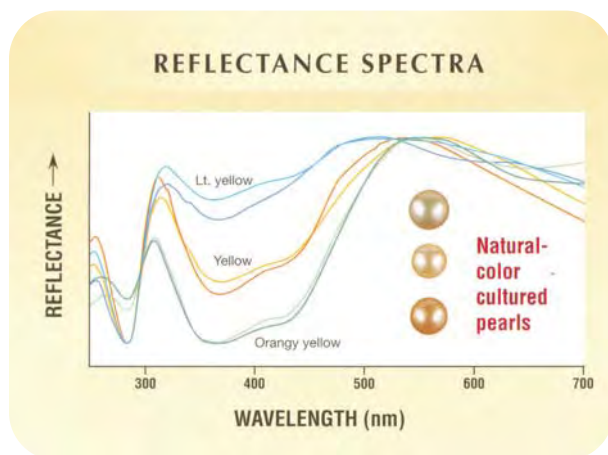
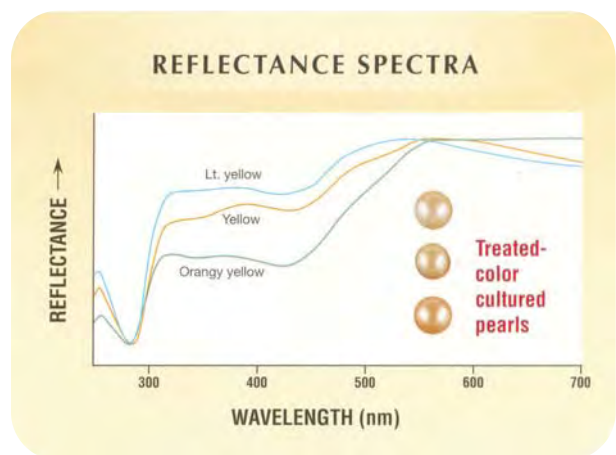


Figure 9. The reflectance spectra of the heat-treated yellow cultured pearls revealed very weak or no absorption in the 330–385 nm region. The presence of a weak UV absorption feature around 345 nm suggests that the orangy yellow cultured pearl exhibited some natural yellow coloration prior to treatment.



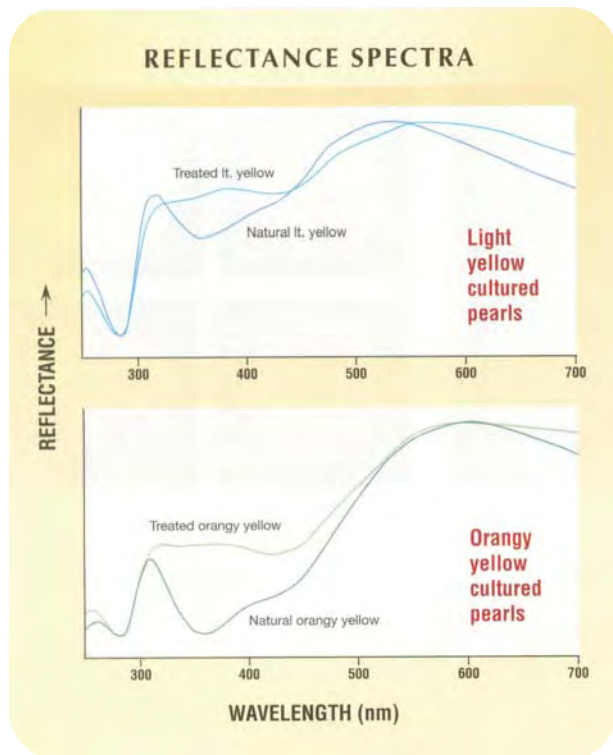


Figure 10. These reflectance spectra of natural and treated light yellow (top) and orangy yellow (bottom) cultured pearls show a distinct difference in absorption in the 330–385 nm region. Note the lack of absorption in this region shown by the treated-color samples.

most saturated orangy yellow bodycolor fluoresced a light brownish orange. The spots of concentrated color seen in some HTYCPs (see figure 5) fluoresced a strong orange to long-wave UV.

DISCUSSION

Confirmation of Reported Origin of Color. One of the main challenges of performing a study of this kind is obtaining samples of known species and color origin. Ideally for pearls of natural color, witnessing the removal of the pearl from the oyster would be the method of choice. However, this is not always practical, so instead we must look to very reliable sources. Similarly, obtaining pearls treated by specific methods also can be very challenging.

None of the cultured pearls represented as being of natural yellow color showed any visible indications of treatment, whereas most of the cultured pearls reported to be heat treated did exhibit some visible evidence in the form of spots with concentrated color. In most cases, too, there was a distinct difference in reflectance spectra between yellow

cultured pearls stated to be natural color and those that were reportedly heat treated. In addition, those stated to be natural color exhibited reflectance and fluorescence characteristics similar to the samples of shell nacre of similar color. These findings would appear to support the reported color origins for the cultured pearl samples used in this study.

Although no chemical study of the zoochrome (a naturally occurring pigment molecule found in the animal kingdom; Needham, 1974) was performed, the reflectance and fluorescence results indicate that the yellow coloration in *P. maxima* shells and NYCPs appears to be due to a common zoochrome regardless of their geographic origin.

Spectral Reflectance Characteristics. A broad absorption between 330 and 460 nm in the reflectance spectra was seen in the yellow nacre from both the gold-lipped *P. maxima* shell and the NYCP samples (figures 6 and 8), and thus appears to be characteristic of natural-color yellow nacre produced by this species. The strength of this absorption appeared to increase as the color became more saturated. The 420–435 nm maximum (in the blue region of the visible spectrum) is typical of reflectance spectra for yellow objects (Lamb and Bourriau, 1995), and is responsible for the yellow color observed. Although UV absorption is not necessary to produce yellow coloration, it does appear to be related to the same zoochrome that is responsible for the absorption in the blue region of the visible spectrum. The absence of this absorption maximum in the UV reflectance spectra obtained from white areas on unevenly colored cultured pearls is consistent with the reflectance results obtained for white shell nacre.

The HTYCPs exhibited an absorption in the blue region, as would be expected for a yellow cultured pearl, but there was a significant difference in the strength of UV absorption between similarly colored natural and treated cultured “golden” pearls (figure 10). The absence of the UV absorption feature in the HTYCPs indicates that the cause of their yellow coloration is different from that of the NYCPs tested. The fact that some areas of the treated cultured pearls showed a weak UV absorption feature suggests that these areas were a light yellow prior to treatment.

Ultraviolet Fluorescence. Fluorescence can be a valuable yet challenging identification technique, since many of the effects and color differences are

TABLE 1. Summary of identification characteristics for natural-color and heat-treated yellow cultured pearls produced by *P. maxima*.

Nacre color	UV absorption feature (330–385 nm)	Visible absorption feature (385–460 nm)	Fluorescence to long-wave UV	Comments
Natural white	None	None	Moderate to strong; very light blue or very light yellow	Generally very light blue fluorescence
Natural yellow	Distinct to strong	Present	Moderate; light yellow or light brown, to greenish yellow, greenish brown, or brown	Even distribution of body color will be accompanied by even fluorescence
Heated yellow	None to weak	Present	Moderate to strong; light yellow, very light blue, or light brownish orange	Even distribution of body color may be accompanied by uneven fluorescence

quite subtle and can vary depending on the type of long-wave UV source used. It is important to observe the relationship between (1) the tonal distribution of the yellow color, and (2) the distribution and hue of the fluorescence (again, see figure 7). For the natural-color samples, the distribution of fluorescence matched the evenness or unevenness of the color distribution: An even yellow distribution corresponded to an even fluorescence distribution, and uneven color showed uneven fluorescence. An even color distribution with a patchy fluorescence is indicative of treatment. In lighter samples, however, slight tonal variations in nacre color can be quite difficult to see compared to the more obvious patchy fluorescence.

In addition, the fluorescence colors emitted by both natural- and treated-color light yellow cultured pearls can be similar, and thus they are less reliable as an indicator of treatment. The exception to this is the very light blue fluorescence observed in natural white nacre and in some light yellow HTYCPs. The fact that no NYCPs of light yellow color exhibited this fluorescence color would imply that the treated-yellow sample was originally white. (Caution must be observed, however, because some long-wave UV lamps emit enough blue visible light to render this observation unreliable.) The HTYCPs also lacked the greenish fluorescence component noted in many of the yellow shell nacre samples and NYCPs. Neither the NYCPs nor the yellow shell nacre exhibited the strong orange fluorescence seen in the spots of concentrated color of some of the HTYCPs; therefore, distinct spots of strong orange fluorescence would indicate treatment.

Inasmuch as the details of the heat-treatment process are unavailable, the effect that heat treatment might have on the individual components that contribute to fluorescence (i.e., conchiolin, aragonite plates, and pigments) was not investigat-

ed. It has been reported that the fluorescence of conchiolin can be affected by certain treatments (S. Akamatsu, pers. comm., 2001). However, the differences in fluorescence between natural- and treated-color cultured pearls may result from a combination of these components and not necessarily from any one component in particular.

Identification of Heat-Treated Yellow Cultured Pearls. Table 1 summarizes key identification characteristics for natural-color and heat-treated yellow cultured pearls produced by the *P. maxima* oyster. As indicated below, the ease with which HTYCPs can be identified depends greatly on whether the original cultured pearl had even or uneven color.

1. An HTYCP that exhibited white and yellow areas prior to treatment is likely to be the easiest to separate from natural color. After treatment, the white areas would appear yellow but would exhibit the UV spectral characteristics of white nacre; that is, the UV absorption characteristic of yellow nacre between 330 and 385 nm would be absent. In this type of treated cultured pearl, areas that formerly were white fluoresce a lighter color than do the yellow zones. The uneven fluorescence also may contrast with an even yellow coloration of the treated cultured pearl.
2. An HTYCP that exhibited evenly distributed, very light color prior to treatment may exhibit a UV absorption feature that is too weak for its apparent color (figure 10). Also, the fluorescence color might appear too light for the apparent tone and saturation of the treated cultured pearl.
3. Probably the most difficult to identify would be HTYCPs that were originally unevenly colored light and dark yellow. Nevertheless, this type of HTYCP is likely to exhibit uneven fluorescence, possibly in contrast to an even yellow coloration.



Figure 11. Large, fine “golden” cultured pearls are a popular item in the jewelry mix. The natural-color cultured pearls in this strand range from 13.0 to 17.3 mm. Courtesy of Tara & Sons, New York; photo © Harold & Erica Van Pelt.

Again, the UV absorption feature would likely appear too weak for the apparent color of the treated cultured pearl.

If heat-treated cultured pearls are subsequently drilled, the color may appear to be concentrated in the surface layers of nacre when observed through the drill hole (T. Moses, pers. comm., 2000).

CONCLUSION

As “golden” cultured pearls from *P. maxima* become increasingly popular in the marketplace (figure 11), there is growing incentive to treat off-color cultured pearls to produce these rich yellow to orangy yellow colors. As a result, the separation of treated-color from natural-color pearls has become a constant challenge for the gemologist. Although color treatment is relatively straightforward to identify in many drilled cultured pearls because of distinctive color differences in the layers visible

through the drill hole, certain treatments—especially heat treatment—may be very difficult to detect in some undrilled cultured pearls.

The present study of white and yellow shell nacre from gold-lipped *P. maxima* shells showed a characteristic increase in absorption between 330 and 385 nm in the UV spectrum as tone and saturation increased from white to dark yellow. This absorption appears to be related to the zochrome responsible for absorption in the blue region, which results in the yellow color of the nacre. The change in absorption with increasing tone and saturation was accompanied by a similar change in long-wave UV fluorescence, which progressed from very light blue or very light yellow, to light yellow or light brown, to greenish yellow, greenish brown, or brown as the colors of the shell nacre samples changed from white to dark yellow.

NYCPs from the *P. maxima* oyster exhibited characteristics similar to those of the yellow shell

nacre. However, the UV reflectance and fluorescence properties of HTYCPs of comparable color appeared more like those of very light yellow or white nacre. Although only 12 treated samples were obtained for the study, all 12 lacked the UV absorption feature characteristic of natural yellow color in *P. maxima*. Therefore, the fluorescence and, more importantly, the absence of UV absorption can help identify heat-treated undrilled “golden” cultured pearls.

Given that the UV absorption feature is a characteristic of natural-color yellow nacre in *P. maxima*, the absence of this feature would indicate a treated yellow color regardless of the treatment method used. Unfortunately, without further study of chemically processed or dyed “golden” pearls, we cannot state that the presence of this feature proves that the color is natural. Fortunately, these latter methods typically are applied to drilled cultured pearls and thus generally are easier to identify.

ABOUT THE AUTHOR

Mr. Elen is a research gemologist at GIA Research, Carlsbad, California.

ACKNOWLEDGMENTS: The author thanks the following persons for providing samples of cultured pearls and shells for this study: Alex Vock of ProVocative Gems, New York; Jacques Branellec of Jeweler International, the Philippines; Salvador Assael of Assael International, New York; Terry D'Elia of D'Elia & Tasaki Co., New York; Nicholas Paspaley of Paspaley Pearlring Co., Darwin, Australia; and David Norman of Broome Pearls Pty, Broome, Western Australia. Thanks also to Dr. Peter Buerki of GIA Research and Matt Hall of the GIA Gem Trade Laboratory, for helping collect some of the spectroscopic data; to Karin Hurwit and Cheryl Wentzell of the GIA Gem Trade Laboratory for aiding with color determination; and to Tom Moses of the GIA Gem Trade Laboratory, Dr. Jim Shigley of GIA Research and Shigeru Akamatsu, former manager of the Pearl Research Laboratory and currently general manager, Sales Promotion Department, at K. Mikimoto and Co. Ltd., Tokyo, for their constructive comments.

REFERENCES

- Federman D. (1995) Gem Profile: Philippine pearl—The quest for gold. *Modern Jeweler*, Vol. 94, No. 1, pp. 11–12.
- (1998) The ABCs of pearl processing. *Modern Jeweler*, Vol. 97, No. 3, pp. 53–57.
- Gauthier J-P., Lasnier B. (1990) La perle noire obtenue par traitement a l'argent. *Revue de Gemmologie a.f.g.*, No. 103, pp. 3–6.
- Gervis M.H., Sims N.A. (1992) *The Biology and Culture of Pearl Oysters (Bivalvia: Pteriidae)*. International Center for Living Aquatic Resources Management Contribution No. 837, Studies and Reviews 21, 49 pp.
- Hargett D. (1989) Gem Trade Lab notes: Pearls—“Pinked.” *Gems & Gemology*, Vol. 25, No. 3, p. 174.
- Ken-Tang Chow (1963) *Process for irradiating pearls and product resulting therefrom*. U.S. Patent 3,075,906, issued January 29.
- Komatsu H. (1999) The identification of pearls in Japan—A status quo summary. *Journal of the Gemmological Society of Japan*, Vol. 20, No. 1–4, pp. 111–119.
- Komatsu H., Akamatsu S. (1978) Studies on differentiation of true and artificially coloured black and blue pearls. *Journal of the Gemmological Society of Japan*, Vol. 5, No. 4, pp. 3–8.
- Lamb T., Bourriau J. (1995) *Color: Art & Science*. Darwin College Lectures, Cambridge University Press, figure 12g, p. 86.
- Miyoshi T., Matsuda Y., Komatsu H. (1987) Fluorescence from pearls and shells of black-lip oyster, *Pinctada margaritifera*, and its contribution to the distinction of mother oysters used in pearl culture. *Japanese Journal of Applied Physics*, Vol. 26, No. 7, pp. 1069–1072.
- Needham A.E. (1974) *Zoophysiology and Ecology 3: The Significance of Zoochromes*. Springer-Verlag, Berlin.
- Newman R. (1999) *Pearl Buying Guide*, 3rd ed. International Jewelry Publications, Los Angeles.
- Prices of golden South Sea pearls likely to rise. (2000) *Jewellery News Asia*, No. 192, August, pp. 45, 59.
- Sheung B. (1998) Concern about treatments rises. *Jewellery News Asia*, No. 168, March, pp. 49–52.
- South Sea Pearl Consortium (1996) Guide to South Sea cultured pearl quality. *Modern Jeweler*, Vol. 95, No. 9, special supplement.
- Vock A. (1997) Disclosure needed for a healthy industry. *Jewellery News Asia*, No. 158, October, pp. 52–54.
- Webster R. (1994) *Gems: Their Sources, Descriptions and Identification*, 5th ed. Revised by P. G. Read, Butterworth-Heinemann, Oxford, England, 1026 pp.

A NEW METHOD FOR IMITATING ASTERISM

By Shane F. McClure and John I. Koivula

Several gems were recently examined that showed stars with an unnatural appearance or an unusual number of rays. Asterism in some of these gem materials is very rare, or has not been seen previously by the authors. Microscopic examination revealed that these “stars” were produced by using what appeared to be a rough polish to scratch lines in an oriented fashion onto the upper surface of the cabochons.

Asterism and chatoyancy (i.e., the phenomena of stars and cat’s-eyes, respectively) can potentially occur in almost any gemstone. Chatoyancy will occur if a sufficient volume and concentration of acicular (needle-like) inclusions line up parallel to one another within a gem material, and the gem material then is cut into a properly oriented cabochon. To create asterism, these concentrations of needles must line up in more than one direction—almost always in specific relationship to crystallographic axes—which gives rise to stars with four, six, and sometimes more rays. Chatoyancy can actually be caused by mechanisms other than acicular inclusions, such as the fibrous structure in some cat’s-eye opal, or by other phenomena, such as the oriented adularescence in cat’s-eye moonstone (Hurlbut and Kammerling, 1991). For those not familiar with phenomena such as asterism and adularescence in gems, a good general reference is Webster’s *Gems* (1994).

Nevertheless, even though the potential for asterism exists in almost any gemstone (see, e.g.,

Kumaratilake, 1997, 1998), asterism has never been observed in many gemstones and is very rare in others. The presence of asterism in a gemstone can add significant value, especially if it occurs in a material in which it has not previously been observed, such as sinhalite (figure 1). Collectors of phenomenal gems have been known to pay handsomely for such a stone, even if the gem material itself is unattractive, or otherwise of little value.

Many methods have been used over the years to imitate asterism. These include: engraving a series of intersecting parallel lines on the back of a transparent cabochon which is then covered by a reflective backing, or adding a thin engraved metallic plate to the back of a transparent cabochon (figure 2; see also Hurlbut and Kammerling, 1991); or using a diffusion process to put fine, oriented rutile needles in a thin layer just under the surface of a cabochon (figure 3; Fryer et al., 1985). These star imitations can be quite effective, but usually they are found only in gem materials that are known for asterism, such as rubies and sapphires.

Therefore, we were surprised to learn that an evidently new process was being used to create the appearance of asterism in gems that had not shown this phenomenon previously. The first such stones seen at the GIA Gem Trade Laboratory had been represented to our client as rare examples of stars in unusual materials. Some of these stars showed as many as 15 or 16 rays. Subsequently, we received more asteriated stones, many of which were

See end of article for About the Authors information and Acknowledgments.
 GEMS & GEMOLOGY, Vol. 37, No. 2, pp. 124–128
 © 2001 Gemological Institute of America



Figure 1. This 6.17 ct sinhalite, a gemstone that has not been reported to display asterism, showed a very unusual 11-rayed star that ultimately proved to be manufactured. Photo by Maha Tannous.

opaque, that represented an array of different materials. One even sported a double star. Most of the stars showed essentially straight rays, but in some cases the rays were obviously curved down the sides of the cabochon (figure 4). These stones were supplied to us by three dealers from three very different locations (Louisville, Colorado; Bangkok, Thailand; and Falls Church, Virginia), and were purported to

be from Sri Lanka and India. Because of the types of gem materials involved, the superficial appearance of the stars, and the odd number and orientation of some of the rays in the stars, the dealers suspected that the asterism had been artificially created. We conducted the present study to learn more about this new technique and to establish the best means of identifying this imitation asterism.

Figure 2. Oriented lines engraved on this thin metal plate give the appearance of asterism in the synthetic ruby cabochon to which it is attached. Photomicrograph, taken through the dome of the cabochon, by John I. Koivula; magnified 30×.

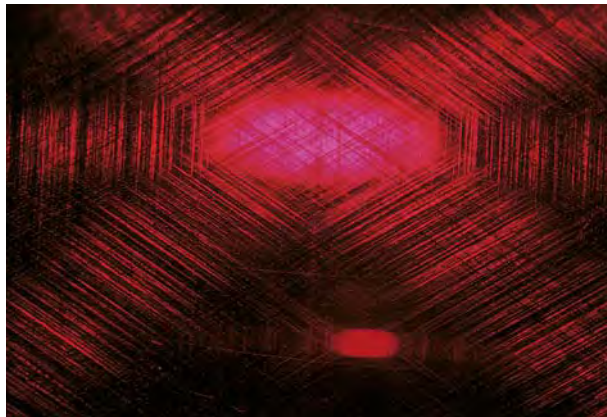


Figure 3. This very fine, unnatural-looking silk (similar in appearance to the silk found in flame-fusion synthetic star rubies or sapphires) is typically seen in a star created by diffusion treatment. Photomicrograph by John I. Koivula; magnified 40×.





Figure 4. This rutile cabochon displayed at least 16 rays, most of which showed a noticeable curve as they approached the girdle. Photo by Maha Tannous.

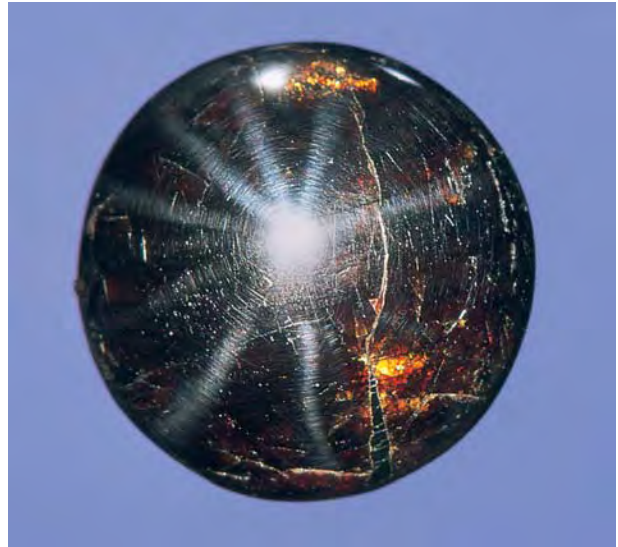


Figure 6. The stars made by the “scratching” process described here often displayed asymmetrical rays, such as in this 17.08 ct cassiterite that shows nine rays. Photo by Maha Tannous.

MATERIALS AND METHODS

Altogether, we examined a dozen stones that displayed evidence of this new method of imitating asterism. We studied one each of sinhalite, cassiterite, chrysoberyl, and garnet, and one stone that was represented to be scheelite but turned out to be a member of a series of naturally radioactive rare earth-bearing minerals, possibly samarskite. Chrysoberyl is well known for chatoyancy, but it rarely shows asterism. Star garnet is relatively common, but cat’s-eye garnet is rare. The authors have not seen examples of either phenomenon in

Figure 5. The eye of this natural cat’s-eye rutile shows a very dense concentration of needles that are clearly inside the stone. Photomicrograph by John I. Koivula; magnified 45 \times .



sinhalite, cassiterite, and scheelite (or samarskite). The balance of the cabochons were rutile, in which natural chatoyancy is occasionally seen (figure 5) and asterism is reported to be very rare (Kumaratilake, 1997).

The 12 cabochons in this study ranged from 3.29 ct to more than 20 ct; all were oval or round and semi-transparent to opaque.

All of the gem materials were identified by standard gemological procedures. To determine the cause of the asterism, we used a GIA Gem Instruments Mark VII Gemolite gemological microscope, at magnifications up to 45 \times , with fiber-optic illumination.

RESULTS AND DISCUSSION

Each stone displayed a star that had as few as six rays (in the case of the chrysoberyl), to more than a dozen rays (in the case of several rutiles). The garnet showed a double star, one with four rays and the other with eight. The first thing anyone familiar with natural asterism will notice is the unusual appearance of most of these stars. In many of the stones, the stars had too many rays and the rays were not symmetrical (figure 6). Many stars also displayed an unusual number of rays, such as eight or 10, or an odd number such as 11 (again, see figure 1), which is not typical for any material. Also, the asterism appeared to be very superficial, even in stones that were almost transparent, whereas true asterism usually has depth to it.

Microscopic examination quickly identified the

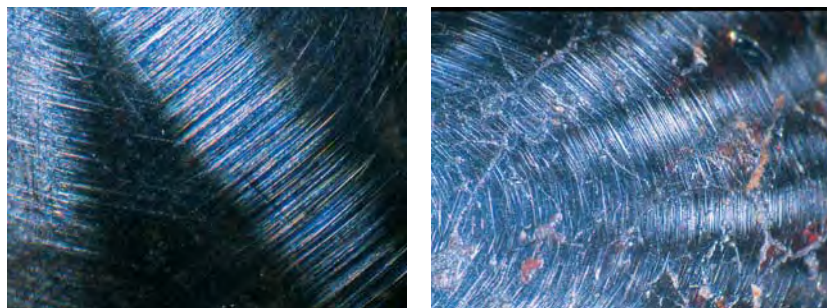


Figure 7. These photos illustrate how superficial the imitation stars are and that they are being created by oriented “polishing” lines. The specimen on the left may be samarskite; the cabochon on the right is rutile. Photomicrographs by Shane F. McClure; magnified 40×.

source of the asterism: oriented, coarse, parallel lines scratched on the domed surfaces of the stones (figure 7). At first one might think the lines were the result of a bad polishing job, but close inspection revealed that this “bad polish” was deliberate. By making the lines coarse and keeping them parallel in certain directions, the treater was able to use them to reflect light in essentially the same way that natural subsurface needle-like inclusions do.

As mentioned above, some of the stones displayed too many rays or an unnatural number of rays, so that the asterism was not believable. In one case, however, the illusion was very well executed. A 3.29 ct chrysoberyl showed an almost perfectly symmetrical six-rayed star (figure 8). The authors have seen a few examples of chrysoberyl with a natural six-rayed star over the years (figure 9), but they are so rare that most references do not even acknowledge their existence.

Perhaps the most interesting stone in our sample group was a 4.28 ct purplish red garnet that dis-

played a double star, that is, two stars adjacent to one another (in contrast to multiple stars that manifest themselves in different areas of the stone). Double stars have been noted in some corundums (Moses et al., 1998), and multiple stars actually are common in some materials, such as quartz (see, e.g., Johnson and Koivula, 1999). To our knowledge, though, no such double star has been reported in garnet. Even more suspicious was the fact that one of the stars had four rays and the other had eight. The authors are not aware of any reports of double stars with this kind of asymmetry. In this case, microscopic examination revealed that the four-rayed star was natural, and the eight-rayed star was manufactured by the method described above. The four-rayed star clearly showed the individual needle-like inclusions that one normally expects from a natural star, while the eight-rayed star was obviously caused by oriented “polish lines” and was evident only on the surface of the stone (figure 10). The close juxtaposition of a natural star to a

Figure 8. The almost-perfect six-rayed star in this transparent 3.29 ct chrysoberyl was found to be manufactured. Photomicrograph by Shane F. McClure; magnified 10×.



Figure 9. Natural six-rayed stars in chrysoberyl, as seen in this 2.29 ct cabochon, are very rare. Photo by Maha Tannous.



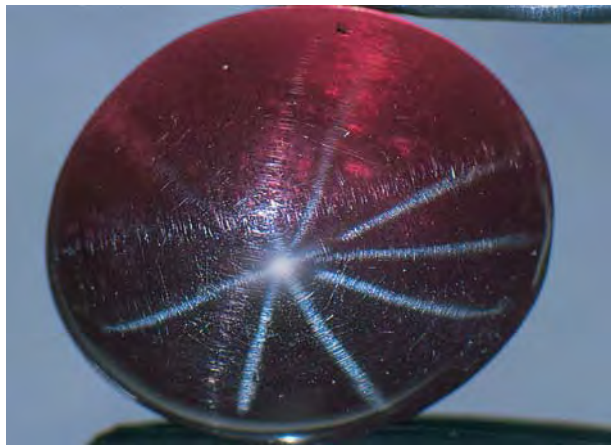


Figure 10. The double star in this 4.28 ct garnet cabochon consisted of one natural four-rayed star and one manufactured eight-rayed star. Note the difference in appearance between the two stars. Photomicrograph by Shane F. McClure; magnified 10 \times .



Figure 11. Natural 12-rayed stars (such as in this 4.41 ct sapphire) do exist, but they are easily distinguished from the manufactured stars discussed in this article. Photomicrograph by Shane F. McClure; magnified 10 \times .

manufactured one illustrates quite effectively the striking differences between the two.

It is interesting to note that one of the groups of suspect stones we received had a sapphire with a 12-rayed star (figure 11). The phenomenon in this stone was completely natural. For this reason it was not included as part of the study group.

Although no one has come forward to say exactly how this process is being done, the appearance of the stones suggests that it involves the use of a polishing wheel with a coarse grit. The oriented scratches are numerous and packed tightly together, so some type of spinning wheel is probably involved. Also, the asymmetry of most of the specimens would suggest that the process is being done by hand, rather than by some form of automation.

CONCLUSION

These imitation stars are not difficult to detect in most cases because of their unnatural appearance. The key, as is often the case in gemology, is in knowing that such a treatment exists, understanding the sources and appearances of naturally occurring

phenomena such as asterism, and questioning any stone that appears suspicious. Microscopic examination should easily permit the identification, especially with the assistance of a fiber-optic light source.

The presence of a natural 12-rayed star sapphire in one of the groups of suspect stones we received serves as a reminder that while stones with such a large number of rays are rare, they do exist. Only with careful microscopic examination can you conclusively prove the origin of the asterism. Even if a stone appears suspicious, you should follow through with the proper examination before pronouncing judgment.

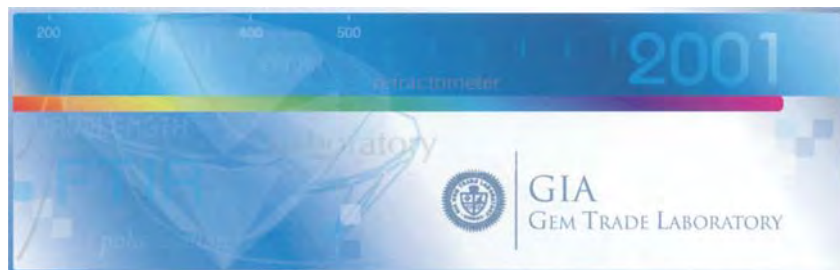
ABOUT THE AUTHORS

Mr. McClure is director of identification services, and Mr. Koivula is chief research gemologist, at the GIA Gem Trade Laboratory in Carlsbad.

ACKNOWLEDGMENTS: The authors wish to thank the following for providing the samples for this study: K & K International of Falls Church, Virginia; Mark Smith of Bangkok, Thailand; and Dudley Blauwet of Louisville, Colorado.

REFERENCES

- Fryer C., Crowningshield R., Hurwit K., Kane R. (1985) Gem Trade Lab notes: Corundum. *Gems & Gemology*, Vol. 21, No. 3, p. 171.
- Hurlbut S., Kammerling R. (1991) *Gemology*, 2nd ed. John Wiley & Sons, New York, 336 pp.
- Johnson M.L., Koivula J.I., Eds. (1999) Gem news: Twelve-rayed star quartz from Sri Lanka. *Gems & Gemology*, Vol. 35, No. 1, pp. 54–55.
- Kumaratilake W.L.D.R.A. (1997) Gems of Sri Lanka: A list of cat's-eyes and stars. *Journal of Gemmology*, Vol. 25, No. 7, pp. 453–516.
- (1998) Spinel and garnet star networks: An interesting asterism in gems from Sri Lanka. *Journal of Gemmology*, Vol. 26, No. 1, pp. 24–28.
- Moses T., Reinitz I., McClure S. (1998) Gem Trade Lab notes: Ruby, with a true double star. *Gems & Gemology*, Vol. 34, No. 3, p. 217.
- Webster R. (1994) *Gems: Their Sources, Descriptions and Identification*, 5th ed. Revised by P.G. Read, Butterworth-Heinemann, Oxford, England, 1026 pp.



Editors

Thomas M. Moses, Ilene Reinitz,
Shane F. McClure, and Mary L. Johnson
GIA Gem Trade Laboratory

Contributing Editors

G. Robert Crowningshield
GIA Gem Trade Laboratory, East Coast
Karin N. Hurwit, John I. Koivula, and
Cheryl Y. Wentzell
GIA Gem Trade Laboratory, West Coast

DIAMOND

“Banded” Twinned Crystal

Diamond manufacturers commonly encounter a wide range of colors and shapes in the crystals they facet. They are routinely required to make quick cutting decisions throughout the faceting process. Occasionally, however, a crystal is so unusual that the manufacturer stops to ponder it. Such a crystal recently was brought to the attention of the East Coast laboratory by one of our clients. Although the appearance of the crystal was intriguing, we were also interested in gaining a better understanding of its growth history.

The 14.07 ct elongated diamond crystal (measuring $21.78 \times 7.62 \times 7.59$ mm) appeared “banded,” with near-colorless portions on each end and a black area in the middle (figure 1). Stepped twin boundaries (twinned according to the spinel law, that is,

Figure 1. The unusual “banded” structure of this 14.07 ct twinned diamond crystal is the result of a complicated growth history.



with the twin plane parallel to one of the octahedron's faces) were found in both near-colorless portions. The twin planes, although parallel, were shifted slightly in position. However, the two near-colorless portions had different morphologies. The portion on the left in figure 1 had a flattened triangular twinned morphology with typical re-entrant corners in the boundaries, whereas the near-colorless portion on the right had a slightly elongated triangular shape without clearly visible twin re-entrant corners. The black portion was irregular in shape, but roughly spherical, with very rough surfaces; it had a submetallic luster. The boundaries between the black center and the near-colorless ends were clearly demarcated.

Because the black center section appeared so different from the end portions, we thought there might have been another material involved. However, the measured specific gravity of the piece was 3.51 (compared to 3.52 for diamond), which indicated that only diamond was present in significant amounts. Infrared spectra suggested that all three parts of the diamond were type Ia, with high levels of nitrogen. Raman spectra collected from the three portions confirmed this result. Several black inclusions with irregular shapes were observed in the near-colorless portions, but none of these was located close enough to the surface of the crystal for Raman analysis.

Detailed observations at high mag-

nification, using an optical microscope (up to $150\times$) and a scanning electron microscope (up to $500\times$) at the California Institute of Technology (Caltech), revealed entirely different surface features for the near-colorless and black portions, which were apparently due to a combination of growth and dissolution (figure 2). On the flat surfaces of the near-colorless portions, the growth features appeared as macroscopic parallel steps and triangular hillocks, particularly in the boundary areas close to the black portion. The dissolution features included tiny etched trigons, with an orientation opposite that of the triangular hillocks, and etch figures with rhombic forms that followed the symmetry of the structure of the twin boundary. Also, the twin boundaries were slightly bent in several places. The rough surface of the black portion consisted of irregular steps and small crystallites with polygonal forms. When examined with strong transmitted light, this portion revealed a rather complex internal structure, with a near-colorless transparent core and a black rim.

We concluded that this diamond was a single crystal with a complicat-

Editor's note: The initials at the end of each item identify the editor(s) or contributing editor(s) who provided that item. Full names are given for other GIA Gem Trade Laboratory contributors.

Gems & Gemology, Vol. 37, No. 2, pp. 130–136

© 2001 Gemological Institute of America

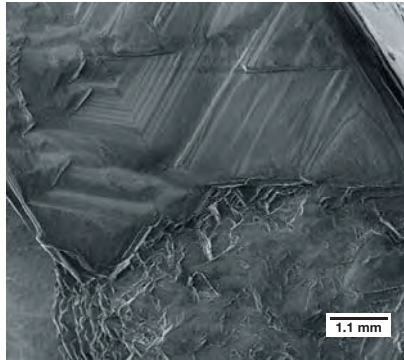


Figure 2. The surface features of this near-colorless portion (top of photo) were very different from those of the black portion (bottom of photo) of the diamond crystal. This backscattered-electron SEM image shows parallel steps, triangular growth hillocks, a twin boundary (upper right), and rhombic dissolution figures on the colorless portion, while it also reveals the rough surface with irregular steps and small crystallites in the black portion.

ed growth history. The black and near-colorless portions represent different stages and conditions of growth. The spherical central portion was formed first and grew rapidly (as evidenced by the small crystallites on its surface). The black color is probably due to numerous tiny and black inclusions located mainly on grain boundaries of the small diamond crystallites. The two flattened and twinned near-colorless portions then grew from both sides of the central portion, by means of a spiral growth mechanism.

Taijin Lu and John M. King

With a Carbonate Inclusion

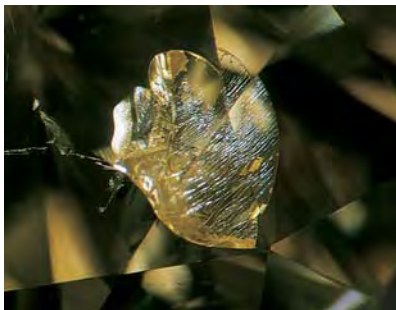
Recently one of the diamond graders in the West Coast laboratory became suspicious of the appearance of a surface-reaching inclusion in a 1.43 ct diamond that could be described as a wide feather or a deep, narrow cavity. The grader thought that the crackled texture observed in the interior of the

inclusion might be due to the presence of some type of artificial filling. When the diamond was brought into the Gem Identification laboratory, we immediately noticed that this texture was very similar to what we had seen in some wide cleavages that had been artificially filled.

Close examination with 15× magnification revealed that where the cavity reached the surface, the transparent material in it was slightly undercut and had a rough texture; it also contained numerous highly reflective, nearly parallel compression cracks (figure 3). The width of the cavity at the surface made it possible to analyze the filler using the laser Raman microspectrometer. The results were both immediate and surprising. The analysis showed the undeniable presence of a carbonate in the crack, although an exact match to a specific carbonate could not be made. To confirm this visually, we placed a minute droplet of 10% hydrochloric acid solution on the crack at the surface of the diamond. The resulting effervescent reaction was as expected for a positive carbonate-HCl acid spot test.

The carbonate calcite has been identified previously as an epigenetic inclusion in diamond (that is, it entered the diamond some time after its formation; see J. W. Harris, "Diamond geology," in J. E. Field, Ed.,

Figure 3. Numerous subparallel, reflective compression cracks in the carbonate inclusion in this diamond resemble a texture noted in some fillings in diamonds. Magnified 15×.



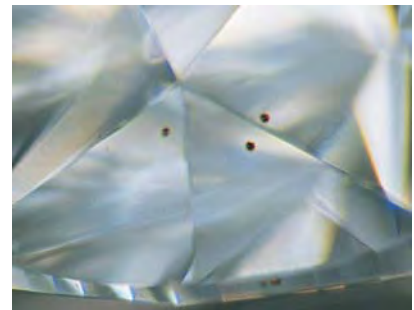
The Properties of Natural and Synthetic Diamond, Academic Press, London, 1992, p. 363). Therefore, the possibility of a carbonate filling the interior of a surface-reaching cavity in a diamond is not unheard of. This, however, is the first time we have identified a carbonate in a polished diamond. Whether or not it would be possible to use a molten carbonate as a diamond filler is not known, although its susceptibility to attack by acid makes this unlikely. We therefore concluded that this was a naturally occurring epigenetic inclusion.

JIK and Maha Tannous

With Unusual Mineral Inclusions

An approximately 1 ct near-colorless round-brilliant-cut diamond recently submitted to the East Coast laboratory was found to contain some rather interesting inclusions. During the clarity grading process, three tiny (0.05 mm) dark red-brown to black inclusions, each surrounded by what appeared to be a brown radiation halo, were observed under the crown (figure 4). These inclusions looked rounded

Figure 4. Too deep in the host diamond to be analyzed by laser Raman microspectrometry, these three tiny (0.05 mm) dark red-brown to black inclusions are surrounded by what appear to be brown radiation halos. They are believed to be either strontian K-Cr loparite or Cr-chevkinite. The inclusion seen here through the girdle of the stone is a reflection artifact. Magnified 40×.



or semi-spherical in form, and proved to be too deep within the diamond host for Raman analysis.

On the basis of visual examination of similar inclusions in about five other diamonds, as well as a search through the literature, we suspected that these inclusions were either strontian K-Cr loparite or Cr-chevkinite. These rather unusual radioactive inclusions are similar in color to those found in this particular diamond, although the latter were too small to provide a radioactivity reading. Loparite is isometric and chevkinite is monoclinic. Because the inclusions in this diamond looked somewhat spherical, loparite is perhaps the more probable choice (chevkinite tends to form as somewhat elongated, spike-shaped crystals). Mineral inclusions in diamonds, however, are often influenced by the diamond structure. Through a process known as xenomorphism, even inclusions that are not isometric, such as chrome diopside, can look as if they have an isometric form. This means that chevkinite could not be ruled out as a possibility.

Strontian K-Cr loparite and Cr-chevkinite were first discovered as inclusions in diamonds that were tiny fragments (approximately 1.5 × 1.5 mm) from the River Ranch kimberlite in Zimbabwe. These inclusions had a high content of radioactive thorium, and contained the highest amounts of rare-earth and radioactive elements ever reported in inclusions in diamonds; small, bright green radiation clouds surrounded each of the radioactive inclusions. The green color indicated that the clouds had developed at a temperature below 600°C, and had not been exposed to a temperature higher than that since they were formed. The fact that the clouds in the diamond we examined were brown indicates that the stone was heated above 600°C at some point (in nature or artificially), as illustrated in J. I. Koivula's *Micro-world of Diamonds*, Gemworld International, Northbrook, Illinois, 2000. A good reference for chevkinite and loparite as inclusions in diamond is

M. G. Kopylova et al., "First occurrence of strontian K-Cr loparite and Cr-chevkinite in diamonds," *Russian Geology and Geophysics*, Vol. 38, No. 2, *Proceedings of the Sixth International Kimberlite Conference*, Vol. 2: *Diamonds: Characterization, Genesis and Exploration*, Allerton Press, New York, 1997, pp. 405–420.

JIK and Maha Tannous

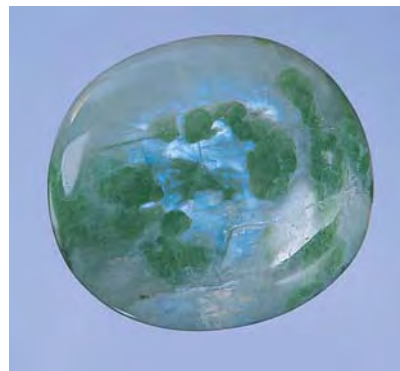
FELDSPAR

With Chrome Diopside Inclusions

The West Coast lab recently examined an unusual double cabochon that standard gemological testing confirmed to be orthoclase feldspar. The 40.14 ct cabochon, which was 22.48 mm long (figure 5), was obtained in Mogok, Myanmar, by Mark Smith, a gemologist and gem dealer in Bangkok. The stone contained a number of relatively large green inclusions, so that in general appearance it resembled the white plagioclase feldspars from the Philippines that contain deep green uvarovite garnet inclusions. Those feldspars, however, do not show adularescence, which this Burmese moonstone did.

Examination with a microscope

Figure 5. This 40.14 ct double cabochon from Myanmar is an interesting mixture of adularescent orthoclase feldspar and chrome diopside.



revealed that the randomly arranged, transparent-to-translucent green inclusions were cracked and well rounded, with no recognizable crystal faces (figure 6). These features suggested a protogenetic origin for these inclusions with respect to the feldspar; that is, they formed before their host. Raman analysis established that the inclusions were diopside, and not (as first suspected) a species of garnet. EDXRF analysis of the inclusions detected the presence of chromium, which is the probable cause of their green color. This is the first example of moonstone with chrome diopside inclusions we have encountered in the laboratory.

JIK, Maha Tannous,
and Sam Muhlmeister

GIBBSITE

Dyed to Imitate Nephrite

Recently, the West Coast laboratory received a 10 × 7 × 3.5 mm oval bead for an identification report. At first glance, the "spinach" green color of the bead (figure 7) appeared to be typical for nephrite jade. However, the optical properties and structural characteristics were quite different from those expected for nephrite.

Using a standard gemological refractometer, we obtained a spot

Figure 6. The rounded appearance and cracked texture of the chrome diopside inclusions in their orthoclase host suggest that the inclusions are protogenetic. Magnified 5×.





Figure 7. This 10×7×3.5 mm bead, which looks like nephrite jade, was identified as dyed gibbsite.

R.I. of 1.58. This reading was too low for nephrite jade (which has an average R.I. of 1.61). The specific gravity, determined by the hydrostatic method, was approximately 2.09. This figure is also significantly lower than nephrite (about 2.95). When we examined the bead with a gemological microscope, we observed a dense granular structure; an even coloration; some small, irregular-shaped, opaque whitish particles; and a few dark brown needle-like inclusions. The material was very soft, and was easily scratched with a needle probe. These properties also indicated that the bead had not been fashioned from nephrite jade.

Next, using a desk-model spectroscope, we noticed strong absorption bands at 560, 600, and 650 nm. The bead fluoresced moderate yellowish green to long-wave ultraviolet radiation, but was inert to short-wave UV. Since the standard gemological tests were inconclusive, advanced testing was required to identify this material. With the client's permission, a minute scraping was taken from an inconspicuous place (the inside of the drill hole) for X-ray diffraction analysis. The pattern obtained matched gibbsite, a clay-like aluminum hydroxide. The material had been dyed to simulate nephrite jade. This was the first jade imitation of this type we have seen in the Gem Trade Laboratory, although on a number of occasions we have

encountered dyed gibbsite as a realistic imitation for turquoise (see Lab Notes: Summer 1983, p.117; Spring 1988, p. 52).
KNH

Devitrified GLASS Resembling Jade

Although jadeite is one of the more common gem materials to be imitated, seldom is the imitation mounted in an ornate setting made with quality craftsmanship. The East Coast lab recently received just such a piece in the form of a pendant.

The fully backed white metal pendant was stamped "18K." It included numerous channel-set transparent near-colorless baguettes, as well as some transparent near-colorless marquise brilliants, all bordered by mill-grain detailing. The pendant showcased a large, thin, semi-transparent to translucent green tablet—carved

with the image of a stork—which measured approximately 33.40 × 40.25 × 1.65 mm (figure 8).

The carved material showed an uneven "patchy" green color throughout, which to the untrained observer might have appeared similar to the aggregate structure of jadeite. We obtained a spot refractive index of 1.60 using a standard gemological refractometer. Patches of the tablet fluoresced a medium chalky yellow to long-wave UV radiation and a very weak chalky yellow to short-wave UV. Using a standard gemological microscope (50×) and fiber-optic lighting, we observed patches of tiny gas bubbles. Higher magnification (200×) revealed a fern-like structure that is commonly seen in the manufactured glass known in the trade as "Meta-jade." The partially devitrified structure confirmed that the carving was a manufactured glass.

Ann-Marie Walker
and Wendi M. Mayerson

Figure 8. The 33.40×40.25×1.65 mm green carving in this pendant proved to be devitrified glass.





Figure 9. Assembled cultured blister pearls such as the ones in this ring (left) were first produced by Kokichi Mikimoto in 1890. Note on the back the concave cups into which they fit precisely (right).

PEARLS

Early Japanese Assembled Cultured Blister Pearls

The East Coast lab recently received for identification an intricate white metal ring set with three pearls (figure 9, left). The setting was stamped “18KT WHITE GOLD” and included numerous old European- and single-cut stones. The ring had a concave cup setting for each of the three partially drilled pearls (figure 9, right), which measured an average of 5.18 mm in diameter.

Magnification revealed a nacreous appearance consistent with natural

Figure 10. This X-radiograph reveals the unusual assemblage of the cultured blister pearls shown in figure 9.



and cultured pearls. X-radiography, however, suggested that the internal structure was not typical of the natural or cultured pearls generally seen in the lab today. Each “pearl” had three components: a layer of nacre, a shell bead with a square notch cut into it, and an oddly shaped mother-of-pearl backing cut to fit into the square notch (figure 10). Most unusual was the fact that the mother-of-pearl backing was rounded on the bottom to give the overall appearance of a fully round pearl. We therefore concluded that these were assembled cultured blister pearls.

We have previously reported on similar cultured pearls in the Lab Notes section (Summer 1983, p. 116; Spring 1988, pp. 49–50; Spring 1994, pp. 44–45). They were produced in Japan prior to the successful culturing of solid round pearls. Although the lab has not seen very many of them, we know that Kokichi Mikimoto was marketing assembled cultured blister pearls as early as 1890, with production exceeding 50,000 annually.

While one might at first assume that these assembled cultured blister pearls were set in the ring to replace lost or worn natural pearls, the fact that they probably represent early Mikimoto production makes it more likely that they were original to the

ring itself. In addition, they fit precisely into the cupped backs, another indication that they were original to the ring. Knowledge of their history can aid in dating this piece of estate jewelry.

Ann-Marie Walker
and Wendi M. Mayerson

Faceted Cultured Pearls, Dyed Black

An 8 mm black faceted pearl was sent to our West Coast laboratory for an identification report. The client had noticed unusual “color spots” that made him question whether it was indeed a natural-color Tahitian cultured pearl. Although we cannot determine a pearl’s provenance, we can determine its identity, whether it is natural or cultured, and whether or not it has been treated.

The item had an attractive black bodycolor and showed strong purplish pink overtones (figure 11). Most of the polygonal facets had been well placed and polished, leaving the surface with a smooth finish. X-radiography revealed a fairly large bead nucleus, which confirmed that this was a cultured pearl. Using 10× magnification with strong overhead illumination, we observed that the nacre was actually dark brown. This color was unevenly distributed, and concentrations in some areas gave the surface a slightly spotted appearance. Magnification also revealed that some facets had been damaged extensively during fashioning. Fairly deep grooves (some straight and others circular) were noticeable. On some facets the top nacre layer had been removed, exposing an almost colorless layer of nacre (figure 12). Along the rims of those exposed areas was an opaque, light brown deposit of unknown identity.

The reaction to long-wave UV radiation was quite peculiar. The exposed near-colorless nacre layer fluoresced chalky yellowish white, similar in appearance to natural-color light nacre shell layers. The black nacre surface, however, did not show

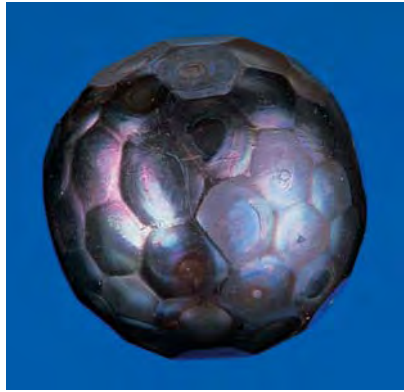


Figure 11. This 8 mm black faceted cultured pearl revealed evidence of treatment. Note the different color of the lower nacre layer that was exposed on some facets during fashioning.

any fluorescence. Natural-color black nacre fluoresces either reddish brown or red to long-wave UV. The absence of this type of fluorescence in the top nacre layer proved that it had been treated. EDXRF chemical analysis revealed the presence of silver, which

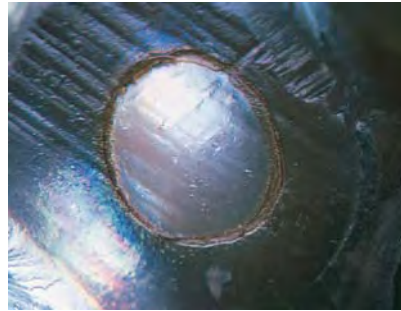


Figure 12. With magnification (here, 15x) a second, almost colorless, nacre layer was revealed, and a light brown deposit was seen where the top nacre layer had been removed during fashioning.

further substantiated our conclusion that the cultured pearl had been treated to attain its black color. As to the cause and nature of the brown deposit around the rims of exposed areas, we could only speculate that it was a byproduct of the faceting and treatment process. *KNH*

Figure 13. This strand of 34 “baroque” imitation pearls was sold as “shell pearls.”



A New Imitation: “Shell Pearls” with a Calcite Bead

This year in Tucson, we purchased a strand of 34 imitation “baroque” pearls (12.50–11.60 mm × 10.30–9.75 mm; figure 13), which were sold as “shell pearls” by Tiger Trading, Fresh Meadows, New York, at the GJX Show. These imitation pearls were offered in rounds ranging from 8 to 14 mm, as well as in “baroque” shapes such as those in the strand we purchased. They came in a variety of colors. Besides the “Tahitian” color scheme of our strand, “South Sea” and standard “akoya” colors were available. The seller reported that they were mother-of-pearl beads—as are sometimes used in imitation pearls—that had been coated to look like many different types of pearls.

The regularity of shape of the “baroque pearls” and the multiple layers visible at the drill holes (figure 14) seemed to support the seller’s description. However, a close inspection in reflected light also revealed what appeared to be facets under the coating. Given the unusual shape and uniformity of these “pearls,” we were curious to learn whether their centers were in fact shell.

To examine the core material, we decided to sacrifice one of the

Figure 14. The view down the drill hole readily revealed that this imitation pearl had multiple layers of some type of coating. Magnified 50x.

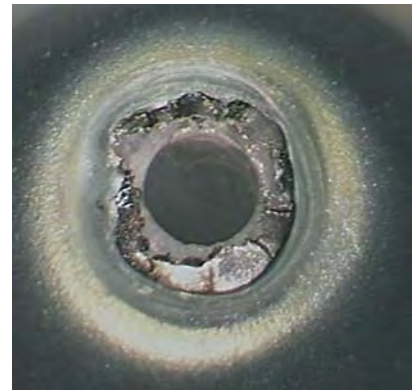




Figure 15. The coating removed from the imitation "shell" pearl was found to consist of two types of layers (left): external transparent colorless layers and internal opaque light gray metallic layers. Gemological testing identified the bead nucleus (right) as calcite.

imitation pearls in the strand. Using a procedure we normally would not perform, we immersed a light gray "shell pearl" in acetone (standard nail polish remover) in an attempt to break down the coating and expose the bead. After 30 minutes, the coating was soft enough to be squeezed with tweezers. In fact, the coating fit loosely, like a plastic bag around a hard center. When the object was squeezed with tweezers, a dark cloud or "puff" was exuded through the drill hole into the nail polish remover. More squeezing ruptured the coating and released the bead nucleus.

As can be seen in figure 15, the coating was quite thick and consisted of two different types of layers—transparent colorless external layers and opaque metallic light gray internal layers. It was part of the internal colored material that, because it was in the process of dissolving, had squirted out of the drill hole when the assemblage was squeezed in acetone.

The bead was translucent white and banded (again, see figure 15). The spot reading, taken with a standard refractometer, revealed a carbonate blink from 1.48 to 1.65, and the polariscope established that the

material was a crystalline aggregate. On the basis of these findings and a specific gravity of 2.75, we identified the bead as calcite, rather than mother-of-pearl. Although both materials consist mainly of CaCO_3 , mother-of-pearl—a shell material—contains organic matter and water in its structure as a result of being excreted by a living creature. It should be noted that shell beads, not calcite, are the standard nucleus for cultured pearls in the industry today. A strand of very similar appearing pearls was recently advertised for sale as "mother of pearl jewelry" in the catalogue of a major department store. A special note stated that "Mother of pearl jewelry is derived from the inner lining of an oyster shell. This collection's magnificent luster is enhanced by a man-made protective coating. Again, we say *caveat emptor*—"buyer beware."

Wendi M. Mayerson

PHOTO CREDITS

Maha Tannous—figures 1, 5, 7, 11, and 12; Taijin Lu—figure 2; John I. Koivula—figures 3, 4, and 6; Jennifer Vaccaro—figures 8 and 13; Elizabeth Schrader—figures 9 and 15; Ann-Marie Walker—figure 10; Wendi Mayerson—figure 14.

GEMS & GEMOLOGY

For regular updates from the world of GEMS & GEMOLOGY, visit our website at:
www.gia.edu/gandg/

Thank You, Donors

The Treasured Gifts Council, chaired by Richard Greenwood, was established to encourage individual and corporate gifts-in-kind of stones, library materials, and other non-cash assets that can be used directly in GIA's educational and research activities. Gifts-in-kind help GIA serve the gem and jewelry industry worldwide while offering donors significant philanthropic and tax benefits. We extend a sincere thank you to all those who contributed to the Treasured Gifts Council in 2000.

\$100,000 or Higher

Daniel & Bo Banks

\$10,000 to \$49,999

Robert & Marlene Anderson
Harry G. Kazanjian & Sons, Inc.
Kennecott Exploration
Company
William and Jeanne Larson
Oro America
Frederick H. Pough, Ph.D.
John & Laura Ramsey
Ken Roberts
Marc Sarosi
Leo F. Stornelli, M.D.

\$5,000 to \$9,999

Theodore & Corinne Grussing
Scott D. Isslieb, G.G.
Christopher LaVarco
Elena Villa Hamann
World Sapphire

\$2,500 to \$4,999

Lee Allison
Argyle Diamonds
Richard E. Brown
Capalion Enterprises
Martin B. de Silva, G.G.
Ebert & Company
Inland Empire Alumni Chapter
Island Legacy, Ltd.

Jewelmer International
Corporation
Leo Hamel & Company
Donald K. Olson & Associates
Tycoon
Jim Yaras

\$1,000 to \$2,499

Associated Gem & Jewelry
Appraisal Service
Heitor Dimas Barbosa
Gary W. Bowersox, G.G.
Douglas Burleigh
Esther Fortunoff
GIA Research
Ben Gordon, G.G.
Barbara Hess
Johannes Hunter Jewelers
Linda Koenig
William C. Reiman
Sara Gem Corporation
Sirimitr Mining Co., Ltd.
Velma Touraine

\$500 to \$999

Allerton Cushman & Co.
Irv Brown
Equatorial Imports, Inc.
Erbgem Company
Brian Hudson

Kwiat, Inc.
Raul Haas/Hyde Park Jewelers
J. Blue Sheppard
Sherry Stuckey

Under \$500

Ronnie Alkalay
American Deepwater
Engineering
Beija-Flor Gems
K. C. Bell
William E. Boyajian, G.G.
Ann D. Broussard
Carl Chilstrom, G.G.
Donald Clary
Professor Jório Coelho
Jo Ellen Cole, G.G., F.G.A.
Companhia Baiana de Pesquisa
Mineral
Stevie Dillon
Dona M. Dirlam, G.G., F.G.A.
Pete J. Dunn, Ph.D.
David S. Epstein
Elaine Ferrari-Santhon, G.G.,
C.G.
Sondra Francis, G.G.
Gebrüder Bank Gemstones
Maggi R. Gunn
Barbara E. Haner

Hearts On Fire Company
Claus Hedegaard, Ph.D.
Herteen & Stocker
Jan David Design Goldsmith
A. J. A. Janse, Ph.D.
Jewelry by Gail, Inc.
Mary L. Johnson, Ph.D.
Jonté Berlon Gems
Joseph's Jewelers
Robert E. Kane, G.G.
Joachim Karfunkel, Ph.D.
Gail Brett Levine, G.G.
Veston Malango
Wendi M. Mayerson, G.G.
Yves Morrier
Primary Industries & Resources
SA
Dwight Rodrigues Soares
Douglas Rountree
Jackie Russell
Scheherazade Jewelers
Art Sexauer
Thorsten A. Strom, G.G.
Topázio Imperial
Paige S. Tullos, G.G.
United States Pearl Co., Ltd.
Martha M. Wampler, G.G.
Betty Waznis
Victor E. Zagorsky, Ph.D.

In its efforts to serve the gem and jewelry industry, GIA can use a wide variety of gifts. These include natural untreated and treated stones, as well as synthetics and simulants, media resources for the Richard T. Liddicoat Library, and equipment and instruments for ongoing research support. If you are interested in making a donation, and receiving tax deduction information, please call Heather Childers at (800) 421-7250, ext. 4139. From outside the U.S. call (760) 603-4139, fax (760) 603-4199. Every effort has been made to avoid errors in this listing. If we have accidentally omitted or misprinted your name, please notify us at one of the above numbers.



EDITOR

Brendan M. Laurs (blaurs@gia.edu)

CONTRIBUTING EDITORS

Emmanuel Fritsch, *IMN, University of Nantes, France* (fritsch@cnrs-imn.fr)

Henry A. Hänni, *SSEF, Basel, Switzerland* (gemlab@ssef.ch)

Kenneth Scarratt, *AGTA Gemological Testing Center, New York* (kscarratt@email.msn.com)

Karl Schmetzer, *Petershausen, Germany*

James E. Shigley, *GIA Research, Carlsbad, California* (jshigley@gia.edu)

Christopher P. Smith, *Gübelin Gem Lab, Lucerne, Switzerland* (cpsgg12@hotmail.com)

DIAMONDS

Royal Asscher cut. Amsterdam's Royal Asscher Diamond Co., cutters of the Cullinan diamond, recently debuted the Royal Asscher cut (figure 1) at the JCK show in Las Vegas. The original Asscher cut (patented in 1902) was a squarish diamond with large corners, a high crown, a small table, and a deep pavilion (see, e.g., p. 165 of the Fall 1999 issue of *Gems & Gemology*). With 74 facets and a more geometric look, the Royal Asscher still retains the distinctive appearance of its predecessor. Both loose stones and a Royal Asscher cut diamond jewelry line are being marketed through M. Fabrikant & Sons, New York. Each diamond is accompanied by a GIA Gem Trade Laboratory diamond certificate.

Figure 1. Updating a traditional look, the Royal Asscher cut (here, 6.35 ct), debuted at the June 2001 JCK show in Las Vegas. Courtesy of M. Fabrikant & Sons.



Diamonds in Canada: An update. In 1991, Canada's Northwest Territories (NWT) was catapulted into the world spotlight with the discovery of diamond-bearing kimberlites in the Lac de Gras area of the Slave Geological Province (see, e.g., A. A. Levinson et al., "Diamond sources and production: Past, present, and future," Winter 1992 *Gems & Gemology*, pp. 234–254). Success has been swift, with several major developments in the last 10 years. The Ekati mine started production in 1998 (see, e.g., Winter 1998 *Gem News*, pp. 290–292), and the Diavik project is scheduled to begin production in 2003 (see the following entry by K. A. Mychaluk on a field excursion to these two mines). The Jericho and Snap Lake projects are in the "permitting" stage, with anticipated production slated to begin in 2003 and 2004, respectively. At least 250 additional occurrences of kimberlite, many of which are diamond bearing, have been discovered in the Slave Geological Province.

Three cutting factories (Sirius, Deton'Cho, and Arslanian) are operating in Yellowknife (the capital of the NWT). These factories provide training and employment for aboriginal people, as they supply the world market with Canadian mined, cut, and polished diamonds. Several brands of Canadian diamonds are now available with laser-inscribed logos (e.g., polar bear, snowflake, and maple leaf); in April 2001, BHP Diamonds, operator of the Ekati mine, began marketing EKATI™ diamonds.

The discovery of diamonds in the NWT led to accelerated exploration activity elsewhere in Canada as well. Currently, exploration is fueled primarily by the efforts of three major mining companies (De Beers Canada Mining, BHP Diamonds, and Rio Tinto) and about 30 smaller, junior to mid-sized companies. In recent years, numerous kimberlites have been found in western Canada (i.e., northern Alberta—44 pipes in two separate areas, discovered since 1996; and Saskatchewan—71 kimberlites, found primarily in the Fort à la Come area since 1988). Encouraging results from surveys of diamond indicator minerals in Manitoba

glacial tills have generated exploration activity there, but no diamond-bearing kimberlite has yet been found.

In central and eastern Canada, most exploration activity is taking place in two areas of Ontario: Wawa and the James Bay Lowlands (JBL; part of which is also in Quebec); the potential for diamonds in the JBL was first suggested a century ago (again, see Levinson et al., 1992). The large (16.7 ha) Victor pipe in the Attawapiskat area of the JBL is the most advanced Canadian diamond project outside the NWT, and is currently being evaluated by De Beers Canada Mining. Diamond exploration is gaining momentum in Quebec, primarily in three widely separated areas: the JBL, the Otish Mountains, and Torngat. In the Torngat area of the Ungava Peninsula (northeastern Quebec), at least 60 dikes of kimberlitic affinity, up to 5 m thick, can be traced for up to 10 km; although many contain diamonds, thus far these are uneconomic.

In 2000, the Ekati mine produced about 2.6 million carats of rough with an average value of nearly US\$170/ct; this represents approximately 2.5% of world production by weight and 5% by value. By 2005, if the Diavik, Jericho, and Snap Lake mines are in full production, Canada's contribution to the world supply of rough diamonds could be approximately 10% by weight and 15% by value. Yet, the exploration component of the Canadian diamond industry is still at an early stage, as compared to major producing countries (e.g., Botswana, South Africa, and Russia). The importance of the fledgling Canadian diamond industry apparently has not escaped the notice of unsavory (even criminal) elements. As early as May 1999, a mere six months after the opening of the Ekati mine, polished diamonds purported to be Canadian—but in far greater abundance than could conceivably have been mined and polished in that time frame—were being offered for sale on the world market (see, e.g., B. Avery, "That Canadian diamond may be bogus," *Calgary Herald*, May 15, 1999, p. D11). More recently, and of far greater concern, it has been suggested that "conflict" diamonds have been smuggled into Canada to circumvent international embargos (see, e.g., A. Mitrovica, "Smuggled 'blood' diamonds are here, police fear," *Globe and Mail*, March 29, 2001, p. A1).

Alfred A. Levinson
University of Calgary, Calgary
levinson@geo.ucalgary.ca

Bruce A. Kjarsgaard
Geological Survey of Canada, Ottawa

Field excursion to Canadian diamond mines. The diamond deposits of Canada's Northwest Territories (NWT) were recently highlighted at the 37th Forum on the Geology of Industrial Minerals, held in Victoria, British Columbia on May 22–25. This contributor participated in a four-day post-meeting field trip to the NWT, led by Dr. George Simandl of the British Columbia Ministry of



Figure 2. The Panda pit at the Ekati mine, currently 150 m deep, is now at half its projected open-pit depth of 300 m. The predominant rocks in the photo are granitic country rocks that surround the diamond-bearing kimberlite (not visible). The rectangular area in the lower left corner of the pit has been drilled in preparation for blasting. The ore trucks are designed to haul 240 tons of rock. Photo taken on May 27, 2001, by K. A. Mychaluk.

Energy and Mines. The itinerary included visits to the Ekati mine (operated by BHP Diamonds), the Diavik project (a joint venture between Diavik Diamond Mines and Aber Diamond Corp.), the Snap Lake project (owned by De Beers Canada Mining) and a diamond cutting facility operated by Sirius Diamonds in Yellowknife (for locations, see map accompanying D. Paget's "Canadian diamond production: A government perspective," Fall 1999 *Gems & Gemology*, pp. 40–41).

Darren Dyck, senior project geologist for BHP Diamonds, was our host at Ekati. We toured the mine, processing plant, tailings containment area, and living quarters for the mine's 400 personnel. The mine is currently extracting ore only from the Panda pit; eventually, a total of five kimberlites will be exploited (see Winter 1998 *Gem News*, pp. 290–292). The Panda pit, now at half its projected open-pit depth of 300 m, is 500 m in diameter at the top (see figure 2). Large amounts of granitic country

Editor's note: Bylines are provided for contributing editors and outside contributors; items without bylines were prepared by the section editor or other G&G staff. All contributions should be sent to Brendan Laurs at blaurs@gia.edu (e-mail), 760-603-4595 (fax), or GIA, 5345 Armada Drive, Carlsbad, CA 92008.

GEMS & GEMOLOGY, Vol. 37, No. 1, pp. 138–159
© 2001 Gemological Institute of America



Figure 3. At the future Diavik diamond mine, a kimberlite processing plant is being constructed. The tower in the left center of the photo will be the exhaust stack for the processing plant, and the low, white buildings in the distance are temporary living quarters for 700 people. The four kimberlite pipes that will be mined are located under the shallow waters of the ice-covered Lac de Gras in the far distance. Photo taken on May 28, 2001, by K. A. Mychaluk.

rock must be removed to mine the kimberlite; the stripping ratio is 14:1 (14 tonnes of granite for each tonne of kimberlite). Excavation of the pit has also exposed a smaller kimberlite pipe and several kimberlitic dikes. Eocene-age fossils have been recovered from crater-facies kimberlite in the Panda pit, including *Metasequoia* logs, fish teeth and scales, and a turtle femur; these suggest that the Panda kimberlite erupted 50 million years ago. Pre-stripping of two of the other four pipes, the Misery and the Koala, has already begun, with production expected to start in mid-2001 and spring 2002, respectively.

Currently, 10,000 tonnes of Ekati kimberlite are processed each day. After initial crushing and screening, about 4,000 tonnes/day undergo heavy-media separation. The resulting 200 tonnes/day of concentrate are processed by X-ray sorting (a small amount is also sent to a grease table). Security protocols prevented our visiting the X-ray sorting facility; in fact, security was tight throughout the tour. Using data gathered through a continuous series of audits, BHP Diamonds believes that they are recovering 99.9% of the diamonds larger than 1 mm (diamonds smaller than 1 mm are rejected into the tailings). A display of rough diamonds, typical of a day's production, was shown to our group. These stones, which would fill a coffee can, consisted primarily of sharp, near-colorless octahedrons and macles.

We saw evidence of many safety and environmental protection measures at Ekati. The most impressive was the Panda Diversion Channel, a >3-km-long canal that diverted water and fish from Panda Lake (which covered part of the Panda kimberlite) to Kodiak Lake. As part of the effort to minimize the environmental impact of mining the Panda pit, the canal reportedly channeled over 3,000 fish to Kodiak Lake last year.

At the Diavik project, more than 850 employees (a number that was expected to grow to 1,100 this summer) are constructing Canada's second diamond mine, which is projected to begin production in 2003. Arnold Enge, public affairs officer for Diavik Diamond Mines, navigated our group through the very busy site. The mine will extract ore from four Eocene-age kimberlite pipes (A-154S, A-154N, A-418, and A-21) under the shallow waters of Lac de Gras, via three open pits. Construction has begun on the processing plant (figure 3), living quarters, a myriad of roads, and the first of several dikes designed to hold back the waters of Lac de Gras. An estimated 8.9 million m³ of rock will be used in dike construction, and 26.5 million m³ of water will be pumped out before mining can begin. Over this past winter, 4,089 truckloads of materials, including 44 million liters of diesel fuel, were transported to the site on a 425 km "ice road" that connects Diavik with Yellowknife during the winter months.

Our hosts at the Snap Lake project were geologist Mike Allen and assistant site manager Jack Haynes, both of De Beers Canada Mining. Highlights included an underground tour of the diamondiferous kimberlite dike, which dips 5°–15° east under Snap Lake. A tunnel from which a bulk sample of the dike is being extracted has advanced 1,250 m along dip, and there are 600 m of additional workings along strike of the dike. On the basis of its composition and texture, the dike is believed to consist of a single intrusion of spinel-bearing phlogopite-monticellite kimberlite. It has been dated at 523 million years old, which is much older than the kimberlites at Ekati and Diavik. In 2000, approximately 6,000 tonnes of kimberlite from the tunnel were processed for ore-grade estimation. Future development will include several activities: extending the decline (500 m along dip and 400 m along strike), processing 9,000 tonnes of kimberlite, auditing the tailings, conducting an experimental seismic survey (with Diamondex Resources Ltd. and the University of British Columbia), implementing a fish habitat compensation program, and performing environmental baseline studies. Commercial diamond production is slated for 2004.

In Yellowknife, Jennifer Burgess, diamond resource specialist with Diavik Diamond Mines, gave us a technical presentation on the geology of the Diavik project. A drill core (from A-154S) and rough diamonds from the project were made available for microscopic examination. The core samples clearly showed the layered volcaniclastic nature of the Diavik kimberlites. Each kimberlite pipe at Diavik contains several volcaniclastic units with different ore grades. Diamondiferous nodules of eclogite (garnet lherzolite) have been found in the Diavik kimberlites, and both eclogitic and peridotitic diamonds have been identified.

Ten percent of Ekati's production is sold to Yellowknife-based cutting operations. Our tour of the Sirius Diamonds facility in Yellowknife was led by manager Peter Finnemore. About twenty cutters (see, e.g., fig-

ure 4) facet about 500–600 carats of rough (with finished weight averaging 50 points each) per month (average color G or better). With less than two years in operation, Sirius has faced high labor costs and a 50% turnover among its cutters. As such, the talent base for cutting fancies is not yet available, according to Mr. Finnemore. Currently, 80% of Sirius's sales are domestic. Mr. Finnemore stated that two other Yellowknife-based cutting facilities, Arslanian and Deton'Cho Diamond, employ approximately 55 and 25 cutters, respectively. A diamond-sorting facility in Yellowknife, owned and operated by BHP Diamonds, employs about a dozen people.

*Keith A. Mychaluk
Calgary, Alberta, Canada*

Diamond presentations at the PDAC conference. With an attendance of nearly 7,000, this year's annual conference of the Prospectors and Developers Association of Canada was held March 11–14 in Toronto. The main focus was exploration for diamonds and platinum group metals. The atmosphere was reminiscent of the diamond rush in the early 1990s, when scores of junior exploration companies promoted their properties (though only a few ultimately reached production status). Aside from the usual updates on specific projects, this year's diamond presentations included several market forecasts aimed at the investor, as well as projections about future demand.

De Beers's **Gary Ralfe** gave a lunchtime address in which he outlined the company's future role, specifically its transition from being a custodian of the diamond industry by controlling the availability of rough, to becoming the "supplier of choice." In the more formal presentations, **Matt Manson** of Aber Diamond Corp. observed that there is now pressure to shorten the diamond pipeline from both ends—retailer as well as producer—through tighter relationships and amalgamations. He added that with brand names, hallmarks, and e-commerce gaining widespread acceptance, the long-term outlook remains bright. Aber's **Bob Gannicott** examined preferences among buyers in the U.S., Southeast Asia, and Japan for diamond color, size, and clarity. He observed that Canadian diamonds show an unusually good fit to the demands of the American market, where the "baby boomer" generation (now 45–55 years old) has more disposable income to spend on luxury goods.

Malcolm Thurston of MRDI USA discussed how investors can evaluate information on diamond projects, from prospect to feasibility. He introduced the "four Q's": quality of data, quality of geologic modeling, quality of ore and cost estimates, and quantity of risk. All data must be collected and interpreted under a well-designed, properly supervised program of quality assurance and control. **Dr. Johan Ferreira** of De Beers downplayed the significance of micro- and macro-diamond size distribution in diamond resource estimation. He maintained that although the relationship is real, many other factors such

as sample site, volume, recovery method, and analysis of shapes and sizes must be considered. **Dr. Larry Heaman** of the University of Alberta noted the wide range in the ages of kimberlite emplacement, in some instances for pipes separated by short distances (as in the Slave Geological Province of Canada's Northwest Territories [NWT]). Episodes of kimberlite/lamproite emplacement that are currently known to be most economic are Precambrian (e.g., Premier pipe, South Africa; Argyle pipe, Australia), Devonian (Republic of Sakha, Russia), Cretaceous (South Africa), and Tertiary (NWT, Canada). **John McConnell** of De Beers Canada Mining presented the latest results on the Snap Lake project, which may become Canada's third diamond mine.

In the less formal Exchange Forum presentations, the directors of several junior exploration companies briefed attendees on the latest developments in Africa, Canada, and elsewhere. The projects discussed included: alluvial diamonds and potential pipe targets in South Africa, offshore operations near Lüderitz in Namibia, alluvial operations along the lower Orange River at Baken and the middle Orange River near Douglas (both in South Africa), discoveries in western Liberia's Mano River kimberlite field, the Aylmer West property in Canada's NWT, the latest kimberlite discovery in the Fort à la Corne kimberlite field in Saskatchewan, kimberlite and diamond discoveries in the Buffalo Hills area of Alberta, an update on the NWT's Jericho kimberlite, and the possibility of kimberlite pipes at the NWT's Snap Lake (in addition to the proven diamondiferous dike). Also presented were the results of exploration in Brazil and in the Wawa and James Bay Lowland areas of Ontario, Canada; the evalua-

Figure 4. Shane Fox, one of about 20 cutters presently working at the Sirius Diamonds factory in Yellowknife, is shown faceting a round brilliant. The company currently cuts 500–600 carats of rough Ekati diamonds per month. Photo by K. A. Mychaluk.



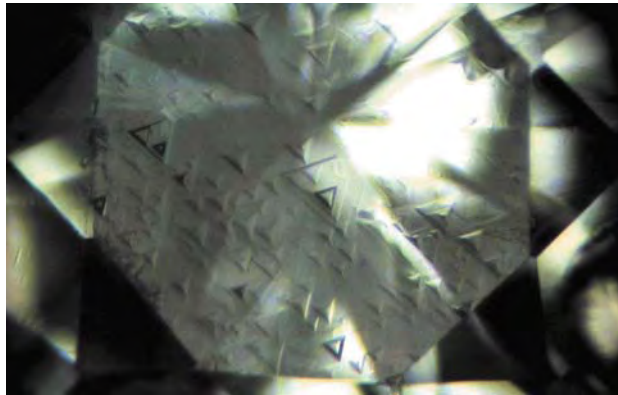


Figure 5. The table of this 2.4-mm-diameter diamond is covered with trigons. Photomicrograph by Robert Cloutier.

tion of the Payaliland kimberlite pipe in the new state of Chhattisgarh in India; and the problems of estimating the average value per carat in mine evaluation studies.

Overall, the mood of the conference was optimistic, with the number of diamond exploration projects increasing as venture capital is forthcoming once again.

A. J. A. (Bram) Janse
Archon Exploration, Carine, Western Australia
archon@space.net.au

A table with trigons. Diamond crystals commonly display triangular growth features on their surface, called trigons. After faceting, such features may be preserved on tiny relict crystal faces ("naturals") along the girdle or, less commonly, elsewhere on the diamond. It was with great surprise, therefore, when Richard Cloutier (Gemteck Appraisal Service, Phoenix, Arizona) observed trigons covering the table of a faceted diamond.

Figure 6. Swirls of color are commonly seen in polished Burmite from the Hukawng Valley, Myanmar. The earring pendants each measure 2.1 × 3.0 cm. Photo by Maha Tannous.



Mr. Cloutier was appraising an antique 18K yellow gold pin set with 13 diamonds when he noticed trigons on the table of one of the stones during his preliminary examination with a 10× loupe. Examination of the 2.4-mm-diameter diamond with a microscope revealed trigons over the entire surface of the table (figure 5). Perhaps an unusual shape to the rough caused the cutter to use the trigon-containing octahedral face for the table.

COLORED STONES AND ORGANIC MATERIALS

Amber ("Burmite") from Myanmar: Production resumes. Amber from Myanmar (Burma) has been used by Chinese craftsmen to produce art objects since the 1st century AD (see V. V. Zherikhin and A. J. Ross, "A review of the history, geology and age of Burmese amber [Burmite]," *Bulletin of the Natural History Museum [London], Geology Series*, Vol. 56, No. 1, 2000, pp. 3–10). However, it rarely reached Western markets before the late 19th century. The deposits are located in the Hukawng Valley, northern Kachin State, about 80 km north-northeast of the famous jadeite mining area in the Uru River valley (U Tin Hlaing, "Burmite—Burmese amber," *Australian Gemmologist*, Vol. 20, No. 6, 1999, pp. 250–253). The amber, sometimes called "Burmite," shows many differences from material derived from the Baltic and the Dominican Republic. Specifically, it ranges from almost perfectly transparent to opaque, has more-saturated and darker colors (which vary from yellow to red, with dark reddish brown being typical), and, with respect to the Baltic material, is reported to have greater hardness and density (R. Webster, *Gems*, 5th ed., revised by P. G. Read, Butterworth-Heinemann, 1994, p. 573). The last two characteristics make Burmite particularly amenable to carving and manufacture into jewelry (figure 6).

Prior to World War II, while the country was still under British rule, commercial quantities of Burmese amber were produced. Since the 1940s, however, the material has been essentially unavailable due to internal problems. Mining resumed in the mid-1990s, and from 1995 to 1997 several commercial shipments of Burmite were made to China. Since then, for various reasons including low prices for the amber, there has been little formal mining and essentially no export of either rough or polished material.

Recently, however, a new joint venture has begun to exploit the material, with the goal of exporting 500 kg (1,100 pounds) of Burmite annually during the next few years. In 2000, Leeward Capital Corp., a Calgary-based Canadian company, made a contractual arrangement with a Myanmar company to purchase all the Burmite produced in the mining area located near the town of Tanai along the Ledo Road (of World War II fame). Using simple recovery methods (figure 7), as many as 60 miners work the deposits during the dry season. First they dig test pits to locate an unweathered amber-containing seam, and then they use open-pit methods to mine this



Figure 7. Miners follow the dark-colored amber-bearing horizon in search of Burmite at the Noiye Bum mine, near Tanai, Kachin State, Myanmar. The open-pit area at this mine measures 30 × 120 m. Photo by R. D. Cruickshank.

horizon. Most of the amber is found as disc-shaped fragments that range from a few millimeters up to several centimeters in diameter. Large-scale mechanized mining is not feasible, because the material is too delicate and the seams are too narrow. In 2000, Leeward Capital obtained 78 kg of Burmite, and by June 2001 a total of 300 kg of mixed-grade material had been obtained in pieces up to 25 cm in maximum dimension.

Inclusions of insects and other biological materials (e.g., pollen and plant remains) appear to be more abundant in Burmite than they are in Baltic amber (J. W. Davis, pers. comm., 2001; see also abstract of "The history, geology, age, and fauna [mainly insects] of Burmese amber, Myanmar" in the Gemological Abstracts section). So far, inclusions have been found in an average of 30 pieces per kilogram of current production. The entombed insects

Figure 8. This 1 mm parasitic wasp (Serphitidae) in Burmite is characteristic of the Cretaceous Period, and provides evidence that the amber is about 100 million years old. Photo © Dr. D. A. Grimaldi, American Museum of Natural History, New York.



Figure 9. This 19.39 ct amethyst from Brazil displays chatoyancy. Photo by Jaroslav Hyrsl.

(see, e.g., figure 8) indicate a Cretaceous age of ~100 million years (Dr. D. A. Grimaldi, pers. comm., 2001), which is significantly older than amber from the Dominican Republic (~30 My) or the Baltic (~40 My; see, e.g., D. A. Grimaldi, *Amber: Window to the Past*, Harry N. Abrams, New York, 1996).

Alfred A. Levinson

Cat's-eye amethyst from Brazil. Amethyst is one of the more common gems, but it rarely displays chatoyancy. Therefore, this contributor was most intrigued by two cat's-eye amethysts he purchased during a visit to Brazil in summer 2000.

The translucent, dark violet stones weighed 30.91 and 19.39 ct (figure 9). With standard gemological testing, they both had a spot R.I. of 1.55 and a specific gravity of 2.65. When examined with a polariscope, both stones showed normal extinction (whereas purple chalcedony would have exhibited an aggregate structure). With magnification, the amethysts revealed distinct color zoning, as well as a dense array of fibrous inclusions oriented perpendicular to the color zones (figure 10). These inclusions were distributed homogeneously in both stones, and were responsible for their chatoyancy.

With high magnification, the fibrous inclusions appeared to consist of tiny elongate negative crystals and two-phase inclusions. They also were visible in two other orientations, at an angle of approximately 45° to the main direction. Their exact crystallographic orientations could not be measured, because the translucency of the stones



Figure 10. Numerous fibrous inclusions are present in the cat's-eye amethyst shown in figure 9, and are oriented perpendicular to subtle color zoning. Note also the smaller fibrous inclusions oriented at approximately 45° to the main direction. Photo by Jaroslav Hyrsl; width of view 5.4 mm.

hindered determination of the optic-axis direction. Although present in both stones, fibrous inclusions with these suborientations were more common in the larger sample. Therefore, the smaller amethyst showed more pronounced chatoyancy.

Jaroslav Hyrsl
Kolin, Czech Republic
hyrsl@kuryr.cz

Brownish red to orange gems from Afghanistan/Pakistan misrepresented as bastnäsite and other materials. During the 2001 Tucson show, one of us (DB) received from the cutting factory a number of faceted brownish red to orange stones that were reportedly bastnäsite. The rough was purchased in Peshawar, Pakistan, and the location was given as a tribal area on the Pakistan/Afghanistan border northwest of Peshawar. Examination of several stones by JH revealed that one of them was actually grossular garnet.

Also at the 2001 Tucson show, one of us (JH) purchased two brownish orange stones that were represented as sphene from Afghanistan or Pakistan. Gemological testing showed that one of the stones was indeed sphene, but the other was zircon. Subsequent gem testing of five "bastnäsites" from DB revealed that one of them also was a sphene. DB also submitted a brownish yellow-orange gemstone to the GIA Gem Trade Laboratory in Carlsbad, which was subsequently identified as sphene (figure 11). Clearly, these four red-to-orange gem materials are easily misidentified by the miners and dealers. Identification of the rough is especially difficult because it is typically broken and weathered.

It is easy to separate grossular from the other gems by its isotropic optic character. The doubly refractive gems may show distinctive features with the spectroscope: Zircon has a distinctive spectrum, bastnäsite shows many

strong lines due to rare-earth elements (see Summer 1999 Lab Notes, pp. 136–137), and sphene has a faint "didymium" spectrum that is identical to that of yellow apatite (see, e.g., R. Webster, *Gems*, 5th ed., revised by P. G. Read, Butterworth-Heinemann, Oxford, 1994, pp. 315–316). The specific gravity values of the three anisotropic stones also differ, and a standard refractometer will give one of the refractive indices (around 1.722) for bastnäsite, whereas grossular is 1.74 and zircon and sphene are over-the-limit of most refractometers. Examination with a gemological microscope revealed brown needle-like inclusions in almost all of the bastnäsite samples; these were recently identified as astrophyllite in bastnäsite from Pakistan (see G. Niedermayr, "Bastnaesit aus Pakistan—ein neuer Schmuckstein?" *Mineralien Welt*, Vol. 12, No. 3, 2001, p. 51). When exposed to long- or short-wave UV radiation, only the zircon showed fluorescence (yellow), while the other gems were inert. As is typically the case in gemology, more than one test is necessary to make a positive identification.

Dudley Blauwet
Dudley Blauwet Gems, Louisville, Colorado
Jaroslav Hyrsl

Spinel with clinohumite from Mahenge, Tanzania. The Mahenge region in southern Tanzania is well known for the marble-hosted ruby deposits found there (see, e.g., J. Kanis, "Morogoro and Mahenge ruby occurrences, Tanzania," 27th International Gemological Congress

Figure 11. Represented as bastnäsite, this 2.12 ct brownish yellow-orange stone was identified as sphene. Photo by Maha Tannous; courtesy of Dudley Blauwet.



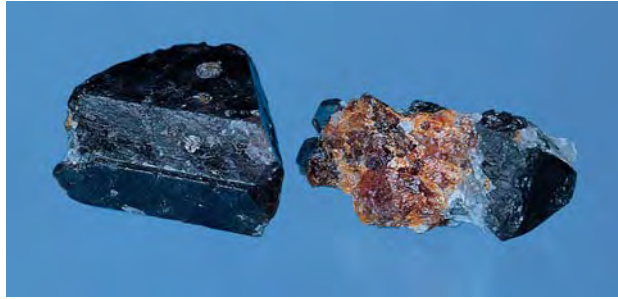


Figure 12. Crystals of dark purple spinel from a new find near Mahenge, Tanzania, were found associated with an orange mineral that proved to be gem-quality clinohumite. The specimen on the right (with the clinohumite) measures 3.5×1.5 cm. Photo by Jaroslav Hyrsl.

handbook, Mumbai, India, 1999, pp. 70–73). In summer 2000, a small mine near the town of Mahenge produced some attractive spinel specimens—dark purple crystals in a matrix of white marble. The crystals ranged up to about 5 cm as octahedrons and, rarely, flattened spinel-law twins (figure 12).

Although small portions of the spinel are facetable, the real interest for gemologists lies in an associated orange mineral, which the dealer presumed was spessartine garnet. The specimens show a striking similarity to material from Kuchi-Lal in the Pamir Mountains of Tajikistan—a famous locality for gemmy pink spinel and clinohumite. X-ray diffraction analysis confirmed that the orange mineral from Mahenge was clinohumite, a rare Mg-silicate that is known in cuttable quality from very few places in the world. Unlike spessartine (which has a hardness of 7–7.5), clinohumite has a hardness of only 6 on the Mohs scale. Clinohumite also has different optical properties. However, the fastest way to distinguish the two minerals, both for faceted gems and rough, is with UV fluorescence: Spessartine is inert, whereas clinohumite glows strong orange to short-wave UV radiation. The dealer informed this contributor that the better-quality material had already been cut in Tanzania and sold as spessartine.

Jaroslav Hyrsl

An interesting engraved emerald. The 1.72 ct carved and faceted emerald shown in figure 13 was part of a large parcel of broken stones that William Larson (Pala International, Fallbrook, California) recently purchased from a major jeweler. After several hours of sifting through what turned out to be mostly glass and synthetics, one of these contributors (RWH) noticed an emerald that initially appeared to be badly scratched. Closer examination with a microscope revealed that the table was actually engraved in Arabic (again, see figure 13). The engraving translates as “Please God, announce good tidings.” Curiously, the writing is engraved in reverse, and

can only be read correctly through the faceted side of the stone. In addition, the facet orientations and inclusions in the stone make it very difficult to read. However, an impression from the engraved side of the stone (in, for example, wax) would read in the correct manner, which leads us to surmise that the stone was once mounted in a ring and used as a seal.

The stone measured $9.54 \times 7.50 \times 2.80$ mm, and had R.I. values of 1.572–1.580. When examined with a Chelsea filter, the stone appeared orangy red. Some small cracks exhibited a weak yellow fluorescence to long-wave UV radiation, but the stone was inert to short-wave UV. Examination with the microscope revealed both a classic three-phase inclusion and a modified cube of pyrite, which suggests a Colombian origin. A similar engraved Colombian emerald was featured on the cover of the Summer 1981 issue of *Gems & Gemology*: That 217.8 ct Mogul emerald was engraved with an Islamic prayer, although not in reverse. Such stones are representative of the early Colombian emeralds that were treasured by the Mogul nobility in India.

Maha Tannous and John I. Koivula
GIA Gem Trade Laboratory, Carlsbad
mtannous@gia.edu

Richard W. Hughes
Pala International
Fallbrook, California

Figure 13. This 1.72 ct engraved natural emerald was found in a large parcel of stones, most of which were glass or synthetics. The Arabic inscription was done in reverse, so it can only be read through the faceted stone or as an impression in wax. For this reason, it is believed that the stone was originally used in a seal ring. Photo by Maha Tannous.





Figure 14. A jewelry designer could use the light coppery reflective display of rutile in this 79.66 ct freeform polished quartz to create an interesting one-of-a-kind brooch. Photo by Maha Tannous.

Unusual rutilated quartz. Rutilated quartz is never in short supply at the Tucson shows. Faceted stones, cabochons, beads, and polished crystals are just some of the forms encountered. While most of this material is composed of randomly oriented needles of rutile scattered in colorless or smoky quartz, occasionally an unusual exam-

Figure 15. With magnification (here 5×), the complex branching growth of the twinned rutile structure is seen in detail. In darkfield illumination, the red-brown color of the rutile is also apparent. Photomicrograph by John I. Koivula.



ple of this relatively common mineral combination is encountered. One of the most sought-after forms of rutilated quartz, for jewelry designers in particular, occurs when the rutile fibers radiate outward from six-sided black ilmenite-hematite inclusions. Less well known, and perhaps even rarer than these rutile “stars,” are macrodisplays of rutile that form geometric “scaffolds” of elongated twinned crystals.

A relatively large rutilated quartz of this latter type was discovered at the Tucson show booth of Tucson jewelry designer and lapidary, Kevin Lane Smith. Weighing 79.66 ct and measuring 54.4 × 34.9 × 5.2 mm, this unusual freeform polished quartz (figure 14) could be used as the centerpiece in an impressive piece of jewelry. It is also attractive under magnification, with the translucent red-brown color of the rutile and the complex branching growth of the twinned sagenitic structure (figure 15) adding an element of intrigue that seems to draw an observer in for a closer look. While rutilated quartz is relatively common, examples such as this are not often seen.

John I. Koivula and Maha Tannous
jkoivula@gia.edu

Important new ruby deposits in eastern Madagascar:

Chemistry and internal features. In January 2001, rough stone buyer Werner Spaltenstein informed staff members at SSEF that two important new ruby deposits had been found in eastern Madagascar—near Vatoman-dry and Andilamena. To investigate the new rubies, this contributor recently traveled to Chanthaburi, Thailand, where a significant amount of the material is processed and sold (figure 16). Several dozen rough and cut rubies (both heated and unheated) were examined in Chanthaburi, and some were selected for further study at the SSEF laboratory in Basel.

Vatoman-dry is located east of the capital city of Antananarivo. The rough from this area is typically a saturated purplish red that responds well to heat treatment; it occurs as rounded fragments up to 1 cm (again, see figure 16). Faceted rubies as large as 6 ct have been cut. Microscopic examination revealed veils of fluid inclusions, as well as mineral inclusions formed by isolated crystals or clusters of tiny crystals (figure 17, left). Using laser Raman microspectrometry, SSEF identified the minerals in the clusters as zircon; they resemble the zircon clusters commonly seen in gem corundum from Umba, Tanzania. The larger isolated inclusions were identified as apatite (colorless) and rutile (dark orange-brown); the latter also formed oriented needles (silk; figure 17, right). The large individual rutile inclusions are protogenetic (i.e., formed before the ruby host), whereas the rutile as silk is epigenetic (i.e., formed after ruby crystallization). Most of the ruby crystals also showed thin twin lamellae in all three rhombohedral directions (see figure 17, left). Trace-element analysis of the two rubies (the lightest and darkest samples available) by

EDXRF at the SSEF laboratory showed significant Cr (0.6–1.2 wt.% Cr₂O₃) and Fe (0.5–0.7 wt.% Fe₂O₃), as well as smaller amounts of Ti, V, and Ga.

The other new ruby source—near Andilamena—is situated 200 km from the eastern coastline near the town of Ambatondrazaka. This area is already known for its beautiful yellow chrysoberyl twins (see, e.g., F. Pezzotta, *Madagascar, extraLapis* No. 17, 1999, pp. 47–48). The ruby typically occurs as euhedral, tabular, saturated purplish red crystals (again, see figure 16); faceted gems up to 12 ct are known. Asterism has been seen in some stones. Inclusions of zircon and rutile (the latter as silk and dark isolated crystals) were identified by Raman analysis (figure 18), and scaffold-like intersections of twin lamellae were seen with the microscope. EDXRF analyses of two samples (again, the lightest and darkest) showed significant amounts of Cr (0.4–1.8 wt.%) and Fe (approximately 0.9 wt.%), and smaller amounts of Ti, V, and Ga.

HAH

The new ruby deposits in eastern Madagascar: Mining and production. This contributor, who is involved with a company that is trading material from Vatomandry and Andilamena (see, e.g., figure 19), supplied further details on accessing and mining these deposits, as well as some preliminary observations about the rough.

The Vatomandry deposit was discovered in September 2000. Access to the mining area, which lies along the Sakanila River, requires traveling on a dirt road approximately 30 km southwest of the coastal town of Vatomandry, which is located 140 km south of Tamatave (Toamasina). Most of the rainforest in this area was cleared in the past by periodic slash-and-burn cultivation.

Soon after the ruby discovery, several thousand miners moved to the region and started mining with basic equipment (i.e., shovels and hand-sieves). Many areas, each measuring 1–3 km², have been worked. So far, the most productive area is located near the village of Tetezampaho. The rubies are found in a layer of gravel about 30 cm thick that generally lies less than 2 m below the surface. The miners wash the gem-bearing gravel in small rivers using hand sieves. Grayish or greenish blue sapphires are also



Figure 16. These heat-treated rubies are from two new mining areas in Madagascar: Vatomandry (rough and cut, left) and Andilamena (two crystals on the right; up to 14 mm long). The inset shows parcels of unheated ruby from Vatomandry (left) and Andilamena (right). Photos by H. A. Hänni.

found in the gravel, many weighing 0.5 grams and larger, but initial heat treatment of this material has proved unsatisfactory. The majority of the ruby rough weighs 0.1–0.3 grams, and rough stones exceeding one gram are rare. Although most of the rubies are purplish red, some show an attractive color that is similar to that of fine Burmese rubies. About 30%–40% of the Vatomandry rubies are marketable without heat treatment.

After the initial rush, the Malagasy government closed the area to mining in February 2001. The closure was done to avoid the environmental and tax problems attendant to uncontrolled exploitation of the region by thousands of independent miners, as has been the case with the Ilakaka gem rush over the past two years. The military enforced the closure, and all trading and exporting of gems from this area were prohibited. Many of the miners have left the region, and ruby production has decreased substantially. The government has since divided the area into claims (2.5 × 2.5 km each) that will be auctioned to companies that meet specific criteria. These criteria were announced by the Ministry of Mines in mid-June. At press-time, interested companies had until mid-July to bid for claims. The minimum bid for each claim was

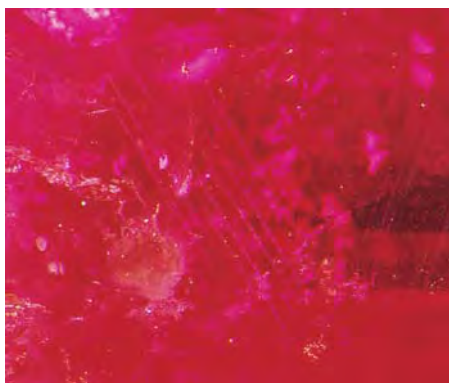


Figure 17. The heat-treated ruby from Vatomandry on the left contains clusters of tiny zircon crystals, as well as larger inclusions of apatite (colorless) and rutile (dark). Also present are partially healed fractures and lines created by intersecting twin lamellae. On the right, partially resorbed silk and zircon clusters are visible in another heat-treated Vatomandry ruby. Photomicrographs by H. A. Hänni; magnified 20×.

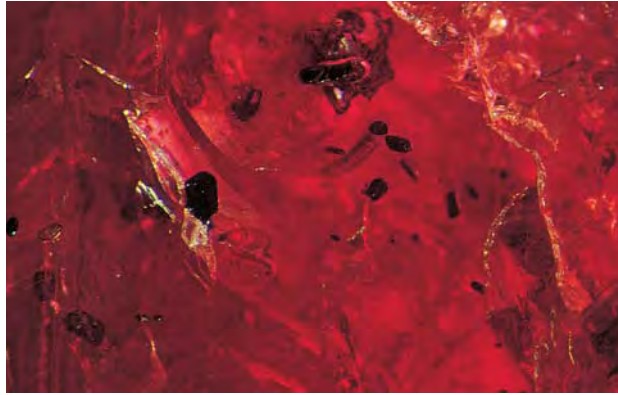


Figure 18. This unheated ruby from Andilamena contains inclusions of dark-appearing rutile crystals and colorless zircon crystals. Photomicrograph by H. A. Hänni; magnified 20 \times .

around US\$30,000, with the claims to be awarded to the highest bidder. It is difficult to estimate the overall ruby production from Vatoman-dry, because most trading was done illegally and the stones were smuggled out of the country. This contributor estimates that more than 70 kg of rough have been recovered, and all indications are that the region has tremendous potential.

The ruby deposit near Andilamena lies within tropical rainforest at the eastern margin of the country's northern high plateau (figure 20). The area can be reached only by foot, following a path that leads about 45 km northeast from Andilamena. An exhausting one to two days of travel is required to visit the mines. The first rubies were dis-

Figure 20. In the Andilamena area of Madagascar, rubies are mined in a remote location within tropical rainforest. Photo by Rakotsoana Nirina.



Figure 19. These unheated rubies (the largest is 2.02 ct) are from the new deposits in eastern Madagascar. Photo by Elizabeth Schrader.

covered in October 2000, but these were not transparent and appeared over-dark. Better-quality material was found in January 2001, and a "gold-rush" atmosphere ensued (figure 21). Hundreds of people arrived each day—many from Ilakaka—and began digging unsystematically without making any attempt at prospecting. By chance, two productive areas were discovered, each about 1–3 km². Within six weeks, nearly 40,000 miners were working in the area, digging with very basic equipment, and living in shacks composed of wood and plastic sheeting. Food and provisions were brought from Andilamena, which also became the headquarters for gem trading. Since foreign buyers are not allowed into the mining area, many have set up offices in Andilamena. Most of the buyers are from Thailand, or are related to Thai companies. The Malagasy government attempted to close the mining area this past April, but their efforts were unsuccessful because of the large number of people who are widely scattered throughout the rather inaccessible area. By late June, several of the major buyers had left Andilamena and many of the miners had returned to Ilakaka. Nevertheless, there was still significant mining and production from the area.

The Andilamena rubies are mined from a layer of gravel that generally lies 2–3 m below the surface. Ore grades can be quite high: More than 100 grams of ruby per cubic meter of gravel have been recovered from some areas. As a result, large quantities were produced in a short time. This contributor estimates that about 2 tons of all grades of ruby had been mined as of May 2001. Most of this material is fractured throughout and appears over-dark. Nevertheless, a significant amount of transparent red to purplish red material has been found. Most of the rough occurs as well-formed tabular crystals (which average 0.5 gram each) with slightly to moderately rounded edges. Clean, attractive rubies showing fine red color are very rare, but they can exceed 5 grams. Some sapphire is also recovered, as at Vatoman-dry.

The new ruby deposits of eastern Madagascar probably share a similar geologic origin. According to Dr. Federico Pezzotta (Museo Civico di Storia Naturale, Milan, Italy), the area between Vatoman-dry and Andilamena is known for the presence of abundant corundum in metamorphic



Figure 21. In a rush to stake their claims, tens of thousands of miners have journeyed to the Andilamena area. The rubies are mined by simple methods from a layer of gravel that typically lies 2–3 m below the surface. Photo by Rakotosaona Nirina.

rocks that apparently formed by the interaction of desilicated granitoid (locally pegmatitic) intrusions with mafic and ultramafic host rocks. The ruby crystals do not appear to have undergone significant alluvial transport. Prospecting is hindered by the lack of detailed geologic studies and the fact that there are few outcrops in either mining area.

The Malagasy rubies have clearly made a significant impact on the ruby trade. During a visit to Chanthaburi in late April 2001, this contributor noted a sharp decrease in the price of medium- to low-quality rubies, which have flooded the market there. According to Thai heat treaters, the over-dark colors cannot be lightened by heating. However, heat treatment is successful in removing some of the purple component from the lighter-colored material.

*Alexander Leuenberger
Isalo Gems & Mining, Antananarivo, Madagascar
a.leu@bluewin.ch*

Ruby crystal with large mobile gas bubble. Southern California gem dealer William Larson is always looking for unique or unusual items during his frequent buying trips to Myanmar. One such gemological curiosity found on a recent trip was a 2.46 ct ruby crystal with four randomly placed polished flats (figure 22).

This specimen (which measured $7.92 \times 5.85 \times 5.38$ mm) was unusual in that it contained a large (almost 4

mm) negative crystal with a 1-mm-diameter free-moving gas bubble (again, see figure 22). Also seen moving within the liquid phase were numerous tiny white solid particles, which make this a three-phase inclusion. Although both primary and secondary fluid inclusions are known to occur in rubies from Myanmar, the very large size of this

Figure 22. This 2.46 ct Burmese ruby crystal contains a fluid inclusion with a free-floating 1-mm-diameter gas bubble. Photomicrograph by John I. Koivula; magnified 5 \times .





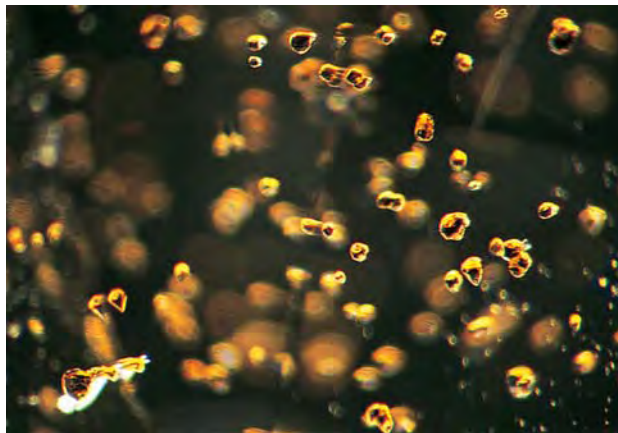
Figure 23. This 28.04 ct natural sapphire was interesting because of its size and color in relation to the stated locality, Myanmar, and because of the inclusions it contained. Photo by Kenneth Scarratt.

primary negative crystal, and the mobility and size of the gas phase and the mobile solid phase(s) inside it, are especially noteworthy.

It is fortunate that the inclusion was not damaged during placement of the polished faces. Large fluid inclusions are very sensitive to heat, and significant heat can be generated by friction during cutting. Also, since the precise extent of this fluid inclusion in the ruby is not clearly visible, the chamber could easily have been opened during the grinding of the flats, causing the fluid to drain out.

John I. Koivula and
Jo Ellen Cole
GIA, Carlsbad

Figure 24. Raman analysis identified these brownish yellow inclusions in the brownish green sapphire shown in figure 23 as pyrochlore. Photomicrograph by John I. Koivula; magnified 15 \times .



A brownish green sapphire, with pyrochlore inclusions. A large, slightly brownish green sapphire, reportedly from Myanmar, was recently seen in both the AGTA laboratory in New York and the GIA Gem Trade Laboratory in Carlsbad. The gem, an oval mixed cut that weighed 28.04 ct and measured 18.80 \times 17.28 \times 10.89 mm (figure 23), was brought to our attention by Joseph Krashes, of Krashes Dirnfeld, New York. It was interesting not only because of its size and color in relation to the stated locality, but also because of the inclusions it contained.

The sapphire played host to a number of transparent to translucent brownish yellow inclusions (figure 24), a few of which had been exposed to the surface during faceting. When we examined some of the inclusions with higher magnification using a digital camera attached to a Raman microscope, we observed a crystal form that suggested that they were isometric, and no pleochroism was visible with polarized light. The slightly rounded surface of the inclusions suggested that dissolution might have occurred prior to their incorporation into the sapphire. The transparency and general condition of these inclusions and their immediate surroundings indicated that the host sapphire had not been subjected to high-temperature heat treatment—an important consideration in today's sapphire market.

Laser Raman microspectrometry of the inclusions at both laboratories identified them as pyrochlore. In the past, the pyrochlore inclusions we have encountered in sapphires have always been dark red to brownish red and observed in blue to blue-green sapphires (see, e.g., figure 25). This is the first time that either laboratory has identified brownish yellow pyrochlore inclusions in sapphire of any color.

John I. Koivula and K. Scarratt

Update on the Vortex sapphire mine, Yogo Gulch, Montana. Last summer, this contributor revisited the Vortex sapphire mine at Yogo Gulch, Montana, for the first time since 1995 (see K. A. Mychaluk, "The Yogo sapphire deposit," Spring 1995 *Gems & Gemology*, pp. 28–41). Vortex Mining Co. provided unrestricted access to their operation. Since 1995, there has been a considerable expansion in surface equipment, manpower, and safety measures, as described in this update.

A new steel head frame (figure 26; compare with figure 12 in Mychaluk, 1995) has been erected, which greatly improves haulage capacity from the underground workings. Ventilation ducts and fans now provide air circulation to the entire mine. In addition to the 76-m-deep main shaft (erroneously reported as 61 m deep in Mychaluk, 1995; depth unchanged since then), a new tunnel is being excavated from the lowest levels to the surface, giving miners increased ventilation and an alternate escape route. Compressed air and electricity are now available on each level, and several mine phones have been added. As in the past, very few timber supports were observed in the mine, because of the competency of the limestone host rock. At

press time a crew of nine was working, and as many as 14 miners worked the mine last winter.

The underground workings follow two distinct, sub-parallel sapphire-bearing dikes (described as E and F by Mychaluk, 1995), which are more than 70 m apart. To excavate the sapphire-bearing ore, the miners drive horizontal tunnels into each dike and then stope upwards. A tunnel at the 76 m level has now advanced 80 m along the E dike, with large stopes reaching almost to the surface. A new crosscut (i.e., a tunnel driven at a right angle to the dikes), also at the 76 m level, has reached the previously unmined F dike, and another horizontal tunnel has explored about 30 m of this dike. Again, large stopes extend upward from this level. A natural cave system, which is actively forming in the limestone adjacent to the dikes, has been exposed at the 76 m level; the layered floor sediments in the cave contain fragments of sapphire-bearing dike rock. The mine yielded 60,000 carats of gem-quality sapphire rough during the period 1995–2000. To help increase production, Vortex has begun excavating a 900-m-long access tunnel (a “decline”), which is currently 460 m long and has reached a level of 82 m below the surface.

The thickness of both the E and F dikes varies widely, although they are predominantly 0.25–0.5 m wide. Xenoliths of limestone host rock are locally present within the dikes. The miners have worked around these obstructions, leaving them as pillars within the tunnels. Very little contact metamorphism was noted between the limestone country rocks and the dike rocks. All of the sapphire-bearing dike rock observed *in situ* was deeply weathered (to clay and carbonate minerals). Because this material is soft and friable, it is easily mined. Limited

Figure 25. In contrast to their brownish yellow color in the sapphire shown in figure 24, pyrochlore inclusions in blue sapphire typically are dark brownish red. Photomicrograph by John I. Koivula; magnified 20×.



Figure 26. Many improvements have been made at the Vortex sapphire mine at Yogo Gulch, Montana, over the last several years, including this new steel head frame. Photo by K. A. Mychaluk.

blasting breaks up the ore, which is then loaded into ore carts, transported to the elevator, and brought to the surface. The procedure for processing the ore was unchanged from that described in Mychaluk (1995), although a new mill with 200-ton-per-day capacity began operating in mid-June 2001. Sapphire grains as small as 2 mm were being collected in Vortex’s gravity-separation plant, which suggests efficient recovery.

A large selection of rough and faceted sapphires and finished jewelry was seen at the mine site. Except for a few well-saturated purple sapphires, all of the stones (none of which had been heat treated) were a consistent “cornflower” blue. Most notable were a 2.78 ct oval-cut sapphire and a 3 ct rough stone, both from the F dike, which are large for Yogo sapphires. Most of the rough is sent to Bangkok for faceting; only larger stones are cut locally. Vortex continues to manufacture their own line of jewelry using contract goldsmiths.

Keith A. Mychaluk

Canary tourmaline from Malawi. A new deposit of “electric” yellow and greenish yellow tourmaline was discovered in fall 2000 in Malawi. The bright yellow



Figure 27. Bright yellow “Canary” tourmaline is being mined from a new deposit in Malawi. Most of the finished gemstones weigh less than 1 ct, and have been heat treated to remove the brown color component. These stones weigh 2.08 and 2.82 ct (bottom; courtesy of Joeb Enterprises) and 11.65 ct (top; courtesy of Pala International); photo by Maha Tannous.

Figure 28. This 5.87 ct crystal of tourmaline from Nigeria has a most interesting chemical composition. It was selected from a parcel of gem tourmaline that was purchased in January 1999 by Nancy Attaway, who subsequently donated it to GIA. Photo by Paul Hlava; inset photo by Maha Tannous.



gems are being marketed as “Canary” tourmaline (figure 27). Although some of the material is natural color, much of it has been heat treated to achieve the “electric” yellow color. Before treatment, this rough was brown to brownish yellow. Because the tourmaline typically contains black needle-like inclusions, 95% of the rough yields faceted gems that are less than one carat. Most of the finished stones are 0.10–0.50 ct, in a variety of calibrated shapes. Production has been quite steady at approximately 1,000 carats per month. Currently, 95% of the production is being sold in Japan, but more may be available by the 2002 Tucson show.

The gemological properties of this material (obtained on two samples by Shane McClure, director of Identification Services at the GIA Gem Trade Laboratory in Carlsbad) were consistent with those for most gem tourmalines: R.I.—1.620–1.641, S.G.—3.10, inert to long- and short-wave UV radiation, weak dichroism (light yellow and moderate yellow), and no distinct features observable with a desk-model spectroscope. Microscopic examination revealed only a few small liquid “fingerprints” and some transparent crystal inclusions. (The black needles usually are removed during cutting.)

Microprobe analysis of the 2.08 ct sample by Dr. W. “Skip” Simmons at the University of New Orleans recorded an enrichment in manganese (6.93 wt.% MnO), fluorine (2.02 wt.% F), and titanium (0.45 wt.% Ti) in this elbaite (all values represent an average of four analyses). Also significant were calcium (0.63 wt.% CaO) and iron (0.13 wt.% FeO). Other elements were either present in very minor amounts or were not detected: K, Mg, V, Cr, Zn, Ba, Pb, and Bi. The composition of this bright yellow tourmaline suggests that its color is due to $Mn^{2+}-Ti^{4+}$ intervalence charge transfer (see G. R. Rossman and S. M. Mattson, “Yellow, Mn-rich elbaite with Mn-Ti intervalence charge transfer,” *American Mineralogist*, Vol. 71, 1986, pp. 599–602). The enriched manganese content is noteworthy, but the sample analyzed does not contain enough of this element to attain the theoretical Mn-tourmaline end member called “tsilaisite” (i.e., 10.7 wt.% MnO; see J. E. Shigley et al., “A notable Mn-rich gem elbaite tourmaline and its relationship to “tsilaisite,” *American Mineralogist*, Vol. 71, 1986, pp. 1214–1216).

Edward Boehm
Joeb Enterprises, Solana Beach, California
joebgem@aol.com

A bismuth-bearing liddicoatite from Nigeria. In a parcel of gem tourmaline from Nigeria (Ogbomosho area) purchased by faceter Nancy Attaway (Sandia Park, New Mexico) in January 1999, this contributor noticed some crystals with unusual coloration: a pale orangy pink core surrounded by a purplish pink rim (figure 28). To investigate the cause of the orangy pink color, one of the smaller, slightly abraded (eluvial) crystals was selected for elec-

tron microprobe analysis. One surface perpendicular to the c-axis of this 5.87 ct crystal was ground and polished, so that the entire 6-mm-diameter cross-section could be analyzed. Gemological properties, collected by GNI editor Brendan Laurs, are as follows: R.I.—1.620–1.638, birefringence—0.018, S.G.—3.07, and UV fluorescence—inert to long-wave radiation and moderate yellow to short-wave (on the outer “skin” of the prism faces only). Microscopic examination revealed feathers, planes of fluid inclusions on partially healed fractures, and a few colorless, low-relief, birefringent mineral inclusions.

The microprobe analyses were obtained at the Sandia National Laboratories in Albuquerque, New Mexico, using a JEOL 8600 instrument controlled by the SandiaTask operating system; data processing was accomplished using the Bence-Albee correction procedure. Initial observations of a few analyses revealed:

1. The pink rim contains Mn, whereas the orangy pink core contains both Mn and Fe.
2. The tourmaline generally contains little Na, Mg, and Fe, and is enriched in Ca, which suggests that it is liddicoatite.
3. Elevated Bi contents are present throughout the crystal, particularly in the rim.

To chemically characterize the material and especially the two color zones, 557 points were analyzed across the width of the polished face. Several major and trace elements were measured: Na, Mg, Al, Si, Ca, Mn, Fe, Zn, and Bi; Cr and Zn were also analyzed, but were below the detection limits of the instrument (i.e., less than approximately 0.03 wt.% Cr_2O_3 and 0.13 wt.% ZnO). Mineral standards and synthetic element oxides were used to standardize the instrument and obtain quantitative analyses.

The analyses reveal that the outer rim of the crystal consists of Ca-rich elbaite, whereas the inner part of the rim and the core is liddicoatite with up to 4.60 wt.% CaO (figure 29); this is more calcium-rich than the type specimen of liddicoatite from Madagascar (4.21 wt.% CaO; see P. J. Dunn et al., “Liddicoatite, a new calcium end-member of the tourmaline group,” *American Mineralogist*, Vol. 62, No. 11/12, 1977, pp. 1121–1124). Also surprising is the amount of bismuth enrichment: Besides the relatively high Bi contents in the core (averaging about 0.3 wt.% Bi_2O_3), up to 1.23 wt.% Bi_2O_3 was measured in the rim. This is apparently the first mention of Bi in liddicoatite, and the enriched rim contains much more Bi than has been reported for elbaite in the gemological literature to date (compare up to 0.83 wt.% Bi_2O_3 in E. Fritsch et al., “Gem-quality cuprian-elbaite tourmalines from São José da Batalha, Paraíba, Brazil,” Fall 1990 *Gems & Gemology*, pp. 189–205). In general, Bi levels in the crystal are inversely proportional to Ca contents. Iron was not detectable (<0.05 wt.% FeO) in the rim of the crystal, and only small amounts of Fe (up to 0.12 wt.% FeO) are present in the core. Manganese is also relatively depleted in

this tourmaline, with the highest values measured in the core (0.45 wt.% MnO). The orange modifier in the core of this pink tourmaline appears to be caused by both Mn and Fe; the highest concentrations of these elements are present in the core, and none of the other elements detected is a known chromophore in tourmaline.

Elbaite and liddicoatite cannot be differentiated by color or standard gemological testing. The interesting chemical data collected from this single sample make one wonder how much of the tourmaline from Nigeria (and elsewhere) is actually liddicoatite.

Paul F. Hlava
Sandia National Laboratories
Albuquerque, New Mexico
pfhlava@sandia.gov

SYNTHETICS AND SIMULANTS

“Jurassic Bugs” amber imitation. Gemological curiosities abound at the Tucson gem and mineral shows in February each year. Many of these are discovered “off the beaten path” and take the form of treated stones, synthetics, or imitations. Such items may be of interest to a laboratory

Figure 29. Electron microprobe data (557 analyses) across the Nigerian tourmaline crystal revealed that the outer part of the purplish pink rim is Ca-rich elbaite, and the pale orangy pink core is liddicoatite. Elevated contents of Bi are present across the entire crystal, but particularly high values (up to 1.23 wt.% Bi_2O_3) were measured in the rim.

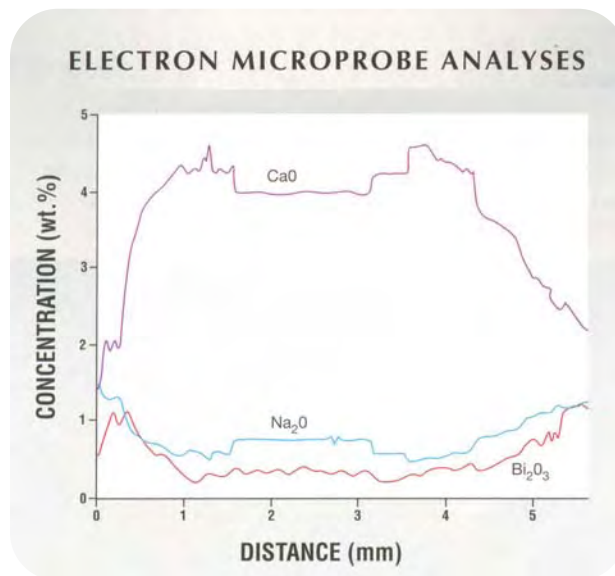




Figure 30. These three freeform brownish yellow plastic nodules were sold as novelty substitutes for natural amber. A single insect is encapsulated in each. The largest nodule, at the bottom of this photo, weighs 8.43 ct and contains a mosquito. The other two insects seen here are a ladybug and an ant. Photo by Maha Tannous.

gemologist as reference specimens, particularly if they have not been encountered previously.

This past February we had the opportunity to purchase three samples of cast-plastic amber substitutes, each of which contained one insect, which were being sold as “Jurassic Bugs.” As seen in figure 30, these polished nodules are a very convincing transparent, slightly brownish yellow, somewhat reminiscent of much of the transparent natural amber from the Dominican Republic. However, the condition and almost perfect positioning of the insect inclusions in the nodules would have raised our suspicions, even if the material had not been marketed as imitation amber at a very low price.

Figure 32. Represented as diamond rough in Brazil, these imitations consist of topaz (23.57 ct, left) and cubic zirconia (8.71 ct, right) to which small fragments of diamond have been attached in discrete crevices. The seller could then place a diamond probe on the small piece of diamond to “prove” that the entire piece was “natural.” Photo by H. A. Hänni.



Figure 31. Magnification and polarized light reveal the zone of encapsulation and the strain pattern that developed when this 7-mm-long ant was encased in liquid plastic that subsequently solidified. Photomicrograph by John I. Koivula.

The dealer had a basket of these nodules, which were packaged individually in small plastic bags. Each had a paper “Jurassic Bug” label imprinted with a cartoon-like mosquito. The choices were ant, ladybug, or mosquito (again, see figure 30). The nodules are formed as plastic blocks. When the plastic is still soft, a depression is created in the surface, the insect is placed and positioned, and a second layer of plastic is added to cover the depression. Then the blocks are rounded off into freeform nodules and polished. The end result is an interesting amber substitute.

Gemologically, the nodules test as plastic. The spot R.I. was consistent at 1.56, which is slightly higher than the 1.54 expected for amber. Unlike amber, all three nodules sank readily in a saturated salt solution, and there was no visible-light absorption spectrum. The nodules fluoresced a weak, slightly chalky bluish green to long-wave UV radiation, with no reaction to short-wave UV. In addition, the zone of encapsulation created by the depression and secondary pour of plastic was easily seen when the insects were examined in polarized light (figure 31).

“Jurassic Bugs” are an interesting amber substitute that is easily separated from natural amber using standard gemological tests and observational skills.

John I. Koivula and
Maha Tannous

Deceptive assembled diamond imitations from Brazil. Last January, a client submitted two pieces of rough (8.71 and 23.57 ct; figure 32) to SSEF for identification. They were represented to him as diamonds in Brazil, where he purchased them for US\$500. A dealer there used a diamond

probe to “confirm” that the stones were diamonds. Both looked like broken crystal fragments, and they did not initially appear to be imitations.

The 23.57 ct stone was approximately 14 × 14 × 11 mm, and had an S.G. of 3.56 (measured hydrostatically); this was identified as topaz. The 8.71 ct sample was approximately 10 × 8 × 7 mm, with an S.G. of 5.89; it was identified as cubic zirconia. (Both identifications were confirmed with laser Raman microspectrometry.) When exposed to long-wave UV radiation, the 8.71 ct sample showed one spot that fluoresced blue. Microscopic examination revealed that the fluorescent area corresponded to a 2 × 1.5 mm colorless fragment that was attached to the surface (see inset, figure 32); testing with a diamond probe indicated that this fragment was diamond, which was confirmed by Raman analysis. Further examination of the 23.57 ct sample revealed that it also had a diamond fragment attached to its surface; in this case, the 2 × 2 mm fragment did not show any fluorescence. On both samples, the pieces of diamond were glued into notches where the dealer could easily place the diamond probe, making them particularly deceptive imitations. HAH

Enamel-backed quartz as a star sapphire imitation.

Recently these contributors received an approximately 10 ct blue cabochon for testing. The stone displayed nice, distinct asterism and was mounted in a ring with diamonds. On first sight, it resembled a star sapphire (figure 33). Closer examination with a microscope, however, revealed features that indicated it was an imitation.

The back of the stone was flat and appeared bruted. Star stones typically have a bruted back that is domed, not flat. With the microscope, it became obvious that the blue color was located solely in a thin (about 1 mm) layer on the base of the cabochon. This layer had a grainy appearance with many air bubbles (figure 34, left). It could not be scratched with a needle. The upper part of the cabochon consisted of a colorless transparent material that contained three sets of tiny colorless needles arranged at 120° angles (figure 34, right). These were the cause of the distinct asterism.

No inclusions typical of sapphire (e.g., negative



Figure 33. This imitation star sapphire was mounted in a ring with diamonds. Photo by H. A. Hänni.

corundum crystals, mica, or zircon with tension fractures) were observed in the sample, although small conchoidal fractures (which are unusual for sapphire) were observed. We also did not see the expected absorption line for sapphire at 450 nm with a desk-model spectroscope; in fact, no distinct absorption bands could be seen. When we examined the cabochon with a polariscope, however, we easily recognized a so-called bull’s-eye figure, which is typical for quartz. EDXRF qualitative chemical analysis and Raman analysis confirmed the identification as quartz.

Although the imitation had a convincing appearance, standard gemological and laboratory testing revealed that it was a star quartz backed with a layer of blue enamel. This is the first time that we have seen such an elaborate, high-quality imitation of a star sapphire.

*Michael S. Krzemnicki and HAH
SSEF Swiss Gemmological Institute
gemlab@ssef.ch*

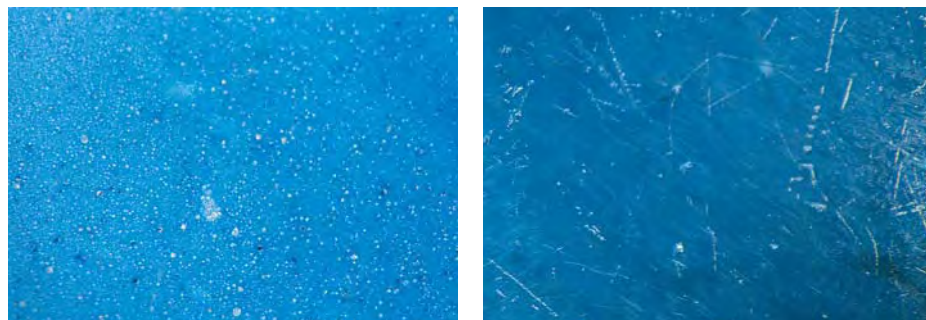


Figure 34. The blue enamel layer at the base of the quartz cabochon, which contained numerous gas bubbles (left). Tiny needle-like inclusions were responsible for the asterism in the quartz (right). Photomicrographs by H. A. Hänni; magnified 30×.



Figure 35. At the 11th Annual V. M. Goldschmidt Conference, Dr. George Rossman received the prestigious Dana medal. He is shown here on the right with Dr. Cornelius Klein, president of the Mineralogical Society of America. Photo by Dr. J. Alex Speer.

MISCELLANEOUS

11th Annual V. M. Goldschmidt Conference. This year's Goldschmidt geochemistry conference was held in Hot Springs, Virginia, May 20–24, and included a session titled "Geochemistry and Mineralogy of Gemstones." The session was well attended, which indicated increasing interest in the study of gem materials on the part of the geochemistry community. **Dr. G. Harlow** (American Museum of Natural History, New York City) introduced the session with a talk on the opportunities that the study of gem materials provides for research and for cross-fertilization of ideas between education and the popular culture. As an example, he cited the American Museum's recent "Nature of Diamonds" exhibition, which introduced many in the public to the science of diamond origin and the technological applications of diamonds, as it dazzled them with diamond jewelry. Next, **Dr. J. Shigley** discussed the identification challenges posed by HPHT-annealed diamonds. Recognition of this kind of treatment is increasingly dependent on the use of visible, infrared, and Raman (photoluminescence) spectroscopic techniques. **Dr. T. Häger** (Johannes-Gutenberg-Universität, Mainz, Germany) described experiments to study the causes of color and heat-treatment behaviors of rubies and sapphires. He presented a graphical representation of sapphire coloration according to various chromogens (Mg^{2+} , Ti^{4+} , and $Fe^{2+/3+}$). **M. Garland** (University of Toronto, Ontario, Canada) reported on the use of trace-element data and inclusion

chemistry to help determine the original source of Montana's alluvial sapphires. She suggested that they formed as a result of contact metamorphism, possibly related to extensive plutonism in this region during the Cretaceous Period. **Dr. L. Groat** (University of British Columbia, Vancouver, Canada) described the geologic setting of a new emerald occurrence, called the Crown Showing, in the southeastern portion of the Yukon Territory in Canada. The emeralds are hosted by quartz veins in schists. **Dr. S. Sorensen** (National Museum of Natural History, Smithsonian Institution, Washington, DC) reported on research into the chemical composition of jadeite-bearing rocks from Nansibon, Myanmar. Studying the rare-earth elements in these jadeites helps provide a record of their deformation and recrystallization. **C. Wright** (Miami University, Oxford, Ohio) discussed the cause of color and paragenesis of several generations of fluorite from the Hansonburg mining district in New Mexico. **Dr. E. Fritsch** (University of Nantes, France) described work on volcanic Mexican opals, which differ in their microstructure from sedimentary gem opals. Sedimentary play-of-color opals are composed of stacked silica spheres in a regular arrangement, whereas volcanic opals display a wider variety of less-regular micro- and nano-structures. **Dr. G. Rossman** (California Institute of Technology, Pasadena) ascribed the coloration of rose quartz to the presence of microscopic fibrous inclusions of an unidentified pink mineral thought to be related to dumortierite. Translucent blue quartz also appears to be colored by microscopic inclusions—of rutile, ilmenite, or similar iron-titanium oxides. **Dr. P. Heaney** (Pennsylvania State University, University Park) proposed that tiger's-eye quartz forms by the fracturing of a crocidolite host rock and deposition of columnar quartz (and enveloped crocidolite inclusions) in the resulting cracks. Incorporation of abundant parallel crocidolite inclusion trails into the quartz results in the tiger's-eye appearance of the rock.

A highlight of the conference was the award of the Dana Medal to Dr. George Rossman (professor of mineralogy at the California Institute of Technology and a member of the *G&G* Editorial Review Board and GIA Board of Governors) by the Mineralogical Society of America (figure 35). This award is given to recognize continued outstanding scientific contributions to the mineralogical sciences; in this case, it was awarded in recognition of Dr. Rossman's many contributions to this field, particularly regarding mineral spectroscopy and the causes of color in minerals. JES

Gemological conference at the Moscow State Geoprospecting Academy. On April 2–6, 2001, a gemological meeting was held in Moscow as part of an international conference with the general theme "New Ideas in the Earth Sciences." The conference was sponsored by several organizations, including the Ministry of Education of the Russian Federation, the Russian Academy of

Sciences, and other professional societies. The gemological session was organized by the Moscow State Geoprospecting Academy, the Russian Gemological Institute, and GIA Moscow. More than 300 participants attended the conference, including scientists, government officials, educators, academics, and students from many regions of the Russian Federation and adjoining countries, as well as some foreign guests.

The presentations covered a wide range of topics, such as the identification of synthetic and treated gem materials, chemical and physical properties of gemstones, new gem materials, and methods for gem appraisal and prospecting. A few of the presentations are summarized here. The meeting organizers published abstracts of all presentations (nearly all in Russian) in a conference proceedings.

Dr. J. Shigley (GIA Research, Carlsbad, California) opened the gemological session with a review of the identification of synthetic and treated diamonds, including those that had undergone HPHT annealing. **Dr. V. Vins** (Institute of Mineralogy and Petrography, Novosibirsk) and others reported on possible color changes that can be produced by the HPHT-annealing of various types of diamonds. **Y. Shelementiev** and co-authors (Lomonosov Moscow State University) discussed spectroscopic and luminescent properties as identification criteria for gem-quality synthetic diamonds and HPHT-treated diamonds. **Dr. M. Meilman** and **Dr. E. Melnikov** (Moscow State Geoprospecting Academy and GIA Moscow, respectively) discussed the identification of synthetic moissanite. Several presentations covered the properties of diamonds from various areas of Russia as well as studies of their inclusions. Mineralogical and gemological descriptions of gem materials from Russia and Central Asia were provided for alexandrite, apatite, charoite, chrysoberyl, sapphire, scapolite, sunstone (feldspar), tourmaline, turquoise, and zircon.

Dr. V. Bukanov (Gemological Association of Russia, St. Petersburg) described his work on a gemological dictionary. **Dr. V. Balitsky** (Institute of Experimental Mineralogy, Moscow) reviewed the status of synthetic gem materials produced in Russia and adjoining countries. **Dr. L. Demianets** (Institute of Crystallography, Russian Academy of Sciences, Moscow) described her work on synthesizing various colors of synthetic beryl, including red. Several gem identification techniques were discussed during the conference, including the presentation by **Dr. S. Mikhailov** and others (Institute of Electrophysics, Ural Division, Russian Academy of Sciences, Ekaterinburg) that described a pulsed-laser instrument for recording the cathodoluminescence spectra of gems.

A number of presentations focused on the use of gems in jewelry and for ornamental purposes. Among these were descriptions of museum gem collections, such as the Hermitage in St. Petersburg. Various investigators (including **Dr. Julia Solodova** and others at GIA Moscow) report-

ed on methods of quality grading colored gemstones such as ruby, sapphire, and emerald. Methods to appraise pearls and other nontransparent gem materials also were discussed. **B. Borisov** and **L. Tsunskaya** (Moscow Hallmark Office) reviewed efforts to implement an internationally recognized diamond grading system within the Russian Federation. The final presentations covered aspects of prospecting for various gem materials. The success of the gemological session promises that similar meetings will be held at future geological conferences in Moscow.

Julia Solodova
GIA Moscow, Russia
(gi-gia@cityline.ru)

JES

A visit to the Harvard tourmaline exhibit. A new exhibit, "Romancing the Stone: The Many Facets of Tourmaline," opened on February 10, 2001, at the Harvard Museum of Natural History. Curated by Dr. Carl Francis, this exhibit is the perfect vehicle for displaying Harvard's extensive collection of tourmalines, which dates from 1892 when the museum accepted the historically important Augustus Hamlin collection of Maine tourmalines. In fact, the viewer is drawn into the exhibit with the mining history of southwestern Maine's Mt. Mica and Dunton deposits. This section includes impressive crystal specimens, beautiful cut stones, and the famous Hamlin Necklace, which incorporates 70 tourmalines of different colors weighing a total of 228.12 carats.

The exhibit also explores the geology of tourmaline formation and occurrence, with examples of rough and cut tourmaline specimens from most sources worldwide represented. In addition, the complex chemical composition of the different tourmaline species is demonstrated in a clever interactive display. An impressive light box shows several multicolored liddicoatite slices to great advantage, and there are many beautiful examples of tourmaline carvings through the ages, notably from China and Germany. Compact, yet thorough, this interesting exhibit will remain on display through January 20, 2002.

Elise B. Misirowski
Director, GIA Museum
emisioro@gia.edu

ANNOUNCEMENTS

AGTA announces changes to Spectrum Awards. The American Gem Trade Association has announced significant changes to its Spectrum Awards, the annual competition for natural colored gemstone and cultured pearl jewelry design. Formerly limited to design entries, the 2002 Spectrum Awards will include AGTA's Cutting Edge lapidary arts competition. Another major difference is that design entries will be judged in fashion categories (evening, business, casual, men's, and bridal) rather than by price.



Figure 36. This 845-ct (62 × 53 × 30 mm) natural pearl was recently discovered near Zadetkyi Island of southern Myanmar. Photo courtesy of Myanma Pearl Enterprise.

Additionally, there will be no limit on the number of entries allowed, and the judging panel has been expanded from three judges to five. The deadline for entering the 2002 Spectrum Awards is September 28. To obtain an entry form, visit www.agta.org or call 800-972-1162. Outside the U.S., call 214-742-4367.

New Brazilian gemological maps available. The national geologic survey of Brazil (CPRM—Serviço Geológico do Brasil) recently issued two new gemological maps as part of the series *Informe de Recursos Minerais—Série Pedras Preciosas*, which started in 1997. Published in 2000, the maps cover the states of Rio Grande do Sul (No. 5) and Santa Catarina (No. 6) at 1:1,000,000 scale, and are accompanied by detailed reports (in Portuguese) describing the gem resources. Other maps in the series include portions of Rio Grande do Sul (Nos. 1 and 3), the Lajeado/Soledade/Salto do Jacuí region (No. 2), and Piauí/Maranhão (No. 4). To order, visit the CPRM's online bookstore at <http://www.cprm.gov.br/didote/cdot01.htm>, e-mail seus@cprm.gov.br, or fax 55-21-295-5897.

Large natural pearl. Last April, an 845 ct natural pearl measuring 62 × 53 × 30 mm (figure 36) was discovered at the Mukkalauk exploration area near Zadetkyi Island, which is off the southern tip of Myanmar (see www.myanmar.com/pearl/pearl.html). According to this source, the nacreous pearl is the world's largest natural pearl. Myanmar Andaman Pearl Co. Ltd., a company working under a profit-sharing agreement with Myanma Pearl Enterprises, discovered the pearl, which was found in a *Pinctada maxima* oyster. It is considerably larger than the "Pearl of Asia" (605 ct), which has been reported in the literature as the world's largest pearl. GIA has not examined the new specimen.

PCF rock-breaking technology. Rockbreaking Solutions has developed a new technology that offers the mining industry a non-explosive method for the controlled breakage of hard rock. The process, called PCF (Penetrating Cone Fracture), uses a propellant cartridge placed in a drill hole to produce a high-pressure gas pulse. The gas expands within small microfractures created during the percussive drilling process, and fractures the rock in a cone-shaped pattern (see www.rockbreakingsolutions.com). This non-explosive, low-hazard excavation technique has obvious applications for mining gems from many types of primary deposits.

CONFERENCES

World Diamond Conference. The 2nd Annual World Diamond Conference will attract explorers, producers, investors, and brokers to Vancouver August 22–23. Presentations will cover the global diamond market and exploration initiatives, government relations, diamond valuation, "conflict" diamonds, and activities in several important diamond-producing countries. Visit <http://www.iiconf.com>.

Facets 2001. The 11th annual gem and jewelry show organized by the Sri Lanka Gem Traders Association will take place September 3–5 in Colombo. Tours to Ratnapura, Elahera, and other mining areas are being organized, as well as visits to local lapidaries and jewelry manufacturing centers. Visit <http://www.facets-x.com>.

Hong Kong Jewellery and Watch Fair. On September 21–25, this show will take place in the Hong Kong Convention and Exhibition Centre. Special events include workshops and seminars by GIA, the Gemmological Association of Hong Kong, and the Diamond High Council, and an exhibition of Tahitian Pearl Trophy Design Competition by Perles De Tahiti. E-mail info@jewellery-net-asia.com or visit www.jewellery-net-asia.com.

On Sunday, September 23, *Gems & Gemology* Editor Alice Keller will participate in GIA GemFest with noted *G&G* authors Jim Shigley and Tom Moses.

ISA Antique and Period Jewelry course. The International Society of Appraisers (ISA) will conduct an Antique and Period Jewelry course on September 29–October 4 in Atlanta, Georgia. Appraisers, dealers, and collectors will learn to identify period pieces from before the 17th century to the mid-20th century. The course focuses on the history, design elements, construction, gem materials, and makers prominent in each period. Call 888-472-4732, e-mail courses@isa-appraisers.org, or visit www.isa-appraisers.org.

Fourth international business conference in Russia. *Russian Precious Metals and Gemstones Market: Today's Situation and Future Developments* will take place November 1–3 in Moscow.

This conference will cover a wide range of topics pertaining to gemstones and precious metals, including exploration and resource calculation, mining investment, production, certification, legislation, taxation, and current and future markets. Participants will have an opportunity to visit the Kremlin, Diamond Fund of Russia, St. Basil's Cathedral, and museums. Visit <http://www.jewelnet.ru/goldenbook/eng/rdmk.html>.

EXHIBITS

Diamonds exhibition in Canada. Quebec's Musée de la Civilisation is hosting a special exhibition on diamonds until January 6, 2002. This comprehensive exhibition examines the properties, geologic formation, and mining of diamonds, as well as their use in jewelry and industrial applications. Half of the objects on display have been loaned from New York's American Museum of Natural History, which developed the *Nature of Diamonds* exhibition. On display are pieces of extraordinary jewelry and diamonds, including the Aurora Collection, which consists of over 260 colored diamonds. Call 418-692-1151, e-mail pmignault@mcq.org, or visit www.mcq.org.

Carnegie Gem & Mineral Show. The Carnegie Museum of Natural History in Pittsburgh, Pennsylvania, will hold its fourth annual gem and mineral show August 24–26. Gold is the theme of this year's show, and some fine specimens will be displayed by six invited museum exhibitors. Visit www.clpgh.org/cmnh/gemshow.

Pearls at the American Museum of Natural History. A comprehensive exhibition on pearls will take place at the American Museum of Natural History in New York from October 13, 2001 to April 14, 2002. The exhibition will showcase a variety of pearls and pearl-forming mollusks, including white and black pearls from marine *Pinctada* oysters of Japan and Polynesia, freshwater pearls from mussels found in the United States and China, pink conch "pearls" from the Caribbean Queen conch, and more. A section on the decorative use of pearls will feature an extensive collection of jewelry and *objets d'art*. Visit www.amnh.org, or call (212) 769-5100.

ERRATA

1. In the Spring 2001 article on the Argyle diamond mine by Shigley et al., figure 3 (p. 28) shows two kimberlites located near the Argyle mine. These should have been indicated as lamproites. We thank Dr. Bram Janse for this correction.

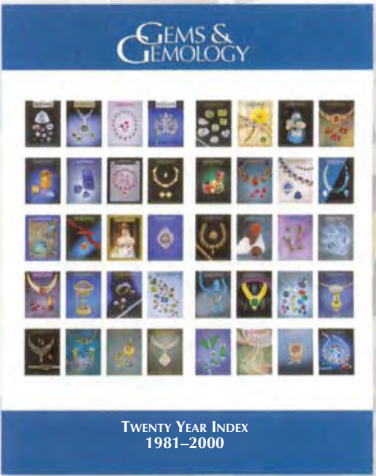
2. In the Spring 2001 article on hydrothermal synthetic red beryl by Shigley et al., the Y-axis of each graph in figure 14 (p. 52) should be labeled "Log (Counts)". Our thanks to Dr. George Rossman for bringing this to our attention.

3. In the Spring 2001 (p. 86) abstract of the article by B. Zhang et al. ("A study of photoluminescence spectrum of black pearl," *China Gems*, Vol. 9, No. 4, 2000, pp. 111–113), an editing mistake changed the meaning of the second paragraph. It should have been stated that the dyed-black freshwater cultured pearls exhibited the same photoluminescence features as those of untreated freshwater cultured pearls.

GEMS & GEMOLOGY

TWENTY YEAR INDEX 1981–2000

GEMS & GEMOLOGY's TWENTY YEAR INDEX, your indispensable reference guide to the 1981–2000 issues, is now available. Search the index by subject or author to locate the articles, Lab Notes, and Gem News entries of interest to you.



Printed copies are on sale for only \$9.95 in the U.S. (\$14.00 elsewhere). Download the index **FREE OF CHARGE** from the G&G website, www.gia.edu/gandg. Or receive a free index by purchasing any three years of back issues.

To order your printed copy of the **TWENTY YEAR INDEX**, contact Subscriptions Manager **Debbie Ortiz** at dortiz@gia.edu, or call toll-free **800-421-7250 ext. 7142**. Outside the U.S. and Canada, call **760-603-4000, ext. 7142**.

Back issues and article reprints are also available.

Book REVIEWS

2001

EDITORS

Susan B. Johnson
Jana E. Miyahira-Smith

Ammolite 2: A Guide for Gemmologists, Jewellers and Lapidaries

By Donna Barnson, 116 pp., illus., publ. by the author, 2000. Can.\$29.95*

At about the same time that I received this book for review, my copy of the Spring 2001 issue of *Gems & Gemology* appeared with its authoritative article on Ammolite by K. A. Mychaluk, A. A. Levinson, and R. L. Hall. The contrast between the two publications is striking, and in my view favors the article over the book despite the latter's larger size, its plethora of illustrations, and its announced purpose to serve as a guide to Ammolite. It is not surprising that almost every important fact covered in *Ammolite 2* is also covered in the article, since the book was published first, but the article authors are more succinct in their presentation and provide greater geological and mineralogical detail.

Ammolite 2, a large format (8.5 ↔ 11 inches; 21.5 ↔ 28 cm) soft cover book, contains nearly 300 color photo illustrations, many of finished Ammolite cabochons and jewelry. It consists of eight chapters covering the history of the industry, important persons connected with it, mining, processing, lapidary instructions, enhancements, optical properties, color and color patterns, and a grading system for finished stones. The grading system is based on a combination of color hue, quality, and the kind of pattern shown by the finished Ammolite. It is summarized by small color photos arranged according to grade on one side of a flap that folds inward from the back cover; a series of perforations allow the user to detach these

illustrations and use them separately for grading purposes. Color photos are present throughout the book and depict not only dozens of cut stones but also jewelry items, mining scenes, lapidary work, the mines and mining country, and persons connected with the industry. On the whole, the color quality is excellent, especially where cut gems are concerned.

Concluding the book are a glossary and a bibliography that both require reworking for the next edition. The glossary contains far too many terms, especially ones that are so common that any reader should know them (e.g., *centimeter*, *class*, *gemstone*, etc.). The "bibliography" is no more than a listing of books and articles, without paginations, and in the case of journal articles, without volume, issue, or page numbers. Misspellings are present throughout the book.

Ammolite 2 contains much interesting material and attractive color photographs. However, it suffers from poor organization and inclusion of matter that could have been omitted entirely without serious loss (such as the Indian legend "Iniskim," which supposedly refers to a fetish made from Ammolite; a description of the mosasaur, a prehistoric aquatic beast that is said to have dined on ammonites; and the glossary). Above all, the manuscript should have been submitted to an expert editor, who presumably would have eliminated awkward statements, purplish prose, abrupt changes in writing style, redundancies, and misspellings.

From a gemologist's standpoint, the article in *Gems & Gemology* says it all. Nevertheless, *Ammolite 2* offers a popular overview plus a host of excellent color illustrations and con-

siderable local color. It is a desirable addition to any geological library.

JOHN SINKANKAS
Peri Lithon Books
San Diego, California

The Dorling Kindersley Handbook of Gemstones

By Cally Hall, with photography by Harry Taylor, 160 pp., illus., publ. by Dorling Kindersley, London, 2000. US\$18.95*

Gemstones promotes itself as a recognition guide "for beginners and established enthusiasts alike" that "enables you to recognize each gemstone instantly." Although instant recognition may not be possible (or advisable), this smart-looking book provides a good start.

Inside are more than 800 full-color photographs of some 130 materials used in jewelry. The Introduction contains short sections on sources, properties, and synthetic gems, as well as a key to gems that occur in each of the different colors. It is followed by chapters on Precious Metals, Cut Stones, and Organic Gems; then a table of properties, a glossary, and an index.

One advantage of *Gemstones* is the numerous photos that provide rough, cut, and set illustrations for each gem material. Another is its ease of use, especially for the layperson. Unlike

**This book is available for purchase through the GIA Bookstore, 5345 Armada Drive, Carlsbad, CA 92008. Telephone: (800) 421-7250, ext. 4200; outside the U.S. (760) 603-4200. Fax: (760) 603-4266.*

most handbooks, the photos are shown on the same pages as the text. Bordering the photos and text in table-like form are the "vitals": R.I., S.G., luster, etc. The binding and materials used are of high quality, giving this book the feel of a rugged field guide.

Nevertheless, there are weaknesses. The book's "vivid, full-color photographs" tend to lack color saturation. Much of the information in the Introduction sections (e.g., Synthetic Gemstones) lacks detail, and inaccuracies occasionally appear. A cluster of albite crystals is used to depict distinct cleavage, and parti-colored tourmaline is misrepresented as the watermelon variety. Adularescence, which is caused by the scattering of light, is wrongly attributed to interference. A quartz perfume bottle first is described as having rutile inclusions, but later is presented correctly as having black needles of tourmaline. Some high-tech treatments, such as diffusion, are not included under enhancements. The Precious Metals chapter asserts that "although nuggets had been set in rings before 1920, most platinum jewelry dates from this time." However, this statement overlooks the fact that many Edwardian pieces, which predate 1920, were made of platinum. In the Cut Stone chapter, sphalerite is stated as showing doubled back facets, yet it is singly refractive. Chile, not Argentina, is a source of fine lapis lazuli. The irritant causing natural pearl formation is usually a parasitic animal instead of a piece of grit. The statement that Japan leads the world in the production of cultured pearls is no longer true, as China now occupies that position.

Gemstones is worthwhile despite such mistakes. It will be helpful particularly to the novice gemologist, and even advanced enthusiasts will gain some knowledge. Be careful, though: You can't do it all with this book alone! Good gemstone identification skills take considerable study, time, and practice to master.

MICHAEL EVANS
Gemological Institute of America
Carlsbad, California

Gem & Jewelry Pocket Guide

By Renee Newman, 156 pp., illus., publ. by International Jewelry Publications, Los Angeles, 2001. US\$11.95*

Picture yourself sitting in a deck chair on a cruise ship, or settling in for a long plane ride to some foreign destination. As part of your trip, you plan to buy a gemstone or piece of jewelry, so you are reading up on the subject. You would have a difficult time finding a better general reference on the subject than this book.

The author draws from her extensive experience as a gemologist, tour director, world traveler, and author of numerous other gem- and jewelry-buying guides to produce a concise, detailed, and interesting guide. Through the use of over 100 color photographs, numerous black-and-white photos, line drawings, and charts, she features dozens of different varieties of gemstones with separate sections for Alexandrite and Cat's Eye (Chrysoberyl); Amethyst and Other Quartz Gems; Chalcedony; Emerald, Aquamarine and Other Beryls; Garnet; Iolite; Jade; Kunzite; Lapis; Malachite; Moonstone and Other Feldspars; Opal; Peridot; Ruby and Sapphire; Spinel; Tanzanite; Topaz; Tourmaline; Turquoise; and Zircon. Additional chapters profile diamonds and gems from living organisms (pearl, amber, coral, and ivory). Other gemstone-specific information is provided in chapters on price factors for colored gems, gem lab documents, notable gem sources, synthetic and imitation gems, and gemstone treatments (with information on stability, frequency, and acceptability of various treatments). Not every gem mentioned has an accompanying photograph, but all are well described.

For those interested in purchasing a finished piece of jewelry, there are chapters on gold and platinum jewelry, jewelry craftsmanship, and how to have jewelry custom-made. Metals fineness markings, types of mountings, and care and cleaning tips also are included.

A subject that is not often covered

in books on gemstones and jewelry is the set of factors that a buyer should know to make a smart and safe purchase decision. These factors are covered throughout the book, and there are specific chapters on choosing a jeweler, finding a good buy, making the purchase, and selecting an appraiser. Another excellent chapter on this subject covers Customs considerations, including regulations, U.S. duty rates on jewelry and gems, and tips on how to avoid problems.

It's sometimes said that a little knowledge can be a dangerous thing. This book certainly doesn't replace gemological training and trade experience, but it goes a long way in helping gem and jewelry consumers make better buying decisions.

The size and readability of this book make it a "perfect fit" for its intended use, and you're likely to see it being put to use in just about any part of the world.

DOUGLAS KENNEDY
Gemological Institute of America
Carlsbad, California

Nature Guide to Gemstones & Minerals of Australia

By Lin Sutherland and Gayle Webb, 128 pp., illus., publ. by Reed New Holland Publishers, Sydney, 2000. Aus\$24.95

This small—6 × 8 inches (15 × 21 cm)—soft cover book is one of a series of Nature Guides published in Australia. It is well bound and printed on glossy paper. The book succeeds in presenting to the general reader the major gems and minerals that occur in Australia. The first part of the book, *What Are Gemstones & Minerals*, gives a succinct summary of crystallography and physical properties. The second, larger part, *Guide to Gemstones & Minerals*, discusses each gem and mineral in a well-written and easy style. It mentions many variations in color and shape, along with areas where these different materials have been found, but it only touches briefly on geology and origin. The size of the book prevents the inclusion of

detailed maps and descriptions of localities, but the last page shows a small-scale map of Australia on which the major areas are marked. The main strength of the book is the many photographs, which, although small—1.5 to 2 × 2.5 inches (4 to 5 × 6 cm)—display the gemstones and minerals in sharp detail and true color.

Text and photographs for each gem and mineral group occupy two pages, except for opal (six pages) and sapphire (four pages). The book is a good introduction for the interested nature lover, but keen rockhounds and amateur mineralogists will find the presentation of the subject matter a bit too superficial.

A. J. A. (BRAM) JANSE
Archon Exploration Pty. Ltd.
Carine, Western Australia

The Practical Guide to Jewelry Appraising

*By Cos Altobelli, 292 pp., publ. by the American Gem Society, Las Vegas, NV, 2000. US\$49.95**

This book presents a comprehensive outline of the appraisal profession's body of knowledge. It touches on everything an appraiser needs to know, but it also invites its readers to seek more comprehensive information on many of its subjects. For instance, the section on gemstones will encourage appraisers to expand their gemological knowledge, and the section on pricing invites the appraiser to establish personal trade sources and supplement their knowledge from the periodicals cited. All appraisers should add to the "time lines" section as the industry evolves.

The Case Histories chapter is especially interesting. It provides examples and pointers for handling jewelry and talking to clients. The

examples are highly relevant to situations that an appraiser may encounter. The situations mentioned in the case histories should persuade the appraiser to research legal precedents as well. The section on Insurance Policies is an eye opener. Clients should be encouraged to use the described points to talk to their insurance brokers regarding coverage.

Although the absence of an index was initially off-putting, I found the Table of Contents specific enough to serve as an index, if the reader has working knowledge of appraisal terminology. The forms and samples included provide basic examples of the various materials necessary for appraisal purposes, but they also encourage appraisers to create their own collateral documents.

This book challenges every jeweler to understand the complexities of the appraisal profession, and serves as a guidepost to further independent studies. Most instructional books become static as soon as they are finished. This one, however, involves appraisers in the material and encourages them to add to its chapters as the industry evolves.

The Practical Guide to Jewelry Appraising reflects Cos Altobelli's considerable experience as a jeweler, a gemologist and, especially, an appraiser. It belongs in the library of every serious appraiser.

GAIL BRETT LEVINE
Publisher, Auction Market Resource
Rego Park, New York

OTHER BOOKS RECEIVED

Ethnic Jewelry: From Africa, Europe and Asia, by Sibylle Jargstorf, 160 pp., illus., publ. by Schiffer Publishing Co., Atglen, PA, 2000, US\$29.95.*

This lavishly illustrated 8.5 × 11 inch soft cover presents a wide range of ethnic jewelry from several continents. The author combines the study of ethnic and traditional folk costumes with the jewelry of those cultures to demonstrate a holistic approach to decorative arts. In addition, by presenting an international variety of ethnic jewelry and traditional dress, she seeks to illustrate the similarities in approach that many cultures have toward these art forms. The traditional jewels of Africa, Europe, and Asia are covered in great detail with hundreds of photos and detailed descriptions. A price guide is included.

BARAK GREEN
Gemological Institute of America
Carlsbad, California

Costume Jewelers: The Golden Age of Design, 3rd Ed., by Joanne Dubbs Ball, 205 pp., illus., publ. by Schiffer Publishing Co., Atglen, PA, 2000, US\$39.95.* All costume jewelry enthusiasts should enjoy this heavily illustrated, 8.5 × 11 inch hardback volume, which focuses on the notable costume jewelers of the 20th century. Christian Dior, Givenchy, "Coco" Chanel, and Hattie Carnegie are just some of the more than 60 designers profiled. Far from being considered only as cheap imitations, many pieces of costume jewelry have grown in popularity and appreciation among jewelers, collectors, and artisans. Unfortunately, along with an increase in appreciation comes an increase in unauthorized reproductions, which the author warns against in her new preface. This revised edition also contains an updated pricing guide for all of the pieces shown.

BARAK GREEN
Gemological Institute of America
Carlsbad, California

Gemological ABSTRACTS

2001

EDITOR

A. A. Levinson
University of Calgary
Calgary, Alberta, Canada

REVIEW BOARD

Anne M. Blumer
Bloomington, Illinois

Jo Ellen Cole
GIA Museum Services, Carlsbad

R. A. Howie
Royal Holloway, University of London

Jeff Lewis
New Orleans, Louisiana

Taijin Lu
GIA Research, Carlsbad

Wendi M. Mayerson
GIA Gem Trade Laboratory, New York

James E. Shigley
GIA Research, Carlsbad

Jana E. Miyahira-Smith
GIA Education, Carlsbad

Kyaw Soe Moe
GIA Gem Trade Laboratory, Carlsbad

Maha Tannous
GIA Gem Trade Laboratory, Carlsbad

Rolf Tatje
Duisburg University, Germany

Lila Taylor
Santa Barbara, California

Paige Tullos
GIA Gem Trade Laboratory, Carlsbad

Sharon Wakefield
Northwest Gem Lab, Boise, Idaho

June York
GIA Gem Trade Laboratory, Carlsbad

Philip G. York
GIA Education, Carlsbad

COLORED STONES AND ORGANIC MATERIALS

Achat [Agate]. *extraLapis*, No. 19, 2000, 96 pp. [in German]

This issue in the special *extraLapis* series contains 15 articles from 12 contributors, and is illustrated with superb color photos. It is no surprise that about half the issue is dedicated to the agates of Idar-Oberstein, as these formed the basis of the Idar-Oberstein cutting industry. Several articles by R. Dröschel, U. Laarmann, and M. Henkel describe the geology of the Saar-Nahe region (which encompasses Idar-Oberstein), the special conditions required for the formation of agate, and the history and development of agate mining and the cutting industry (agate cutting was first mentioned in 1375 and probably did *not* occur in Roman times as is sometimes stated). J. Zang and A. Peth describe the two museums in Idar-Oberstein—Deutsches Edelsteinmuseum and Museum Idar-Oberstein—that display important collections of agate and other gems.

The remaining articles cover general aspects of agates. R. Hochleitner attempts to answer the question “What is an agate?” and (with R. Dröschel, K. Fischer, M. Glas, and U. Henn) compiles a useful glossary of the numerous and sometimes puzzling terms and names (some only in German) applied to chalcidony. M. Glas and M. Landmesser discuss the current theories on the formation of agate (e.g., SiO₂ mobilization and accumulation). L. H. Conklin presents his curious collection of rare Brazilian eye agates, M. Glas tells the story of the Ptolemaios II cameo (the most expensive agate in history), and G. Grundmann explains an almost forgotten printing technique using agates (“Naturselbstdruck”). P. Jeckel describes new finds of agate made during the past decade. H. Zeitvogel demonstrates how to cut and polish your own agates. RT

This section is designed to provide as complete a record as practical of the recent literature on gems and gemology. Articles are selected for abstracting solely at the discretion of the section editor and his reviewers, and space limitations may require that we include only those articles that we feel will be of greatest interest to our readership.

Requests for reprints of articles abstracted must be addressed to the author or publisher of the original material.

The reviewer of each article is identified by his or her initials at the end of each abstract. Guest reviewers are identified by their full names. Opinions expressed in an abstract belong to the abstracter and in no way reflect the position of Gems & Gemology or GIA.

© 2001 Gemological Institute of America

Approaches to improve cultured pearl formation in *Pinctada margaritifera* through use of relaxation, anti-septic application and incision closure during bead insertion. J. H. Norton, J. S. Lucas, I. Turner, R. J. Mayer, and R. Newnham, *Aquaculture*, Vol. 184, No. 1/2, 2000, pp. 1–17.

Cultured pearls from the black-lipped oyster *Pinctada margaritifera* constitute a significant industry in the South Pacific, with current annual production from French Polynesia and the Cook Islands at about US\$117 million and \$2.6 million, respectively. The main problems faced by pearl culturers from this region are post-operative oyster mortality, bead rejection, and poor-quality cultured pearls.

This study was designed to determine the effectiveness of three techniques for improving the quality and quantity of round cultured pearls from *P. margaritifera*: (1) immersion of the oysters in a solution of propylene phenoxetol to induce muscle relaxation before the bead is surgically implanted; (2) disinfection of the operation site with a dilute solution of povidone iodine; and (3) closure of the surgical incision with a flexible cyanoacrylate adhesive. The study showed that although the relaxant lowered the incidence of bead rejection, it significantly increased the oyster mortality rate. Another adverse effect of the relaxant was that the cultured pearls produced were lighter in weight due to reduced nacre secretion. The povidone iodine antiseptic solution had no significant effect on mortality or bead rejection, and was the only treatment that resulted in a lower percentage of total failures compared to the controls. Oysters treated with the adhesive had higher mortality and bead rejection rates, but this treatment did have a positive effect on cultured pearl quality (i.e., improved shape). The study also concluded that better hygiene surrounding the beads and instruments would reduce cell inflammation and infection, thereby improving cultured pearl production. MT

The history, geology, age, and fauna (mainly insects) of Burmese amber, Myanmar. *Bulletin of the Natural History Museum (London), Geology Series*, Vol. 56, No. 1, 2000, 83 pp.

This issue, devoted exclusively to Burmese amber (commonly called Burmite), consists of 11 articles written by 15 authors, most of whom are paleontologists from the Russian Academy of Sciences in Moscow and the Natural History Museum in London. The first article, by V. V. Zherikhin and A. J. Ross, is a thorough overview of current knowledge based on an exhaustive literature search. Early Chinese literature suggests that Burmite has been known since the first century AD and soon thereafter was traded in Yunnan Province. It was not mentioned in European literature until 1613. The first visit by a Westerner to the Hukawng Valley—one of five known Burmite-producing regions, but the only one that has been commercially mined—was by Captain S. F. Hannay

in 1836. Subsequent visits by members of the Geological Survey of India established that the amber occurs in sandstones and shales of Middle Eocene age. The archaic insects entrapped in the Burmite are assigned a probable Cretaceous age, thus suggesting that the amber had been reworked into the younger (Middle Eocene) sediment horizons.

The remaining 10 articles describe and tabulate the abundant fauna (mainly arthropods) found in Burmite. All the data reported in these articles are based on studies of specimens in the extensive collection of the Natural History Museum. Several new genera and species are described for the first time. The fauna are well illustrated, some in color. As the value of amber is frequently influenced by the type, abundance, and quality of included fauna, this issue will be of interest to amber collectors and dealers alike. AAL

PIXE studies of emeralds. K. N. Yu, S. M. Tang, and T. S. Tay, *X-Ray Spectrometry*, Vol. 29, 2000, pp. 267–278.

This study attempts to identify chemical characteristics that will separate natural from synthetic emeralds and also distinguish their source (i.e., geographic or manufacturer). Fifty-six natural emeralds (from Colombia, Pakistan, Zambia, and Brazil) and 26 synthetic emeralds (both flux-grown and hydrothermal, from eight manufacturers), all faceted, were analyzed nondestructively for 33 elements by PIXE (proton-induced X-ray emission).

Although the chemical characteristics of the emeralds sometimes varied significantly for a single locality or manufacturer, certain generalizations were possible. The concentrations of three elements—Cr, V, and Fe—enabled the distinction of Pakistani emeralds, as well as flux-grown synthetic emeralds from Chatham, Gilson, Taiwan, and Lennix. No single element, or combination of a small number (<4) of elements, gave satisfactory results for the other samples. When a larger number of element concentrations were analyzed by principal component analysis (PCA), an advanced statistical technique, unequivocal identifications were possible. With PCA, the separation of all the natural emeralds from their synthetic counterparts was achieved. The technique also enabled the identification of country of origin of all the natural emeralds, as well as the manufacturers of most of the synthetic emeralds—only Russian flux-grown and hydrothermal synthetic emeralds could not be distinguished by this technique. PGY

SEM study on jadeite jade. X. Liu, *Kuangwu Yanshi [Journal of Mineralogy and Petrology]*, Vol. 21, No. 1, 2001, pp. 5–7 [in Chinese with English abstract].

The mineral composition, grain size, and microstructural features of the green part of a specimen of jadeite were studied by scanning electron microscopy, and the variations in scattering and intensity of color were correlated with grain size. Images of the cleavage planes show that

they are not smooth, but rather are characterized by linear and "sawtooth" cleavage steps. RAH

La traçabilité des émeraudes: Une avancée décisive obtenue par microscopie infrarouge (μ IRTF) [Tracing the origin of emeralds: Decisive progress obtained by infrared microscopy]. A. Cheilletz, P. de Donato, and O. Barrès, *Revue de Gemmologie*, No. 141/142, 2001, pp. 81–83 [in French].

A new Fourier transform infrared (FTIR) spectroscopy technique has been applied to emeralds. This nondestructive "micro-FTIR" method acquires high-quality data more rapidly than other techniques, and uses an adapter that produces a small (10 micron) IR beam for taking high-resolution spectra. The distinction between natural and synthetic hydrothermal emeralds is made by detecting and interpreting the high-resolution FTIR patterns of water and CO₂ in the samples; the latter component is characteristic of natural emeralds. For natural emeralds, a database of 262 FTIR spectra representing 45 deposits in 15 countries has been assembled, along with oxygen isotope data ($\delta^{18}\text{O}$) and abundances for such elements as Cr and V. According to the authors, taken together these data enable the determination of geographic origin. This is possible because emeralds have characteristic chemical, isotopic, and FTIR spectral variations, which result in part from interactions between the host rocks and hydrothermal fluids in the geologic environments in which they crystallized. MT

DIAMONDS

Diamond Facts 2000/01—NWT Diamond Industry Report.

Northwest Territories Resources, Wildlife and Economic Development, 2001, 22 pp.

This year (2001) is the 10th anniversary of the first diamond discovery in the Northwest Territories (NWT), Canada, and the region has quickly become recognized as a world-class diamond producer. Highlights of activities in the NWT are presented in this informative, well-illustrated booklet prepared by the government agency responsible for economic development. Topics include: a timeline of important events (e.g., discoveries, approval of environmental reviews, and start of production at the Ekati mine); general information on the world diamond industry, with Canada's current and potential future positions; current exploration activities in the NWT; descriptions and status of advanced diamond mining projects; and the role of the Government of the Northwest Territories (GNWT) in various aspects of the diamond industry (e.g., certification of selected diamonds as mined, cut, and polished in the NWT, and sold as Canadian Arctic™ diamonds).

This booklet emphasizes—with an opening message from the Minister of Resources, Wildlife and Economic Development—that the GNWT is committed to maximizing the development of natural resources (including diamonds) and to adding value to Canada's diamonds. In

addition to creating job opportunities at the mines, post-production value-added opportunities are visualized in the form of increased employment in the cutting sector, establishment of grading facilities, jewelry manufacturing, and using NWT diamonds for tourism-related activities. A complimentary copy of this booklet may be requested by e-mailing diamondprojects@gov.nt.ca.

AAL

Etching of diamond crystals in a dry silicate melt at high P-T parameters. V. M. Sonin, E. I. Zhimulev, I. I. Fedorov, A. A. Tomilenko, and A. I. Chepurov, *Geochemistry International*, Vol. 39, No. 3, 2001, pp. 268–274.

Most natural diamond crystals have been subjected to dissolution processes that result in morphological and etch features such as curved faces and edges, and trigons. The authors investigated such dissolution processes using both natural and synthetic diamond crystals. The samples were placed in a silicate melt (corresponding to the chemical composition of an alkali basalt) at high pressure and high temperature, to approximate the conditions experienced by natural diamonds.

Various morphological and etch figures were produced, some very similar to those found in natural diamonds, depending on the experimental conditions. Three types were distinguished:

1. Positive trigons (with edges oriented parallel to the edges of the octahedral faces) and {hhl} surfaces with parallel striations normal to the initial octahedral edges were observed in samples subjected to relatively low pressures and in experiments with silicate melts in contact with air.
2. Negative trigons (with edges oriented opposite to those of the octahedral faces), or hexagonal etch pits and {hhl} surfaces with striations parallel to the initial octahedral edges, occurred only at high pressures.
3. Negative trigons or hexagonal etch pits and {hhl}, {hk0}, and {hkl} surfaces formed only in high-pressure experiments.

In all cases, the dissolution rate increased with increasing H₂O in the experimental systems. TL

Isotope dating of diamonds. D. G. Pearson and S. B. Shirey, in D. Lambert and J. Ruiz, Eds., *Application of Isotopes to Understanding Mineralizing Processes, Reviews in Economic Geology*, Vol. 12, Chap. 6, 1999, pp. 143–171.

The need to know the ages of diamonds is driven by both scientific curiosity and economic necessity. For example, such information should enable scientists to determine whether diamonds formed continuously throughout the earth's history or during discrete episodes. Moreover, diamond ages may be of value in determining new target areas for primary deposits and also in constraining the

sources of alluvial diamonds. Determining ages directly by isotopic methods, however, is not possible because the diamond lattice contains no useful radioisotope. The only reliable method of dating diamonds is based on the isotopic analysis of their mineral inclusions, which is the subject of this critical review.

The mineral inclusions used for diamond dating must be syngenetic (i.e., formed at the same time as the diamond). Criteria are given for recognizing such inclusions. The specific radioisotope system employed generally depends on the nature of the inclusion: Sm-Nd for garnet and clinopyroxenes, Re-Os or Pb-Pb for sulfides, and Ar-Ar for clinopyroxene. Interpretation of the results is often difficult, and many factors must be considered. Conflicting results occasionally are obtained by different methods. Everything involved with the isotopic dating of diamonds, from the isolation of an appropriate inclusion to the operation of the complicated instruments (e.g., mass spectrometers), requires great care and is time consuming.

When all published isotopic diamond ages determined since the mid-1980s are summarized, a wide variety of crystallization ages are evident, but the vast majority are greater than 1 billion years. AAL

A new approach to the exploration of diamond deposits by large-diameter boreholes. V. V. Krotkov, *Doklady Earth Sciences*, Vol. 373A, No. 6, 2000, pp. 930–932.

This article describes the application of a large-diameter (4 m) drilling technique for sampling kimberlite ore at the Lomonosov diamond deposit in the Arkhangelsk province of Russia. The drilling technique could extract an average of 2.58 tons/hour of kimberlite to a depth of 240 m without serious complications. The ability to extract such a large volume of material rapidly and efficiently enhances productivity in sampling diamondiferous rock with low diamond content (but possibly high-quality rough). The technique reduces the time needed to obtain the necessary volume of kimberlite for estimating ore grade, while it minimizes worker exposure to underground working conditions. Repair and maintenance costs are also minimized, and the drill can function at low temperatures (to -38°C).

Joshua Sheby

The source of the Espinhaço diamonds: Evidences from SHRIMP U-Pb zircon ages of the Sopa Conglomerate and Pb-Pb zircon evaporation ages of metavolcanic rocks. M. L. de Sá Carneiro Chaves, T. M. Dussin, and Y. Sano, *Revista Brasileira de Geociências*, Vol. 30, No. 2, 2000, pp. 265–269.

Alluvial diamonds are hosted by the Sopa Conglomerate, which outcrops in the Diamantina region of the Espinhaço Range in Minas Gerais, Brazil. The original source of these diamonds has never been established. One suggestion is that the diamonds might be derived from associated metavolcanic rocks. Using a Sensitive High Resolution Ion Microprobe (SHRIMP), the authors determined radiometric ages for different isotopes (e.g., $^{238}\text{U}/^{206}\text{Pb}$, $^{207}\text{Pb}/^{206}\text{Pb}$) in

zircons separated from both the Sopa Conglomerate and the metavolcanics. The results showed multiple ages (e.g., 3.6, 2.8, 2.0 billion years) for the zircons from the Sopa Conglomerate, all of which were older than the zircons from the metavolcanics (1.7 billion years). Because the metavolcanics are younger than the Sopa Conglomerate, they could not have been the source of the Espinhaço diamonds; hence, the origin of these diamonds remains unknown. PGY

Surface properties of diamonds in kimberlites [sic] processing. V. Chanturiya, V. Zuev, E. Trofimova, Y. Dikov, V. Bogachev, and G. Dvoichenkova, *Proceedings of the XXI International Mineral Processing Congress*, Rome, Italy, 2000, pp. B8b-9–B8b-16.

The use of grease table and froth flotation procedures in the recovery of diamonds from kimberlite ore may result in significant losses, particularly for certain size fractions. The explanation lies in the variable nature of the surfaces of rough diamonds, due to surface characteristics. Some are hydrophilic (have a strong affinity to water), whereas others are hydrophobic (water repellent); the former can be recovered with water-based flotation methods, whereas the latter adhere to grease and are recoverable on a grease table.

Using samples from the Mir pipe in Russia, the authors identified differences in the disparate nature of rough diamond surfaces. Hydrophilic surfaces are covered with a layer of CO_2 gas molecules and HCO_3^- radicals (both of which originate from carbonate minerals in the kimberlite) as well as minerals of the serpentine group. In contrast, hydrophobic surfaces have superficial films of carbonate minerals and minerals of the talc group. A technique patented in Russia (No. 2071836), based on the use of an anolyte (an acid product of water electrolysis), modifies the diamond surface so that recovery losses can be reduced by a factor of 1.5–2.0. AAL

United States diamond market: Analysis of polished diamond consumption 1994–2000. E. Cohen, *Mazal U'Bracha*, Vol. 15, No. 129, January 2001, pp. 45–48.

From 1994 through 2000, the importation (which can be equated with consumption) of polished diamonds into the U.S. increased rather uniformly on an annual basis in terms of both wholesale value and carat weight. During this period, there was a 132% increase in value (from US\$4.94 to \$11.44 billion), and a 91% increase in weight (from 10.70 to 20.47 million carats). The greater increase in polished value compared to weight indicates increasing demand in the U.S. for higher-quality and larger stones during that time period.

In 2000, the three main suppliers of polished diamonds imported into the U.S. as a percentage of total value were Israel (47%), India (23%), and Belgium (21%). By weight, however, India was the predominant supplier, accounting for 62% of the imports; Israel and Belgium supplied significantly less (19% and 10%, respectively).

From 1994 through 2000, the average per-carat value of all sizes of polished diamonds imported into the U.S. increased by a modest 21% (from \$462 to \$559 per carat); this is explained by the fact that the value of diamonds imported from India remained essentially static (\$198 per carat in 1994 compared to \$202 in 2000) throughout this seven-year period. In 2000, the average per-carat values of polished diamonds imported from Israel and Belgium were \$1,359 and \$1,142, respectively. AAL

GEM LOCALITIES

The Alto Ligonha pegmatites—Mozambique. M. B. Dias and W. E. Wilson, *Mineralogical Record*, Vol. 31, No. 6, 2000, pp. 459–497.

The Alto Ligonha pegmatite district of northern Mozambique is significant to mineralogists and gemologists for the quality and variety of gems and minerals it has produced. This comprehensive article provides a history (political and exploration) of the region starting at the end of the 19th century, a summary (with maps) of the geology of the district, and a table of the most important mines (organized into 27 groups, each comprising one-to-six individual pegmatites) together with the most notable gems or minerals found at each. From the 1930s through the 1970s, the district was an important producer of gem-quality tourmaline and beryl, as well as topaz and spodumene. Many rare and economically important ore minerals (of tantalum, beryllium, and lithium) also were mined. Production during the 1980s and 1990s suffered because of political problems, but mining activities are being encouraged by the current government.

The pegmatites are difficult to prospect because vegetation and lateritic soil cover the area, but they are locally revealed by prominent quartz cores or concentrations of mica in the soil. Although hundreds of pegmatite bodies have been mined, they probably represent only a small fraction of the district's potential. The Muiane pegmatite, which measures 400 m wide and 1 km long, is perhaps the most important producer of mineral specimens.

The bulk of the article is an alphabetical listing and brief description (including chemical and physical properties) of the 77 minerals reported from the district. This section is illustrated with superb color photographs of gem and mineral specimens, as well as crystal drawings of selected minerals. A most unusual, and fascinating, feature of this article is the final section, "Memoirs of Alto Ligonha," which contains reminiscences by the senior author of his tenure as a geologist, most of it in Alto Ligonha, from the mid-1930s until the end of the Portuguese colonial period (1975). JEC

Die Pegmatite von Alto Ligonha in Nord-Mozambique [The pegmatites of Alto Ligonha in northern Mozambique]. P. Schäfer and T. Arlt, *Lapis*, Vol. 25, No. 8, 2000, pp. 13–17, 54.

For decades, Alto Ligonha has produced several pegmatite

gem minerals—sometimes in giant crystals. Most of the pegmatites are deeply weathered, so there is little need for explosives. Many of the dumps and old pits are being reworked for overlooked gem crystals.

The authors describe their visit to Muiane, the most important gem mining area, which is dangerous and where bribes are a way of life. They also visited several smaller and less dangerous areas, including the beryl and emerald deposit Maria III at Niame. Because the local mining industry is focused on cuttable material, many pieces of broken gems were offered; it was nearly impossible for the authors to obtain undamaged gem crystals or mineral specimens. RT

Classification and mineralization potential of the pegmatites of the Eastern Brazilian Pegmatite Province.

G. Morteani, C. Preinfalk, and A. H. Horn, *Mineralium Deposita*, Vol. 35, 2000, pp. 638–655.

The Eastern Brazilian Pegmatite Province (EBPP) encompasses the pegmatite districts of Itambé, Araçuaí, Safira, Nova Era, Aimorés, and Espera Feliz, almost all of which are important sources of gems, especially fine tourmaline, aquamarine, and morganite, as well as Li, Sn, Nb, and Ta ore minerals. All of the districts except Itambé are situated in fold belts surrounding the eastern border of the São Francisco craton, and were formed during the Brasiliano tectonothermal event (~600 My) in host rocks that show decreasing grades of metamorphism from east to west. The one exception, the Itambé district, is located within the São Francisco craton, and is of Transamazonian age (~1,900 million years [My]).

To determine the degree of fractionation of the EBPP pegmatites and assess their mineralization potential, major- and trace-element analyses were obtained for 530 K-feldspar and 550 muscovite samples. A wide variety of compositions were recorded, from slightly fractionated muscovite-class pegmatites to highly fractionated pegmatites of the rare-element class. Districts with the widest range in pegmatite fractionation (such as Araçuaí and Safira) are also leaders in the production of gem and rare-element minerals. Emeralds are more likely to be found in Be- and Li-pegmatites of Transamazonian age (i.e., the Itambé district). Within the EBPP, a correlation seems to exist between grade of metamorphism, degree of fractionation, and mineralization of gems and rare-element minerals. The use of geochemical indicators (e.g., plotting Cs vs. K/Rb for K-feldspar or muscovite) appears useful for targeting highly fractionated pegmatites and evaluating their mineralization potential. RT

Emerald mineralisation in Colombia: Fluid chemistry and the role of brine mixing. D. A. Banks, G. Giuliani, B. W. D. Yardley, and A. Cheillett, *Mineralium Deposita*, Vol. 35, 2000, pp. 699–713.

It is generally accepted that Colombian emeralds in both the eastern (Gachalá, Chivor, and Macanal) and western (Peñas Blancas, Muzo, Coscuez, and Yacopi) mining dis-

tricts formed from the interaction of hypersaline brines with the host black shales and evaporites. The purpose of this study was to quantify the composition of these fluids, which were extracted from inclusions in emeralds, calcite, dolomite, quartz, and fluorite by a bulk crush-leach technique and subsequently analyzed by different spectroscopic methods (ICP-AES, FES, and GFAAS).

In contrast to fluids from the other minerals, those in the emeralds (fluid 1) are dominated by Na and Cl and have the lowest concentrations of all other elements. While a range of origins has been proposed for high-salinity brines—with seawater as the most common—the authors found that in both districts, all the fluid inclusions in emeralds have Cl:Br ratios much greater than that of seawater. Therefore, they believe the fluids to be the result of halite dissolution, most probably from the local salt beds. The authors also postulate an origin under low-grade metamorphic conditions.

The fluids from quartz inclusions (fluid 2) are of similar salinity and contain less Na, but significant amounts of Ca, K, Fe, and Cl. Inasmuch as the fluid compositions in both the western and eastern zones are similar, they seem to be controlled by interaction with the local host rocks, which in both cases are black shales and evaporites. The authors suggest that in certain conditions, beryllium may have been leached from wall rocks and introduced into fluid 1. Subsequently, a mixing of both fluids caused precipitation of fluorite and parisite, the destabilization of Be-F complexes, and the growth of emeralds. RT

Emeralds in Greenstone belts: The case of Sandawana, Zimbabwe. J. C. Zwaan and J. L. R. Touret, *Münchner Geologische Hefte*, Series A, Vol. 28, 2000, pp. 245–258.

Most emeralds occur in “schist-type” deposits (Colombian emeralds are a notable exception), which are commonly attributed to the interaction of pegmatitic fluids with Cr-bearing host rocks (e.g., metavolcanics and/or ultramafics). This interaction is usually envisaged as a single-stage contact-metasomatic event, with the emeralds occurring at or close to the border of the pegmatitic veins. However, based on regional and detailed geologic studies, as well as geochemical and mineralogical data, this origin is not appropriate for emeralds in the Mweza Greenstone belt, such as at Sandawana, even though they are normally found very near the contact between green-schists and pegmatites.

The pegmatitic bodies at Sandawana are completely altered (albitized), and are strongly folded and sheared along with their greenstone host rocks. The gem-quality emeralds occur in strongly foliated schists at least 1 mm away from the pegmatites, in relatively low pressure areas called “traps.” The authors suggest that the emeralds formed during folding, shearing, and regional metamorphism, from a pegmatitic fluid rich in F, P, Be, and Li that invaded the contact zones and incorporated various other elements (e.g., Cr) necessary for the formation of emerald. KSM

Edelsteine aus Sambia—Teil 2: Turmalin und Aquamarin [Gemstones from Zambia—Part 2: Tourmaline and aquamarine]. C. C. Milisenda, V. Malango, and K. C. Taupitz, *Zeitschrift der Deutschen Gemmologischen Gesellschaft*, Vol. 49, No. 1, 2000, pp. 31–48 [in German with English abstract].

The important Jagoda pegmatite mining area in Zambia is a source of gem-quality pink, red, and green tourmalines, as well as aquamarine. Geologic descriptions and maps are presented for several of the pegmatites (e.g., Jagoda, Muchinga, and Pela). The gemological properties of the tourmaline and aquamarine are typical. The tourmaline is characterized by inclusions of “trichites” (hair-like capillaries) and growth tubes; the aquamarine has minute fluid inclusions.

These pegmatites are unusual because gem-quality tourmaline and aquamarine rarely occur together in the same deposit, even though both generally form near the cores of zoned pegmatites that are enriched in alkali- and rare-elements. Thus, a special set of growth conditions is required. The Jagoda pegmatites probably formed by the mobilization of fluids during the Pan African metamorphic event (650–450 million years ago), when they were emplaced as relatively thin stratabound bodies into metamorphic host rocks. They apparently did not form in the more usual way, that is, by magmatic differentiation from granitic melts. AAL

The Rist and Ellis tracts, Hiddenite, North Carolina. D. L. Brown and W. E. Wilson, *Mineralogical Record*, Vol. 32, No. 2, 2001, pp. 129–140.

This article reviews the history, geology, and production of the Rist and Ellis gem tracts, near Hiddenite, North Carolina. Although this area is known primarily for the production of emerald and hiddenite (bright green Cr-bearing spodumene), excellent specimens of other minerals also have been mined, including monazite, muscovite, quartz (smoky and amethyst), rutile, tourmaline (schorl), and xenotime.

Two amateur mineralogists, J. A. D. Stephenson and W. E. Hidden, discovered the mineralized pegmatites and hydrothermal veins in the area in 1875 and 1880, respectively. After decades of intermittent mining and several changes in ownership, the area was acquired in 1969 by a partnership of Warren Baltzley and Charles Rist, which operated through 1981 as American Gems Inc. During this period, the adjacent Rist and Ellis tracts were opened to the public for collecting on a daily fee basis. There are no records of the amount or quality of production during this time, but it is generally known that many fine-quality specimens were obtained. In 1969, for example, a 59 ct emerald crystal was found and later cut into a 13.14 ct gem, the “Carolina Emerald,” which now resides in the New York showroom of Tiffany & Co.

Since 1982, ownership of the properties has changed three times, and numerous other stunning specimens have been discovered. These include North America’s

largest emerald crystal (1,686.3 ct), still unnamed, which was found in 1984.

All the important minerals found at this famous locality are described in varying detail, with their typical crystal habit and mode of occurrence noted. Excellent full-color photographs accompany the text. *JEC*

The São Geraldo do Araguaia opal deposit, Pará, Brazil.

T. A. Collyer and B. Kotschoubey, *Revista Brasileira de Geociências*, Vol. 30, No. 2, 2000, pp. 251–255.

The recently discovered opal deposit near São Geraldo do Araguaia, in the state of Pará, contains several types of opal, the main ones being “precious” opal (showing play-of-color; called “noble” opal by the authors), “jasper” (reddish) opal, and fire opal. All occur as fracture fillings, veins, and/or local accumulations within biotite schist of the Xambioa Formation. The opal-bearing zone is approximately 3 km long and up to 6 m thick.

Inclusions within the opal consist mainly of fragments of metamorphic minerals from the host rock, including kyanite and biotite; the latter has been partially altered to chlorite. Other included materials are quartz grains, acicular rutile crystals (with a roughly radial, fan-like habit), and hematite.

It is likely that most of the opal formed as a result of low-temperature hydrothermal activity and tectonism during Jurassic and Cretaceous time, which was associated with the opening of the Atlantic Ocean. Hydrothermal processes mobilized silica at depth within the earth’s crust, and this was subsequently precipitated as opal near the surface. A later episode of opal deposition probably was responsible for the formation of the precious opal. *LT*

JEWELRY MANUFACTURING

Fancy free. A. Skuratowicz and J. Nash, *American Jewelry Manufacturer*, March 2001, pp. 72–74, 76, 78, 80–82.

Setting a fancy-shaped gemstone (e.g., a marquise cut) may pose problems that require the skill of an experienced jeweler. Complications can arise from a stone’s shape and its durability under stress (at the points of a marquise, sharp corners, curved sides), variations in the cut (uneven girdle, pavilion bulge), and its inherent properties (toughness, cleavage, hardness, types of inclusions, susceptibility to thermal shock, and sensitivity to harsh chemicals).

After taking into consideration artistic preferences and a stone’s shape and characteristics, a jeweler can then choose the elements of a setting: style and metal type. Setting style is determined by the stone’s durability and the location of pressure points. Different metal types offer varying degrees of malleability and durability depending on the alloy components; a soft malleable alloy, whether precious or nonprecious, usually works best.

Given the problems inherent in working with fancy cuts, the jeweler may have to make some adjustments at the bench. Some suggestions include annealing hard

metal alloys, laying out and measuring pieces before beginning, and compensating for pressure points with additional burring. *Joshua Sheby*

PRECIOUS METALS

Hard 22 carat [karat] gold alloy. C. Cretu, E. Van Der Lingen, and L. Glaner, *Gold Technology*, No. 29, 2000, pp. 25–29.

Market demand for high-karat gold jewelry is growing, especially in India and the Middle East. Unfortunately, high-karat gold lacks the hardness of lower-karat gold. Mintek, a South African company, has developed a 22K gold alloy with a hardness near that of 18K gold; even greater hardness can be attained by a combination of cold working and heat treating of the metal. Tests conducted by Mintek show that the alloy is similar in color to 22K gold, can be cast using conventional methods, and resists tarnish and corrosion as much as 22K gold. It also can undergo in excess of 99.99% cold rolling without intermediate heating and cracking. Solder testing revealed very good hardness, even greater than that of 22K gold. Standard equipment and techniques can be used with the alloy. Although the other elemental constituents of the alloy are not revealed, the authors state that no hazardous elements are used during its manufacture. *PT*

Rise in shine. *American Jewelry Manufacturer*, Vol. 45, June 2000, p. 33.

Seeking a tarnish-free silver, British silversmith Peter Johns added germanium to the alloy formula. Still considered sterling (at 92.5% silver), the alloy is tarnish resistant and also does not develop firescale (an inorganic substance that develops after cooling). Kultakeskus Oy, a silver manufacturing company in Finland, partnered with Johns because this alloy saves production time. The alloy is conducive to laser welding, and its manufacture is more environmentally friendly than those processes that use acids and other substances to prevent firescale. Although the alloy resists tarnish, it does develop a yellow coating that is easily removed. Other reported drawbacks include its higher price and limited availability. *PT*

SYNTHETICS AND SIMULANTS

Characterization of Verneuil red corundum by X-ray topography. C. Rinaudo and P. Orione, *Materials Chemistry and Physics*, Vol. 66, 2000, pp. 143–148.

Over 90% of the synthetic corundum currently produced worldwide is grown by the Verneuil flame-fusion process. Boules grown by this method tend to crack along their length at the end of the growth process. To explain this phenomenon, the authors analyzed cross-wise and length-wise slices (~1 mm thick) obtained from Verneuil synthetic corundum boules. Optical microscopy, energy-dispersive spectrometry, and X-ray transmission topogra-

phy were used to characterize the samples. Particular emphasis was placed on detecting differences in the crystallographic, physical, and chemical characteristics of the slices relative to their position and orientation within a boule. Only the bottom portion of the boules, corresponding to the initial growth stages, are composed of single crystals. From the middle of the boule upward, there is considerable stress-related deformation (easily observed as intense interference colors with crossed polars), which leads to a macromosaic structure.

The authors attribute boule cracking to the loss of monocrystallinity accompanied by stress in the middle and upper parts of the boule, which corresponds to the latter stages of the growth process. It is suggested that the area of the boule closest to the flame during initial growth undergoes a type of annealing that results in improved crystal quality. MT

Graphite \blacklozenge diamond transition under high pressure: A kinetic approach. J. Sung, *Journal of Materials Science*, Vol. 35, 2000, pp. 6041–6054.

This article reviews the kinetics (i.e., rate) of the graphite-to-diamond transition under high pressure and the effectiveness of various solvent-catalysts (i.e., Fe-Ni, Cu, CaCO₃, P) that can facilitate the process. Two types of transitions are recognized: direct and solvent-assisted. The direct transition occurs without a catalyst, and the temperature of the transition appears to depend on the degree of structural perfection (i.e., polytype composition) of the original graphite. The more “perfect” the graphite, the lower the temperature at which it may transform to diamond.

The effectiveness of various catalysts is discussed, and some disputes are reviewed. The authors conclude that the more carbon a solvent can dissolve at ambient pressure, the more effective it will be as a catalyst for the transition of graphite to diamond at high pressure. Hence, Fe or Ni are more powerful catalysts than Cu, which is more powerful than P or CaCO₃. Wuyi Wang

Simulated diamond gemstones formed of aluminum nitride and aluminum nitride: Silicon carbide alloys.

C. E. Hunter, WO Document No. 00/22204 A2, April 20, 2000; U.S. Patent No. 6,048,813, April 11, 2000.

Diamond-like colorless synthetic gems can be produced by growing and faceting single crystals of pure aluminum nitride (AlN), or an alloy of aluminum nitride and silicon carbide (SiC—synthetic moissanite). Alloys in the compositional range of AlN(0.8):SiC(0.2) to AlN(0.5):SiC(0.5) are preferred. Several dopants (gallium, cerium, gadolinium, and samarium are mentioned) can be added to grow crystals of a desired color. The crystals can be grown by several techniques, and various aspects of the growth procedures are described in detail; the fashioning process is also mentioned. However, gemological and physical prop-

erties (e.g., refractive indices, dispersion, spectra, hardness, specific gravity) are not given other than the statement that the refractive indices of pure AlN and the alloys are comparable to those of diamond. The U.S. patent may be viewed at <http://www.uspto.gov/patft/index.html>.

Karl Schmetzer

Spectroscopic properties of coloured, synthetic corundums and spinels produced in Skawina. M. Czaja,

Mineralogica Polonica, Vol. 31, No. 1, 2000, pp. 55–68.

Electronic absorption, excitation, and luminescence spectra are presented for synthetic α -Al₂O₃ (corundum with a trigonal structure), synthetic α -Al₂O₃ (does not occur naturally; does not have a trigonal structure), and synthetic spinels of various colors grown at the Research and Development Laboratories of the Aluminum Plant at Skawina, near Craców (Kraków), Poland. Different crystal growth orientations, concentrations of impurity ions, and the presence of more than one chromophore were established as the main reasons for the variations in color. All of the colored spinel varieties were found to be non-stoichiometric, with an MgO:Al₂O₃ ratio of 1:2.6. The results indicate tetrahedral coordination of Co²⁺ in the synthetic spinels and Mn²⁺ in synthetic α -Al₂O₃. RAH

TREATMENTS

Gübelin Gem Lab introduces thermal enhancement scale.

G. Roskin, *Jewelers' Circular Keystone*, Vol. 171, No. 11, 2000, pp. 52, 54.

The thermal processes used to enhance the color and appearance of gem corundum are varied, as are their effects. The stones may be heat treated either before or after cutting, with or without chemicals (e.g., borax). Vitreous byproducts of melted chemicals (“glass”), as well as vitreous products of natural inclusions, may result from the heating process. All laboratories will indicate whether a stone has been heat treated; some will also estimate how much glass remains, while others will use only such qualitative terms as *minor*, *moderate*, or *pre-dominant*.

The Gübelin Gem Lab in Lucerne, Switzerland, has developed and initiated a new six-point thermal enhancement (TE) disclosure system to characterize and classify the entire range of heat-induced features in gem corundum; master stones are used for comparison. TE1, for example, indicates only minute traces of residue inside partially “healed” fractures. Conversely, a treated stone designated as TE6 shows large glass-filled cavities, in addition to healed fractures with droplets of residue. The system explains what the thermal enhancement has achieved, rather than attempting to quantify the amount of enhancement. It is hoped that with full disclosure of heat treatments and their effects, consumer confidence will return. AAL